ABSTRACT

Title of Document: A STABLE ISOTOPIC INVESTIGATION OF PRECIPITATION NITRATE

Katherine Suzanne Cooney,
Master of Science, 2005

Directed By: Professor James Farquhar,
Department of Geology

The isotopic composition of precipitation nitrate reflects the processes involved in its formation. Silver nitrates prepared from Maryland precipitation were thermally decomposed to gases for mass spectrometric analyses. Nitrate $\delta^{15}N$ ranged from -5.1±0.5‰ to +5.9±0.5‰ (1σ), $\delta^{18}O$ ranged from +42.6±0.5‰ to +81.9±0.5‰, and $\Delta^{17}O$ ranged from +15.33±0.05‰ to +31.71±0.05‰. Precipitation samples were re-analyzed for $\delta^{15}N$ and $\delta^{18}O$ using a method in which bacteria convert nitrate to N_2O for analyses, and $\delta^{15}N$ ranged from -3.6±0.2‰ to +7.1±0.2‰ and $\delta^{18}O$ ranged from +61.6±0.3‰ to +86.8±0.3‰. Differences between the methods were attributed to organic contaminants in the silver nitrates. Nitrate $\delta^{15}N$, $\delta^{18}O$, and $\Delta^{17}O$ were highest in the winter and lowest in the summer. Ion concentrations, storm track data, and the $\delta^{34}S$ of precipitation sulfate were used for interpretations. Most likely, $\delta^{15}N$ varied due to seasonal changes in the NO_x photo-stationary state, and $\delta^{18}O$ and $\Delta^{17}O$ varied due to changes in oxidation chemistry.

A STABLE ISOTOPE INVESTIGATION OF PRECIPITATION NITRATE

By

Katherine Suzanne Cooney

Thesis submitted to the Faculty of the Graduate School of the
University of Maryland, College Park, in partial fulfillment
of the requirements for the degree of
Master of Science
2005

Advisory Committee:
Professor James Farquhar, Chair
Professor Philip A. Candela
Dr. Marilyn L. Fogel
Professor Bruce R. James
Professor Karen L. Prestegaard

Acknowledgements

This project could not have been accomplished without the encouragement and assistance of several people. James Farquhar supported my choice of a research topic and maintained a positive attitude through the analytical challenges. James provided me with a unique perspective on science and helped me grow as a researcher and communicator. Marilyn Fogel allowed me to analyze nitrate isotopes, ammonium concentrations, and the carbon content of prepared silver nitrates at the Geophysical Laboratory of the Carnegie Institution of Washington and served as a role model and mentor. Philip Candela, Bruce James, and Karen Prestegaard helped me clarify research questions and advised me throughout the project. Rebecca Carmody and Janet Hannon contributed to method development and Debra Baker, Ning Bao, Bradley Burcar, Marla Hertz, and Cara Losey provided invaluable assistance in the laboratory. Jay Kaufman kindly allowed me to analyze sulfate sulfur isotopes in the Stable Isotope Laboratory of the University of Maryland, and Nick Collins and Dan Earnest helped during the analyses. Alan Davis gave me permission to use the ion chromatograph in the Environmental Engineering Laboratory of the University of Maryland, and Hunho Kim and Houng Li assisted with the measurements. Jan Kaiser offered me the opportunity to analyze nitrate isotopes using an exciting set of techniques. Jan and Greg Kane assisted me in conducting these analyses in the laboratory of Danny Sigman at Princeton University. Danny also generously allowed me to analyze nitrate/nitrite concentrations using NO_x chemi-luminescence in his laboratory. Todd Karwoski helped me with all of my computing

needs, and Kate Scheiderich translated several critical journal articles from German to English. Russ Dickerson, Jeff Stehr, and Fang-Zhen Teng provided many insights useful for data interpretations. My family and friends, especially Alan, Sue, Mike, Allie, and Jenn Young, and Will Cooney, provided me with the love and strength that I needed to carry this project to its completion. The Maryland Water Resources Research Center and the National Science Foundation provided partial financial support.

Table of Contents

List of Tables

List of Figures

1. Introduction

1.1. Atmospheric nitrate

Gas-phase nitric oxide, NO, and nitrogen dioxide, NO_2, referred to as NO_x, play a major role in atmospheric chemistry and are smog-forming air pollutants. Globally, NO_x abundances range from a few parts per trillion in remote areas to greater than 100 parts per billion in urban areas (EHHALT et al., 2001). While there are constant emissions of NO_x from automobiles, coal-fired power plants, soils, and lightning channels, NO_x undergoes chemical transformations to nitric acid (HNO_3) or nitrate (NO_3^-) on the order of a day. Within a week, atmospheric nitrate is delivered to the Earth's surface via dry or wet deposition.

The approximately five-fold increase in NO_x emissions since pre-Industrial times translates to larger quantities of atmospheric nitrate (JAWORSKI et al., 1997; PROSPERO et al., 1996) and represents a major perturbation to nitrogen cycling in the atmosphere and biosphere (VITOUSEK et al., 1997). Nitric acid is a significant component of acid rain (GALLOWAY and LIKENS, 1981) and contributes to increased acidity in surface waters (e.g., MURDOCH and STODDARD, 1992). The deposition of atmospheric NO_3^- also has an effect on soil processes and plant biodiversity (e.g., GOULDING et al., 1998). In addition, since nitrogen is frequently the limiting nutrient in surface waters of estuarine and coastal environments (RYTHER and DUNSTAN, 1971), atmospheric NO_3^- affects the productivity of these ecosystems (e.g., PAERL, 1985) and contributes to eutrophication and algal blooms (JAWORSKI et al., 1997; VITOUSEK et al., 1997 and references therein). Furthermore, atmospheric NO_3^-

contaminates drinking water, and the consumption of water with elevated NO_3^- concentrations may have negative effects on human health, such as links to infant methemoglobinemia, or "blue baby" disease, and gastric cancer (BRUNINGFANN and KANEENE, 1993).

Properly managing NO_3^- loading to land and water requires constraints on atmospheric deposition relative to other NO_3^- delivery pathways, such as applications of fertilizers or manure, effluent from waste-water treatment plants, and microbial production via nitrification. If atmospheric deposition delivers an appreciable portion of the total NO_3^-, then other relevant concerns become how and where the precursor NO_x originated.

1.2. Stable isotopes

Stable isotopes provide a tool to distinguish atmospheric nitrate from nitrate formed by non-atmospheric processes. *Isotopes* are atoms of an element that have the same number of protons, or atomic number, but different sums of protons and neutrons, or mass numbers. There are two stable nitrogen isotopes, ^{14}N and ^{15}N, and three stable oxygen isotopes, ^{16}O, ^{17}O, and ^{18}O. Whereas unstable isotopes undergo radioactive decay, stable isotopes maintain their numbers of protons and neutrons over time. In a neutral atom, the number of protons determines the number of electrons. The number and distribution of electrons in an atom's orbitals largely determines its chemical properties, and therefore isotopes exhibit similar behavior and occupy the same place on the periodic table. Even so, there are subtle variations in the properties of isotopes that lead to compounds having slightly different isotopic

compositions. Natural variations in N and O isotope ratios are typically smaller than a few percent and are reported in delta (δ) notation with units of parts per thousand, or *per mil* (‰).

$$\delta = \left(\frac{R_{\text{sample}}}{R_{\text{standard}}} - 1 \right) \times 1000\,‰$$

By convention, R is the ratio of a less abundant isotope over the most abundant isotope. Atmospheric N_2 has a constant $^{15}N/^{14}N$ of 1/272 (COPLEN et al., 1992; JUNK and SVEC, 1958; MARIOTTI, 1983). Nitrogen isotope ratios are typically expressed in δ notation as the ‰ difference from the atmospheric N_2 reference, AIR.

$$\delta^{15}N = \left(\frac{\left(^{15}N/^{14}N\right)_{\text{sample}}}{\left(^{15}N/^{14}N\right)_{\text{AIR}}} - 1 \right) \times 1000\,‰$$

Nitrate oxygen isotope ratios are typically reported relative to Vienna Standard Mean Ocean Water, VSMOW, which has an absolutely calibrated $^{18}O/^{16}O$ of 0.0020052 ± 0.00000045 (BAERTSCHI, 1976) and $^{17}O/^{16}O$ of 0.0003799 ± 0.0000008 (LI et al., 1988).

$$\delta^{18}O = \left(\frac{\left(^{18}O/^{16}O\right)_{\text{sample}}}{\left(^{18}O/^{16}O\right)_{\text{VSMOW}}} - 1 \right) \times 1000\,‰ \qquad \delta^{17}O = \left(\frac{\left(^{17}O/^{16}O\right)_{\text{sample}}}{\left(^{17}O/^{16}O\right)_{\text{VSMOW}}} - 1 \right) \times 1000\,‰$$

Plotting $\delta^{18}O$ versus $\delta^{17}O$ for most terrestrial compounds forms an array, often referred to as the mass-dependent fractionation line, which is shown in Figure 1. The theoretical basis for the mass-dependent fractionation line is presented in section 2.2. The oxygen isotope compositions of several atmospheric compounds plot off the mass-dependent fractionation line. The parameter, $\Delta^{17}O$, shown graphically in Figure 1, is the difference between a measured $\delta^{17}O$ value and the $\delta^{17}O$ value predicted on

the basis of the mass-dependent fractionation line. Whereas most terrestrial compounds have $\Delta^{17}O$ values close to zero, several atmospheric compounds have non-zero $\Delta^{17}O$ values. Of the atmospheric compounds that have been measured, ozone, O_3, exhibits the largest $\Delta^{17}O$ values.

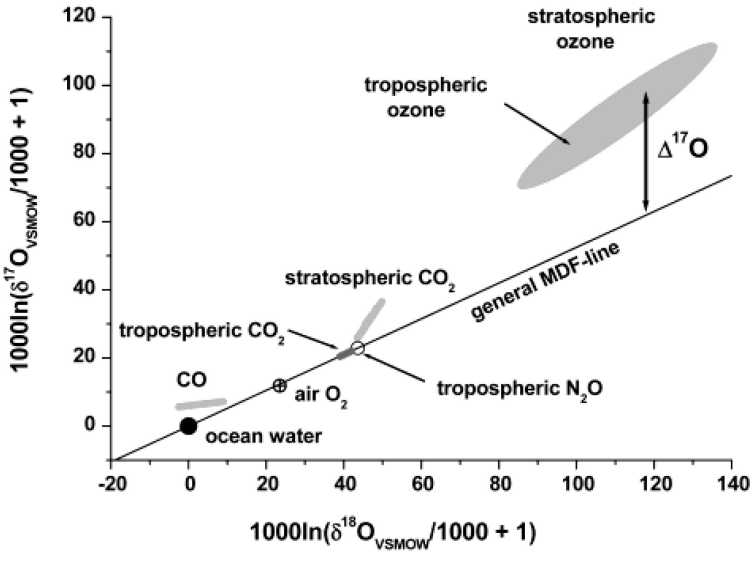

Figure 1: Non-mass dependent isotope effects observed in atmospheric trace compounds as published by Brenninkmeijer and coworkers (2003). Tropospheric refers to compounds collected within the lowest 10-15km of the atmosphere while stratospheric refers to compounds collected from the top of the troposphere to 50km above ground level.

Ozone in the troposphere, the lowest 10-15km of the atmosphere, takes part in a number of atmospheric chemical reactions involving nitrogen oxides (see section 2.1). Michalski and coworkers (2003) showed that during these processes non-mass dependent oxygen atoms can be transferred from ozone to nitrogen oxides, resulting in atmospheric nitrate with $\Delta^{17}O$ values as high as 30‰ (Figure 2). The other oxidants involved in NO_x oxidation have $\Delta^{17}O$ values significantly closer to zero.

Since ozone plays a greater role in NO_x oxidation in the winter than in the summer, the $\Delta^{17}O$ of atmospheric nitrate is higher in the winter and lower in the summer. The seasonal variation of the $\Delta^{17}O$ of atmospheric nitrate was reproduced successfully by Michalski and others (2003) using an isotopic model coupled to a photochemical box model (Figure 2).

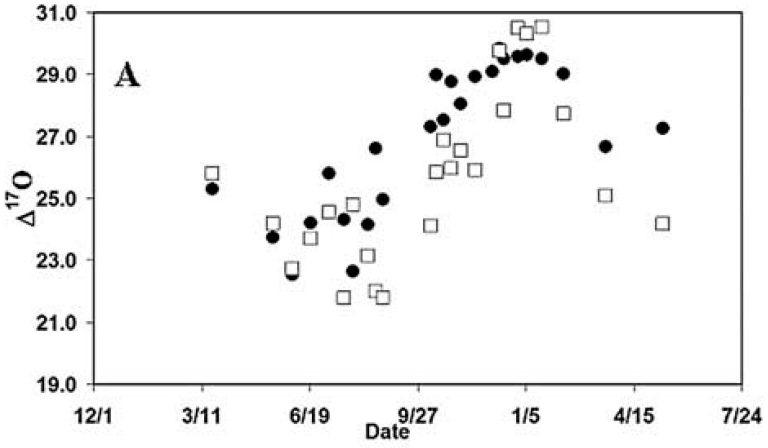

Figure 2: Measurements (open squares) and model predictions (circles) for aerosol nitrate in La Jolla, CA as published by Michalski and colleagues (2003). Described simply, their model showed that lower $\Delta^{17}O$ values in the summer and higher $\Delta^{17}O$ values in the winter were the result of seasonal changes in the role of ozone on NO_x oxidation.

1.3. Research Overview

Atmospheric deposition provides a pathway of delivering non-mass dependent nitrate to the Earth's surface. Measuring the $\Delta^{17}O$ of NO_3^- in surface waters may allow us to address the significance of NO_3^- deposited from the atmosphere (non-zero $\Delta^{17}O$) relative to other NO_3^- delivery pathways ($\Delta^{17}O$ close to zero). However, in order to use $\Delta^{17}O$ as a tool in watershed studies, it is necessary to be able to analyze nitrate isotopes accurately and precisely and to understand potential variations in atmospheric nitrate isotope ratios.

One technique commonly used to analyze nitrate stable isotopes involves the thermal decomposition of prepared silver nitrates. There are numerous challenges associated with the isolation and purification of nitrate salts. Since NO_3^- is a universal solute, nitrate salts cannot be precipitated from solution. Instead, all non-nitrate compounds must be removed from solution, without removing any nitrate in the process, and then solutions are freeze-dried to produce nitrate salts. One of the most challenging aspects is removing organic contaminants. While activated carbon and various resins can be used to extract organic compounds from solution, these treatments can also adsorb NO_3^-. In addition to the possibility of isotope fractionation associated with adsorption, losing significant quantities of nitrate during the wet chemical procedure is not favorable for samples with relatively low NO_3^- concentrations, such as precipitation.

One of our first research objectives was to set up techniques at the University of Maryland to produce contaminant-free nitrate salts that preserved the isotope ratios of precipitation NO_3^-. We established a set of techniques at the University of Maryland based on published methods (CHANG et al., 1999; SILVA et al., 2000) and the techniques used by researchers at the US Geological Survey in Reston (J. Hannon, personal communication). Silver nitrates prepared from precipitation samples were analyzed for $\Delta^{17}O$ using thermal decomposition techniques set up at the University of Maryland and for $\delta^{15}N$ and $\delta^{18}O$ in the laboratory of M. Fogel at the Carnegie Institution of Washington. Despite our efforts to minimize organic contaminants, there was evidence that the prepared silver nitrates were impure. Before we could

interpret the results, we needed to examine the effects of organic contamination on measured isotope ratios.

We were offered the opportunity to re-analyze our samples using an innovative technique developed at Princeton University that avoids issues of organic contamination. Instead of preparing salts that can be decomposed to produce gases, the new approach uses denitrifying bacteria to convert NO_3^- directly to N_2O for mass spectrometric analyses. We analyzed nitrate isotopes using both the $AgNO_3$/decomposition and denitrifier methods. A comparison of the two methods is a major outcome of this research.

Our study of atmospheric nitrate focused on a set of precipitation samples collected in Frederick, Maryland. Reasons for selecting Frederick as the site for sample collection are included in section 4.1. Since precipitation nitrate only represents a portion of the total atmospheric nitrate, we had to consider the effects of in-and-below cloud scavenging processes on nitrate isotope ratios. Other potential influences on the isotopic signature of precipitation NO_3^- include the isotopic composition of precursor NO_x, physical-chemical mechanisms that influence the partitioning of isotopes between atmospheric compounds, and NO_x oxidation pathways. In addition to analyzing $\delta^{15}N$, $\delta^{18}O$, and $\Delta^{17}O$ of NO_3^- and considering the relationships between these parameters, we also collected meteorological data, determined the source regions of air masses, measured the major ion concentrations, and analyzed the $\delta^{34}S$ of precipitation sulfate. Evaluating isotope ratios in the context of these other parameters allowed us to determine the major influences on the isotope ratios of precipitation nitrate.

2. Background

2.1. Tropospheric NO_y Budget

Although long-range transport of NO_x is limited by its short chemical lifetime, the regions that generate NO_x are not necessarily the regions where NO_3^- deposition occurs (e.g., VITOUSEK et al., 1997). Similar to the way upstream activities affect downstream water quality, emissions of NO_x from certain regions can lead to the deposition of atmospheric NO_3^- and environmental consequences in distant areas. Thus, investigations of atmospheric NO_3^- require knowledge of the processes that generate, transform, transport, and remove reactive nitrogen compounds.

2.1.1. NO_x Formation Processes

There are numerous processes by which NO_x enters the troposphere, the lower 10-15 km of the atmosphere where most weather occurs. The Intergovernmental Panel on Climate Change (IPCC) reported that the major processes that contribute to the global NO_x budget, in order of decreasing significance, are fossil-fuel combustion, biomass burning, microbial production in uncultivated and cultivated soils, lightning, emission from aircraft, transport from the stratosphere, which begins above the troposphere and continues to around 50 km above ground level, and atmospheric NH_3 oxidation (EHHALT et al., 2001). The IPCC lists aircraft separately because, at 8 to 12 km above ground level, aircraft emit NO_x directly to the free troposphere, where NO_x has a disproportionately large effect on greenhouse gas concentrations (EHHALT et al., 2001). For the purposes of this discussion, aircraft emissions are considered part of

fossil fuel combustion processes. Fuel combustion sources of NO_x in the United States are estimated to be 40-45% from transportation, 30-35% from power plants, and approximately 20% from industrial sources (SEINFELD and PANDIS, 1998). The relative contributions of NO_x from these processes vary regionally and seasonally (KASIBHATLA et al., 1993; LEVY et al., 1999; PENNER et al., 1991). Figure 3 illustrates the major processes that introduce NO_x to the troposphere.

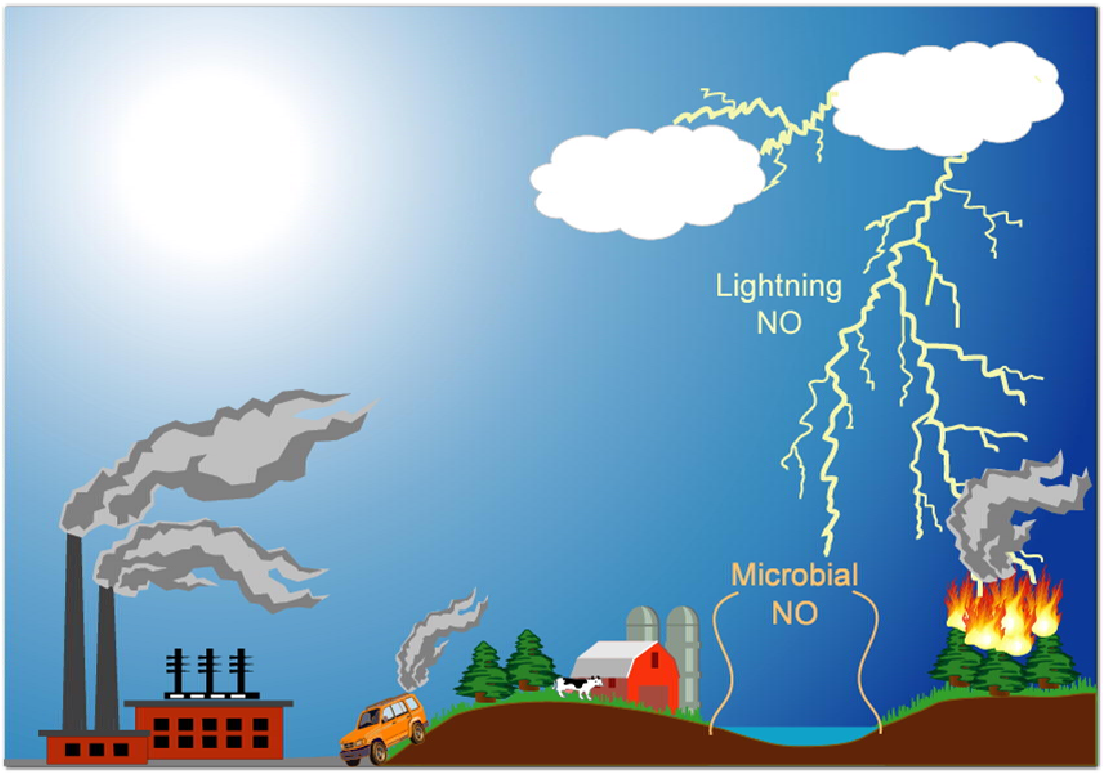

Figure 3: Illustration of the major NO_x formation processes. Fossil fuel combustion by coal-fired power plants, industries, and automobiles, microbial production during nitrification and denitrification in cultivated and uncultivated soils, lightning, and biomass burning account for the majority of NO_x entering the troposphere.

In the formation of NO_x at high-temperatures, N is derived from atmospheric N_2 (thermal NO_x) or organic N (fuel NO_x). Processes that produce thermal NO_x

include lightning discharges and high-temperature industrial processes. Automobile engines also produce mostly thermal NO_x due to low concentrations of organic N in petrol (typically negligible) and high engine temperatures (>2000°C). The production of thermal NO_x can be explained by the Zel'dovich mechanism (ZEL'DOVICH et al., 1947). Molecular oxygen thermally decomposes to form ground state atomic oxygen, $O(^3P)$, by

$$O_2 + \text{heat} \rightarrow 2O(^3P). \quad (1)$$

Atmospheric nitrogen reacts with atomic oxygen to produce NO and atomic nitrogen by

$$N_2 + O(^3P) \rightarrow NO + N, \quad (2)$$

and then molecular oxygen reacts with atomic nitrogen to produce NO and atomic oxygen by

$$O_2 + N \rightarrow NO + O(^3P). \quad (3)$$

Under certain conditions and to a lesser extent, a third reaction contributes to NO formation by

$$N + OH \rightarrow NO + H. \quad (4)$$

At high temperatures, N_2 and NO exist in chemical equilibrium. The most common reaction of NO back to N_2 is

$$NO + N \rightarrow N_2 + O(^3P). \quad (5)$$

The equilibrium concentration of NO decreases as the temperature decreases. If N_2 and NO remain in equilibrium at low temperatures, then the amount of NO produced would be minor. However, the amount of time required to achieve chemical equilibrium increases as the gas cools. When the rate of the gas cooling is

approximately equal to the rate of gas approaching chemical equilibrium, the concentration of NO "freezes out."

Coal-fired power plants typically generate fuel NO_x. Combustion in coal-fired power stations generally occurs at temperatures too low to generate sufficient amounts of thermal NO_x (1300-1400°C), but there are significant quantities of nitrogen in coal (1.0 to 1.2% N). Fuel NO_x is produced by a number of reactions involving the conversion of organic N to reactive N (e.g., N, NH, HCN) and subsequent oxidation by an oxygen-containing radical (e.g., OH) to form NO. Since temperatures of biomass burning and forest fires are generally too low to produce thermal NO_x, the N is likely derived from organic material and can therefore be classified as fuel NO_x.

Bacteria produce microbial NO_x during nitrification (conversion of NH_4^+ to NO_2^- followed by the oxidation of NO_2^- to NO_3^-) and denitrification (reduction of NO_3^- to NO_2^- followed by the conversion of NO_2^- to N_2 and trace amounts of N_2O and NO_x). Atmospheric NH_3 oxidation can also generate small quantities of NO_x (KOHLMANN and POPPE, 1999). Ammonia enters the atmosphere by a number of processes, including the decomposition of animal waste, emissions from fertilized and unfertilized soils, industrial emissions (especially biomass burning), and natural emissions from vegetation and oceans (e.g., DENTENER and CRUTZEN, 1994). Within several hours, NH_3 undergoes heterogeneous reactions to produce aerosols. While the predominant reaction is between NH_3 and sulfuric acid (H_2SO_4) to produce NH_4HSO_4 and $(NH_4)_2SO_4$, NH_3 also reacts with nitric acid (HNO_3) to produce NH_4NO_3 (e.g., STELSON and SEINFELD, 1982). To a much lesser extent, NH_3 can

undergo gas-phase degradation. Kohlmann and Poppe (1999) considered the 27 reactions known to be involved in NH_3 degradation and reported that NH_3 oxidation was a source of NO_x under high NO_x conditions (>1ppb) and a sink under low NO_x conditions (<1ppb). Small amounts of tropospheric NO_x are also the result of reactive nitrogen compounds being transported from the stratosphere.

2.1.2. Tropospheric NO_y Transformations

Atmospheric NO_x oxidation products, termed NO_y, include HNO_3, nitrous acid (HONO), nitrate radical (NO_3), dinitrogen pentoxide (N_2O_5), peroxynitric acid ($HNO_{4)}$), aerosol NO_3^- of various sizes, peroxyacetyl nitrate "PAN" ($RC(O)OONO_2$), alkyl nitrate ($RONO_2$), and peroxyalkyl nitrate ($ROONO_2$), where R represents an organic group. The chemical transformations involving NO_y are highly complex. In particular, transformations to organic nitrates are not straightforward (ATHERTON and PENNER, 1988; 1990). The explanation provided here is simplified to include only the processes that dominate NO_y chemistry, according to current understanding (e.g., SEINFELD and PANDIS, 1998).

Daytime NO_y chemistry is strongly affected by photolysis. Within a few minutes, NO_x introduced to the troposphere photochemically equilibrates. Nitric oxide quickly reacts with ozone, O_3, to produce NO_2 by

$$NO + O_3 \rightarrow NO_2 + O_2. \qquad (6)$$

Then, nitrogen dioxide photolyzes to produce ground state atomic oxygen, $O(^3P)$, by

$$NO_2 + h\nu\ (\lambda < 434nm) \rightarrow NO + O(^3P), \qquad (7)$$

and $O(^3P)$ reacts with O_2 and a third molecule required to absorb energy, called a moderator, M, to regenerate O_3 by

$$O_2 + O(^3P) + M \rightarrow O_3 + M, \qquad (8)$$

and the NO_x cycle (reactions 6-8) continues. Cycling between NO and NO_2 also occurs, to a lesser extent, via the reaction of NO and $O(^3P)$ to form NO_2 by

$$NO + O(^3P) + M \rightarrow NO_2 + M, \qquad (9)$$

and the reaction of NO_2 and $O(^3P)$ to produce NO and O_2 by

$$NO_2 + O(^3P) \rightarrow NO + O_2. \qquad (10)$$

Other atmospheric compounds relevant to the NO_x cycle are the result of the photolysis of ozone, which produces $O(^3P)$ or excited state atomic oxygen, $O(^1D)$ by

$$O_3 + h\nu\ (\lambda < 310nm) \rightarrow O(^3P) + O_2, \text{ or} \qquad (11a)$$

$$O_3 + h\nu\ (\lambda < 463nm) \rightarrow O(^1D) + O_2. \qquad (11b)$$

Once formed, $O(^1D)$ generally collides with another atmospheric compound (most often N_2 or O_2) and transfers its excess energy to the other compound to form $O(^3P)$ by

$$O(^1D) + M \rightarrow O(^3P) + M. \qquad (12)$$

Since $O(^3P)$ quickly reacts with O_2 and M to regenerate ozone (reaction 8), reactions 11a and 11b generally have no net effect. However, a significant exception occurs when $O(^1D)$ reacts with water vapor to produce the highly reactive hydroxyl radical, OH, by

$$O(^1D) + H_2O \rightarrow 2OH. \qquad (13)$$

Once formed, OH reacts with volatile organic compounds (VOCs) to produce the peroxy radical (HO_2) and a number of organic peroxy radicals (RO_x, where again

R represents an organic group). The oxidation of carbon monoxide, CO, provides an example of HO_2 formation. Carbon monoxide reacts with OH to form CO_2 and atomic hydrogen by

$$CO + OH \rightarrow CO_2 + H. \quad (14)$$

Atomic oxygen reacts with molecular oxygen to produce HO_2 by

$$H + O_2 \rightarrow HO_2, \quad (15)$$

and then HO_2 can subsequently oxidize NO to NO_2 by

$$NO + HO_2 \rightarrow NO_2 + OH. \quad (16)$$

Methane, CH_4, reacts with OH to produce CH_3, the methyl radical by

$$CH_4 + OH \rightarrow CH_3 + H_2O. \quad (17)$$

Methyl radical reacts with molecular oxygen to produce the methyl peroxy radical, an example of an organic peroxy radical, by

$$CH_3 + O_2 \rightarrow CH_3O_2, \quad (18)$$

and then CH_3O_2 can subsequently oxidize NO to NO_2 by

$$NO + CH_3O_2 \rightarrow NO_2 + CH_3O. \quad (19)$$

The general form for reactions involving the oxidation of NO by organic peroxy radicals is

$$NO + RO_x \rightarrow NO_2 + RO_{x-1}. \quad (20)$$

Although more complex VOCs than CO and CH_4 dominate the chemistry of the polluted troposphere, the same rules apply: The oxidation of VOCs generates HO_2 and RO_x, which subsequently oxidize NO to NO_2 according to reactions 16 and 20, and the oxidation of NO by HO_2 regenerates OH.

Considerable cycling between NO and NO_2 occurs until there is a termination reaction, which, during the day, is production of HNO_3 by

$$NO_2 + OH + M \rightarrow HNO_3 + M. \quad (21)$$

In addition, reaction of NO_2 with O_3 produces the nitrate radical, NO_3, by

$$NO_2 + O_3 \rightarrow NO_3 + O_2, \quad (22)$$

and, to a much lesser extent, by

$$NO_2 + O(^3P) + M \rightarrow NO_3 + M. \quad (23)$$

The nitrate radical is irrelevant in daylight chemistry because NO_3 is quickly destroyed by photolysis by

$$NO_3 + h\nu\ (\lambda < 700\ nm) \rightarrow NO + O_2, \text{ or} \quad (24a)$$

$$NO_3 + h\nu\ (\lambda < 580\ nm) \rightarrow NO_2 + O(^3P), \quad (24b)$$

and by reaction with NO by

$$NO_3 + NO \rightarrow 2NO_2. \quad (25)$$

At night, photolysis ceases and a different set of atmospheric processes begins to dominate the NO_x cycle. The presence of appreciable levels of NO_3 provides another pathway for NO_x removal. Nitrate radical reacts with NO_2 and a third molecule to produce dinitrogen pentaoxide, N_2O_5, by

$$NO_2 + NO_3 + M \rightarrow N_2O_5 + M. \quad (26)$$

Although N_2O_5 can decompose by

$$N_2O_5 + M \rightarrow NO_2 + NO_3 + M, \quad (27)$$

the majority of N_2O_5 undergoes heterogeneous reaction with water in aerosols or cloud droplets to produce HNO_3 by

$$N_2O_5 + H_2O_{(s)} \rightarrow 2HNO_3. \quad (28)$$

Other reactions determined to be relevant in nighttime chemistry and HNO_3 production involve reaction of NO_3 with organic molecules (e.g., RUSSELL et al., 1985), such as formaldehyde, HCHO, by

$$NO_3 + HCHO \rightarrow HNO_3 + HO_2 + CO, \quad (29)$$

and organic aldehydes, RCHO, by

$$NO_3 + RCHO \rightarrow HNO_3 + RCO_3. \quad (30)$$

There are seasonal variations in NO_y chemistry. During the summer, the conversion of NO to NO_2 is more rapid because of higher abundances of O_3 relative to NO_x. In addition, increased solar insolation accelerates the rate of $O(^1D)$ production (e.g., reaction 11b). Higher $O(^1D)$ and H_2O concentrations in the summer lead to increased OH production by reaction 13, and elevated OH speeds up termination reaction 21. As a result, daylight chemistry (pathway #1 in Figure 4) dominates HNO_3 production. During the winter, conversion of NO to NO_2 is less efficient due to lower O_3/NO_x, and nighttime chemistry by reactions 26-30 (including pathways #2 and #3 in Figure 4) becomes more important.

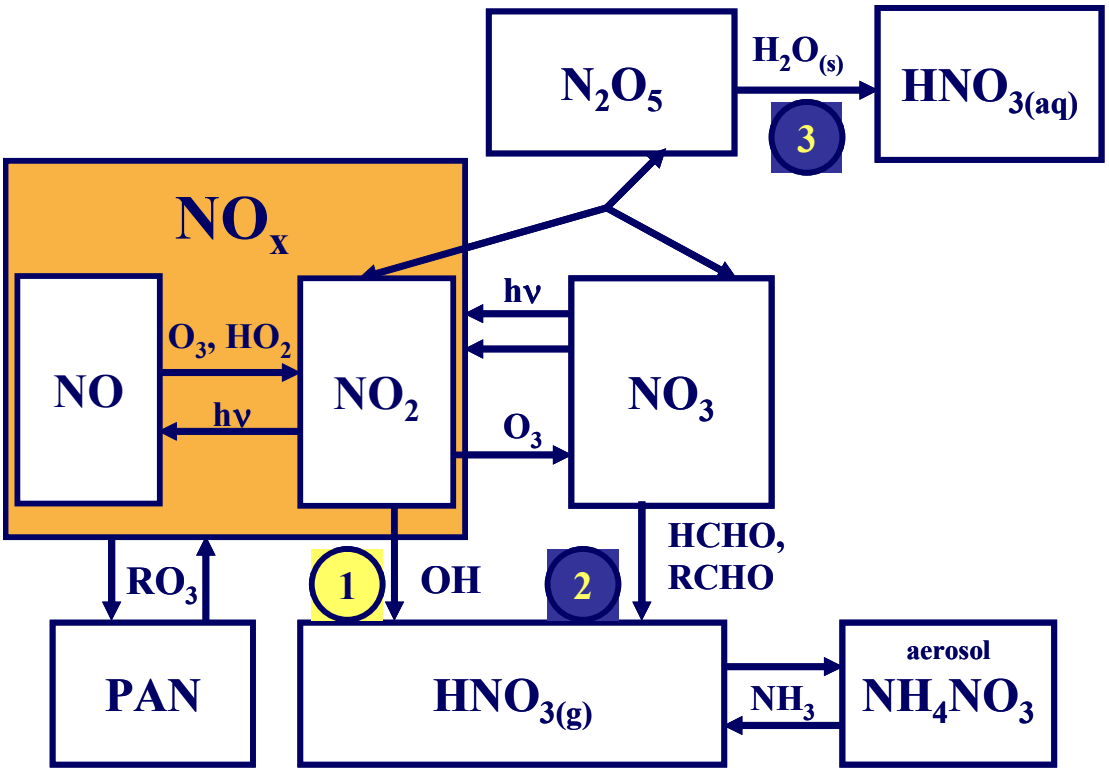

Figure 4: Reaction network of different pathways of atmospheric nitrate formation. The orange box represents the NO_x photo-stationary state, and the white boxes represent pools of N and O in the atmosphere. Arrows between boxes represent individual reactions. Two sided arrows are used when compounds Pathway #1 dominates daytime NO_x chemistry, while Pathways #2 and #3 become more important during nighttime (and winter) chemistry.

2.1.3. Removal of NO_y from the Troposphere

Although the removal of NO_x by chemical transformations occurs on the order of a day, the product HNO_3 typically remains in the atmosphere for days to a week until scavenged by dry or wet deposition (Figure 5). The lifetime of HNO_3 is shorter during wet periods because of more frequent washout of reactive nitrogen compounds. Typically, the lifetime of HNO_3 in the lower troposphere limits long-range transport of reactive nitrogen. The potential for transport increases when NO_x gets vented during storms to the upper troposphere, where transformation of NO_x to HNO_3 and the subsequent removal of HNO_3 occur at slower rates. In areas far from

the location of precursor NO_x production, the photolysis of HNO_3 can regenerate NO_x by

$$HNO_3 + h\nu \rightarrow NO_2 + OH. \qquad (31)$$

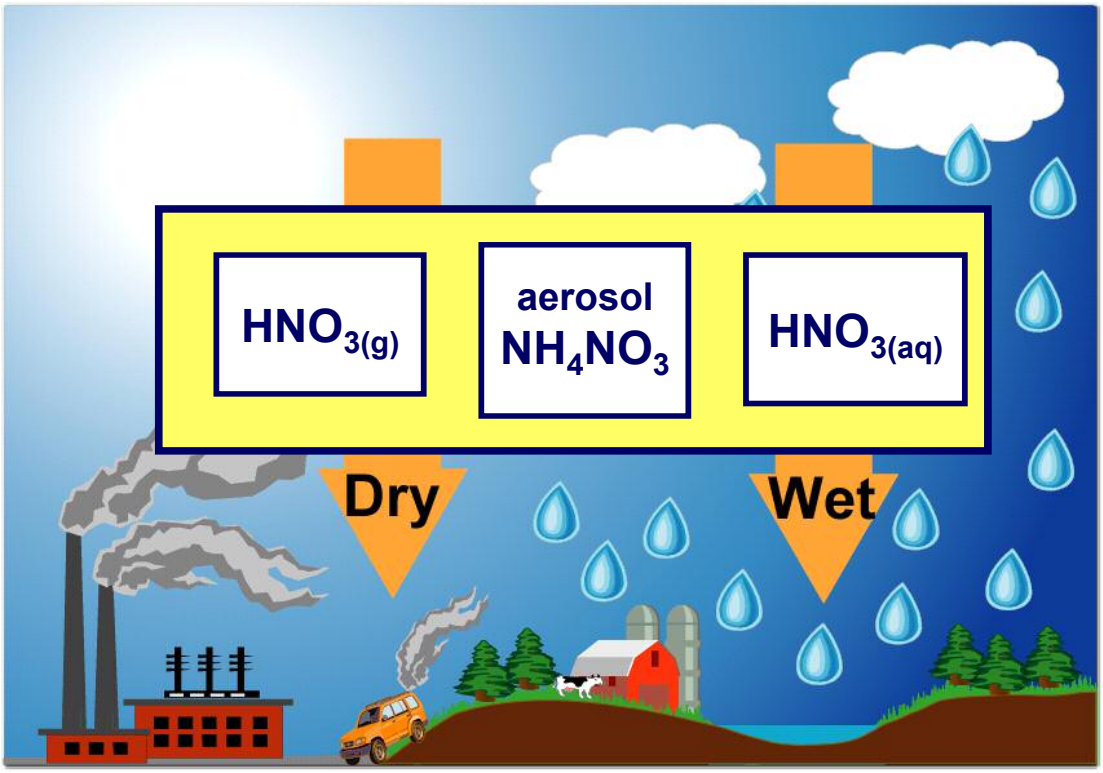

Figure 5: Illustration of the removal of NO_x from the troposphere. Gas phase and aqueous phase nitric acid and aerosol nitrate are removed via dry and wet deposition.

In this sense, HNO_3 serves as a reservoir of NO_x. In addition to HNO_3, there are other important reservoir species, including aerosol NO_3^- and, to a greater extent, organic nitrates. In the polluted troposphere, aerosol NO_3^- exists primarily in the fine-mode (<1μm diameter) as ammonium nitrate aerosol, $NH_4NO_{3(s/aq)}$, which forms when HNO_3 reacts with ammonia by

$$HNO_3 + NH_3 \rightarrow NH_4NO_{3(s/aq)}, \qquad (32)$$

Some $NH_4NO_{3(s)}$ can be transported away from polluted areas. Over the oceans, fine-mode aerosol NO_3^- dissociates by

$$NH_4NO_{3(s/aq)} \rightarrow HNO_3 + NH_3, \qquad (33)$$

and forms coarse-mode sea-salt aerosol NO_3^- (>1μm diameter) by

$$HNO_3 + NaCl \rightarrow NaNO_{3(s)} + HCl, \qquad (34)$$

and conversion to coarse-mode aerosol NO_3^- increases dry and wet deposition rates (SPOKES et al., 2000).

Another class of compounds, organic nitrates, can transport reactive nitrogen even farther from NO_x-generating regions. The most abundant organic nitrate species, peroxyacetyl nitrate, PAN, forms by the reaction of peroxyacetyl radical, $CH_3CO\text{-}O_2$ with NO_2 and a third molecule by

$$CH_3CO\text{-}O_2 + NO_2 + M \rightarrow PAN + M. \qquad (35)$$

Since PAN does not photodissociate in the troposphere or dissolve readily in precipitation, its primary destruction mechanism is thermal decomposition by

$$PAN + heat \rightarrow CH_3CO\text{-}O_2 + NO_2. \qquad (36)$$

Consequently, the chemical lifetime of PAN is strongly temperature dependent, ranging from approximately 30 minutes at 25°C to eight hours at 0°C to many months in the upper troposphere (SEINFELD and PANDIS, 1998). In polluted areas with high hydrocarbon-to-NO_x ratios, nearly one-fourth of NO_x can be transformed to PAN and other organic nitrates (ATHERTON and PENNER, 1988). While some organic nitrates get dry deposited, appreciable amounts can be transported to remote regions, and chemical transport models have demonstrated the importance of PAN on global NO_y distributions (KASIBHATLA et al., 1993).

In brief, NO_x from various processes enters the troposphere and transforms to HNO_3, aerosol NO_3^-, and organic nitrates. Although small quantities of tropospheric NO_y compounds enter the stratosphere during rare storm events, the vast majority of NO_y ultimately gets deposited to the Earth's surface. Although short chemical lifetimes typically limit transport of NO_x, HNO_3, and aerosol NO_3^- in the lower troposphere, the venting of NO_x to the upper troposphere and the formation of PAN permit the movement of NO_y significant distances from the locations of NO_x introduction prior to being deposited as atmospheric NO_3^-.

2.2. Isotope Fractionation

The various NO_y species introduced in the previous section can be considered pools of nitrogen (N) and oxygen (O), and each pool can be characterized by N and O isotopic compositions. This chapter describes the physical-chemical mechanisms that influence the partitioning of isotopes between pools and introduces isotope terminology. Molecules that differ only in their isotopic compositions, called isotopologues, have different energies associated with atomic motions, such as vibrations, rotations, and translations. From a quantum mechanical perspective, these energies are quantized into distinct levels. Using statistical mechanics, a total partition function, Q, can be derived to quantify the total energy of motion over all energy states, where E_i is the total energy and g_i is the degeneracy of state i, k_B is Boltzmann constant, and T is temperature, by

$$Q = \sum_i g_i e^{\frac{-E_i}{k_B T}} .$$

Exact determinations of Q require solutions of the Schrödinger equation (waves that describe the quantized energy). A molecule's total energy is the sum of its internal energy, E_{int}, and translational energy, E_{tr}. Since the contribution of gravitational forces on a molecule's potential energy is small, E_{int} is mostly the energy associated with the potential for interactions within the molecule. Electronic interactions have the greatest potential energy. There are also minor interactions between nuclei and between electrons and nuclei, which are influenced by the masses of the nuclei and the electrons. When all the potentials for interactions are considered, the equation for E_{int} cannot be solved for most molecules. The Born-Oppenheimer (B-O) approximation considers motions of nuclei, relative to electrons, to be insignificant and allows for the cancellation of some energy terms. As a result of the B-O approximation, the potential energy surfaces for isotopologues are treated as identical and the principal differences for E_{int}'s arise primarily because of how the masses of the nuclei affect the energies associated with stretching, compressing, and rotating atoms relative to their optimal distance. A molecule's E_{tr} is the energy associated with the movement of the center of the mass in three-dimensional space and can be determined by solving the translational Schrödinger equation. Isotopologues have different E_{tr}'s due to the effect of mass on molecular velocities. Compared to the light isotopologue, heavy isotopologues have lower E_{int}'s and E_{tr}'s, and thus Q's.

Energy differences between isotopologues result in isotope fractionation, the general term used to describe the processes that cause isotopes to selectively partition into certain pools and are described using partition function ratios. Vibrational

quanta are significantly larger than rotational or translational quanta. Vibrations have characteristic frequencies that depend on the masses of the atoms and the forces, such as bonds, opposing atomic motion. Every substance has a characteristic vibrational energy in their lowest energy state, or zero point energy (ZPE). When a heavier isotope replaces a lighter isotope, the ZPE lowers. When substances undergo isotope exchange, heavier isotopes tend to concentrate in the substance that experiences the greatest shift in ZPE upon substitution. Fractionation processes can be categorized as equilibrium or kinetic. Equilibrium isotope effects (EIEs) occur when there is complete isotope exchange between pools, and these effects are mainly driven by changes in E_{int} upon isotopic substitution. Kinetic isotope effects (KIEs) are generally associated with one-directional processes and involve incomplete isotope exchange. Kinetic isotope effects can be driven by differences in the E_{tr} of isotopologues or by specific features of the reaction paths (e.g., the transition state).

2.2.1. Equilibrium isotope effects

Most observed EIEs can be adequately explained by shifts in zero-point vibrational energies that accompany isotope exchange, although 2nd-order effects may involve non-vibrational, non-mass-dependent mechanisms (BIGELEISEN, 1998). When a heavier isotope replaces a lighter isotope, the energy shift can be represented as the ratio of the partition functions of the heavy and light isotopologues, Q^* and Q. (Asterisks signify terms for heavy isotopologues.) Urey (1947) and Bigeleisen and Mayer (1947) described ways to calculate partition function ratios (Q^*/Q)'s from vibrational frequencies, and their simplifying assumptions allow the calculation of

equilibrium constants for isotope exchange reactions. Several reviews of their approaches were useful in preparing this summary (CHACKO et al., 2001; MATSUHISA et al., 1978; RICHET et al., 1977; SCHAUBLE, 2004; YOUNG et al., 2002).

To a reasonable approximation, (Q^*/Q)'s can be calculated from taking the product of the component partition function ratios for vibrational (vib), translational (tr), and rotational (rot) energies.

$$(Q^*/Q) = (Q^*/Q)_{vib}\ (Q^*/Q)_{rot}\ (Q^*/Q)_{tr}\ .$$

Other terms can be included to account for anharmonic vibrations, $Q^*/Q)_{anh}$, rotational-vibrational interactions, $(Q^*/Q)_{rot\text{-}vib}$, and rotational stretching energies $(Q^*/Q)_{rot\text{-}str}$ (RICHET et al., 1977). Theoretically, there should also be a partition function $_{included}$ for electronic energy associated with excited energy states, $(Q^*/Q)_e$, but the general practice is to assume this energy is negligible.

Determinations of $(Q^*/Q)_{vib}$ require inputs of vibrational frequencies for the isotopologues. For relatively common isotopic compounds, vibrational frequencies are often obtained using spectroscopy, which involves the measurement of the differences between ground state and excited state energies or two excited state energies. Zero-point vibrational frequencies are then calculated from the spectroscopic data using equations that describe the shape of molecules' potential energy surfaces (HERZBERG, 1950). For rarer isotopic compounds, vibrational frequencies are typically calculated from the frequencies of the common forms. Other techniques involve the use of empirical force-field and *ab initio* quantum-mechanical force-field models (see SCHAUBLE, 2004 for a review).

Exact equations used to calculate $(Q^*/Q)_{vib}$ and $(Q^*/Q)_{rot}$, and, if included, $(Q^*/Q)_{anh}$, $(Q^*/Q)_{rot\text{-}vib}$, and $(Q^*/Q)_{rot\text{-}str}$ depend on the expression used for molecules' PE surfaces. Although there are several parameters that influence Q_{tr}, all of the terms cancel in the calculation of $(Q^*/Q)_{tr}$ except the mass term, where M^* and M are the molecular masses of the molecules with heavy and light isotopic compositions, respectively. The expression commonly referred to as the "classical" part of the total partition function is

$$(Q^*/Q)_{tr} = \left(\frac{M^*}{M}\right)^{\frac{3}{2}}.$$

Molecules can also be characterized by a reduced partition function, *f*, which excludes the "classical" term. Where r is the number of atoms being exchanged, *f* is determined by

$$f = (Q^*/Q)\left(\frac{M}{M^*}\right)^{\frac{3r}{2}}.$$

Closely related to *f*'s are β-factors, which have been tabulated for many compounds (RICHET et al., 1977) and are calculated by

$$\beta = f^{\frac{1}{r}}.$$

For isotope exchange reactions, (Q^*/Q)'s and β-factors can be used to predict the equilibrium partitioning of isotopes between compounds. When two substances IX and IY exchange the two isotopes I^* (heavy) and I (light) and a and b are stoichiometric coefficients, the isotope exchange reaction is given by

$$aIX + bI^*Y \Leftrightarrow aI^*X + bIY.$$

The equilibrium constant, K_{eq}, can be written in terms of the Q's of the products over the reactants and in terms of the (Q^*/Q)'s as

$$K_{eq} = \frac{(Q_{I*X})^a (Q_{IY})^b}{(Q_{IX})^a (Q_{I*Y})^b} = \frac{(Q^*/Q)_{IX}^a}{(Q^*/Q)_{IY}^b}.$$

As a result of equilibrium isotope exchange, the compounds IX and IY will have different isotope ratios, which can be expressed as *R*'s or in δ notation. The equilibrium fractionation factor α_{eq} can be determined experimentally by measuring the isotope ratios of the two compounds at equilibrium, or theoretically. The equations used to calculate α_{eq} from measured isotope ratios and theoretical β-factors are

$$\alpha_{EIE(IX-IY)} = \frac{R_{IX}}{R_{IY}} or \frac{\delta_{IX}+1000}{\delta_{IY}+1000} = \frac{\beta_{IX}}{\beta_{IY}}.$$

When a and b are unity, K_{eq} is equivalent to α_{eq}. There are small differences between K_{eq} and α_{eq} for reactions when more than one atom is exchanged. Temperature (T) largely affects the magnitude of α_{eq}, but the relationship between T and α_{eq} is not simple (CRISS, 1991). In general, α_{eq} decreases as temperature increases, but, for most substances, the T dependence of α_{eq} cannot be described with a single equation over a broad range of T's. For particular T ranges, $\ln\alpha_{eq}$ varies continuously from a function of T^{-1} (at low T) to T^{-2} (at high T). At infinite high temperatures, α_{eq} is unity.

2.2.2. Kinetic isotope effects

Compared to equilibrium isotope exchange, kinetic isotope effects (KIEs) result from a wider range of mechanisms, many of which have not been fully described in the isotope literature. KIE's are often described using ratios of the reaction rate constants (k's). The ratio of the k's of light and heavy isotopologues determines the kinetic isotope fractionation factor, α_{kin}, by

$$\alpha_{kin} = \frac{k}{k*}.$$

Isotopologues have different reaction rate constants (k's) due to the effect of molecular masses on translational energies (E_{tr}'s). Whereas the effect of atomic masses on internal energy (E_{int}) is a purely quantum mechanical phenomena, the effect of molecular masses on E_{tr} can also be explained using classical mechanics. The quantum mechanical parameter, E_{tr}, in the translational Schrödinger equation is derived from the classical expression for average translational kinetic energy (KE). In the classical description, KE relates to temperature (T) by the Boltzmann constant (k_B) and is a function of molecular mass (M) and average translational velocity (v) by

$$KE = \frac{3}{2} k_B T = \frac{1}{2} \mathrm{M} \mathrm{v}^2.$$

At a given temperature, the relationship between the M's and v's of two isotopologues is

$$\frac{v*^2}{v^2} = \frac{\mathrm{M}}{\mathrm{M}*}.$$

According to collision theory, higher molecular or translational velocities translate to higher collision frequencies and faster reaction rates. As a result, light

isotopologues tend to have higher reaction rate constants than heavy isotopologues. KIEs occur when there is incomplete isotope exchange during non-reversible reactions, such as dissociation, and reactions in which the reaction products move away from the starting pool, such as evaporation or diffusion.

Fractionations associated with dissociation have been explained by a *transition state* theory (BIGELEISEN, 1949; BIGELEISEN and WOLFSBERG, 1958). The rates of chemical reactions often depend on single "rate-limiting" or "rate-determining" steps, which only occur when a molecule possesses enough energy to achieve an activated complex. In this transition state, the distance between atoms reaches a maximum and the bond can break to permit the formation of products. When a substance becomes activated, the activated complex can either be deactivated or dissociated. The probability of a molecule exceeding the energy barrier, or *activation energy*, can be determined using statistical mechanics by evaluating the (Q^*/Q)'s of the reactants and the activated complexes of the isotopologues. The reaction rate constants for dissociation can also be calculated using a quantum mechanical model, such as the Rice-Ramsperger-Kassel-Marcus (RRKM) theory (MARCUS, 1952; 1965). Although the light isotopologue reacts faster than heavy isotopologues in most cases, there are exceptions that may be related to a phenomenon called the "tunnel effect," in which molecules tunnel through the energy barrier rather than surpassing it (BIGELEISEN, 1949).

2.2.3. Fractionation networks

Fractionations associated with networks, such as those involving geochemical, biological, or atmospheric processes, have been described by some workers as "kinetic." These networks can include both equilibrium isotope effects and kinetic isotope effects, and the fractionation associated with them can produce net isotope effects that reflect the total processing of a material through the network (e.g. (HAYES, 2001). Every reaction has an intrinsic fractionation factor (α_{eq} or α_{kin}). An intrinsic isotope effect, $\varepsilon_{intrinsic}$, can be calculated by

$$\begin{aligned}\varepsilon_{\text{intrinsic}} &= \left(\alpha_{\text{intrinsic}} - 1\right) \times 1000‰ \\ &\cong \ln \alpha_{\text{intrinsic}} \times 1000‰\end{aligned}$$

The isotopic compositions of different pools in nature reflect the various reactions that the molecules in the pools undergo. The net isotope effect, ε_{net} can be defined as

$$\begin{aligned}\varepsilon_{net} &= \left(\alpha_{net} - 1\right) \times 1000‰ \\ &\cong \ln \alpha_{net} \times 1000‰\end{aligned}$$

In applying this approach to atmospheric nitrogen chemistry, there are three ways that isotope fractionation affects the isotopic composition of atmospheric N and O pools: source effects, sink effects, and isotope exchange between different pools (BRENNINKMEIJER et al., 2003; KAYE, 1987; MAUERSBERGER et al., 2003; THIEMENS, 1999; WESTON, 1999) *Source effects* refer to the phenomenon of gases with distinctive isotopic compositions being introduced to the atmospheric from various sources. *Sink effects* include the wide range of mechanisms that affect isotopic compositions during removal reactions, such as chemical transformations, phase changes, and photolysis.

2.2.4. Non-mass dependent isotope effects

Although the processes described thus far occur due to a wide range of mechanisms, the fractionations are driven primarily by the influence of mass on the properties of isotopologues. There are several known examples of non-mass parameters influencing fractionation processes. There are 2nd-order isotope effects associated with shifts in nuclear shape and size upon isotopic substitution (BIGELEISEN, 1998). Nuclear field shifts affect electronic partition function ratios $(Q^*/Q)_e$, which are not considered in the approaches of Urey (1947) and Bigeleisen and Mayer (1947). Although these effects could make a minor effect on equilibrium isotope effects for heavy isotope systems, such as uranium, nuclear field effects are most likely irrelevant in light stable isotope studies.

Another instance of non-mass-dependent (NMD) isotope effects is associated with the effects of nuclear spin on certain chemical reaction rates (TURRO, 1983). Spin refers to an intrinsic property of charged particles that possess magnetic moments. Whereas all electrons possess spin, only odd-mass nuclei, such as ^{13}C and ^{17}O, have spin. During certain reactions involving radicals, the spins of two unpaired electrons, or radical pairs, can orient so that the spins cancel (singlet state) or add to unity (triplet state). Hyperfine interactions between the magnetic moments of electrons and those of odd-mass nuclei can cause changes in nuclear and electron spin that affect the rates of intersystem crossings between the singlet and triplet states. Since certain "self-reactions" only occur when radical pairs are in the singlet state, occurrences of intersystem crossings ultimately affect reaction rates and lead to

magnetic kinetic isotope effects. These effects are very small and are limited to reactions that occur in confined spaces over sufficient time-scales, including certain aqueous-phase photochemical reactions.

Non-mass dependent isotopic compositions also occur in meteorites and meteoritic material (CLAYTON et al., 1973; HULSTON and THODE, 1965). The parameter "Cap Delta 17," $\Delta^{17}O$, was defined as the deviation of a measured $\delta^{17}O$ value from the $\delta^{17}O$ value predicted on the basis of a mass-dependent reference array (MDRA). The slope of the MDRA is the three-isotope coefficient, θ. Matsuihisa and others (1978) defined the slope of the MDRA, "three-isotope coefficient," θ, for the oxygen isotope system as

$$\theta = \frac{\ln \alpha_{(^{17}O/^{16}O)}}{\ln \alpha_{(^{18}O/^{16}O)}} \approx \frac{\mathrm{m}(^{17}O) - \mathrm{m}(^{16}O)}{\mathrm{m}(^{18}O) - \mathrm{m}(^{16}O)}$$

Early definitions used the linear approximation of the MDRA of

$$\delta^{17}O = \theta \times \delta^{18}O,$$

and defined $\Delta^{17}O$ as

$$\Delta^{17}O = \delta^{17}O - \theta \times \delta^{18}O.$$

More recent studies have defined the MDRA as

$$\delta^{17}O = ((1 + \delta^{18}O/1000)^{\theta} - 1) \times 1000,$$

and defined $\Delta^{17}O$ as

$$\Delta^{17}O = \delta^{17}O - ((1 + \delta^{18}O/1000)^{\theta} - 1) \times 1000.$$

Early hypotheses assumed that chemical processes could not produce large NMD anomalies and suggested that the "strange" oxygen isotopic compositions observed in meteorites resulted from nuclear processes involving the production of

isotopes. However, the assumption that ruled out chemical effects was invalidated by the laboratory experiments of Heidenreich and Theimens (1983), in which O_3 generated by electrical discharge exhibited large NMD isotopic compositions. Since their discovery, there has been considerable work dedicated to continuing laboratory experiments, identifying other terrestrial and extraterrestrial compounds with anomalies, understanding the nature of NMD effects in ozone and other gas-phase compounds, and revisiting questions on the origin of meteoritic NMD compositions (BRENNINKMEIJER et al., 2003; THIEMENS, 1999; THIEMENS et al., 2001; WESTON, 1999).

More detailed investigations on the reactions that generate and destroy O_3 and other potential reactions with NMD effects followed the electrical discharge experiments of Heidenreich and Theimens (1983). Other reactions involving O_3 were shown to exhibit unconventional isotope behavior, including O_3 production via O_2 photolysis (MORTON et al., 1990; THIEMENS and JACKSON, 1987; 1988), O_3 destruction by photolysis (BHATTACHARYA and THIEMENS, 1988; VALENTINI, 1987; WEN and THIEMENS, 1991), and O_3 destruction by thermal decomposition (BHATTACHARYA and THIEMENS, 1988; WEN and THIEMENS, 1991). Other laboratory experiments investigated potential effects associated with reactions of oxygen-bearing compounds other than O_3, including the production of CO_2 by reaction of CO+O(^{3}P) (BHATTACHARYA and THIEMENS, 1989), reaction of CO+OH (ROCKMANN et al., 1998), CO_2 destruction by photolysis (BHATTACHARYA et al., 2000), isotope exchange between CO_2 and O(^{1}D) (JOHNSTON et al., 2000; WEN and THIEMENS,

1993), formation of H_2O_2 by reaction of H with O_2 (SAVARINO and THIEMENS, 1999), and the formation of sulfate (SAVARINO et al., 2000).

Other investigators searched for natural compounds with "strange" oxygen isotopic compositions. Whereas most terrestrial compounds have $\Delta^{17}O$ values of zero, many atmospheric trace gases exhibit positive $\Delta^{17}O$ signatures. The greatest anomalies in Earth's atmosphere are observed in tropospheric O_3 (JOHNSTON and THIEMENS, 1997; KRANKOWSKY et al., 1995) and stratospheric O_3 (KRANKOWSKY et al., 2000; MAUERSBERGER et al., 2001). Other compounds with NMD oxygen isotope signatures include CO (ROCKMANN et al., 1998), stratospheric CO_2 (ALEXANDER et al., 2001; ALEXANDER et al., 2002; BOERING et al., 2004; LAMMERZAHL et al., 2002; THIEMENS et al., 1991; THIEMENS et al., 1995), N_2O (KAISER et al., 2004; ROCKMANN et al., 2001), sulfate (LEE et al., 2001), and nitrate (MICHALSKI et al., 2003). Anomalous isotopic compositions are also transferred to the Earth's surface via deposition of these atmospheric compounds. Oxygen isotope measurements of nitrate in desert deposits (MICHALSKI et al., 2003), perchlorate in desert soils (BAO and GU, 2004), and sulfate in numerous deposits (BAO et al., 2000), such as desert varnishes (BAO et al., 2001), Antarctic dry-valley soils (BAO et al., 2000), ash beds (BAO et al., 2003), and desert gypcretes (BAO et al., 2001), reveal non-zero $\Delta^{17}O$.

After two decades of investigations, the physical-chemical origin of $\Delta^{17}O$ in O_3 and other trace atmospheric compounds remains a topic of considerable debate. The reaction identified as being primarily responsible for the O_3 anomaly is the recombination reaction between O_2, $O(^3P)$, and a third body, M. Characteristics of ozone metastable states affect their lifetimes, which affect ozone formation rates.

Some hypotheses ascribe the NMD compositions of O_3 partially to symmetry-induced kinetic isotope effects, SIKIEs (GAO and MARCUS, 2001; GAO and MARCUS, 2002; HATHORN and MARCUS, 1999; HATHORN and MARCUS, 2000). Described simply, the symmetry of activated complexes that form when $O(^3P)$ collides with O_2 can affect the rates of O_3 formation. Others have pointed to non-symmetry mechanisms that influence the lifetimes of metastable states (JANSSEN et al., 1999; MAUERSBERGER et al., 1993). There may also be dependency on the third-body that reacts with the activated complex to stabilize O_3 (GUENTHER et al., 2000). Recently, Babikov and colleagues devised a quantum mechanical model, which incorporates several non-statistical parameters and calculates the positions and lifetimes of different metastable states (BABIKOV et al., 2003; BABIKOV et al., 2003; BABIKOV et al., 2003).

There are also several explanations associated with NMD effects observed during photodissociation. One of the proposed mechanisms stems from the finding that the photodissociation of $^{12}CO_2$ and $^{13}CO_2$ by 185nm radiation to form O and CO with different oxygen isotope effects (BHATTACHARYA et al., 2000). Occurrences of intersections between the potential energy surfaces of pre-dissociative and dissociative states affect the rates of reactions. Another mechanism, called "self-shielding," occurs as a result of isotopologues having slightly different absorption spectra due to shifts in the vibrational frequencies upon isotopic substitution. Photodissociation of the more abundant isotopologue causes saturation, thus shielding the remaining molecules of the same absorption spectra from radiation. As a result, a zone forms where the less abundant isotopologue(s) increase their relative

significance. "Self-shielding" has been recently invoked to explain the anomalies observed in meteorites (CLAYTON, 2002; LYONS and YOUNG, 2005).

Atmospheric nitrate and sulfate have positive $\Delta^{17}O$ values due to the transfer of oxygen atoms from ozone during the oxidation of NO_x and SO_2, respectively (LYONS, 2001). Since the oxygen atoms in nitrate formed by non-atmospheric processes are typically derived from H_2O and/or atmospheric O_2, which have $\Delta^{17}O$ values close to zero, nitrate that exhibits NMD isotopic compositions can be traced back to an atmospheric origin.

3. Previous investigations

3.1. Techniques used to analyze nitrate isotopes

Since the mass spectrometric improvements of McKinney and others (1950), numerous techniques have been developed to analyze nitrate isotope ratios. The first technique used to analyze the $\delta^{15}N$ of nitrate involves collecting NO_3^- on anion exchange resin, eluting NO_3^- from the resin, using an alloy to reduce NO_3^- to NH_3, distilling the NH_3 into an acidic solution, and reacting the distillate with NaBrO under vacuum conditions to produce N_2 (HOERING, 1955 and references therein). The gas then passes over heated copper and copper oxide and through a liquid nitrogen trap to remove CO, which has an interfering mass spectrum (HOERING, 1955). The purified N_2 is then introduced to a mass spectrometer and the relative intensities of ions with mass to charge ratios (m/z) of 28 and 29 are compared to a working N_2 standard.

Combustion techniques are also used to produce N_2 for isotope analyses. There are a suite of "off-line" methods in which nitrate salts (often KNO_3) are combusted in sealed tubes to produce N_2, which gets purified and concentrated prior to analyses (KENDALL and GRIM, 1990 and references therein). "On-line" techniques include thermally decomposing nitrate salts in a thermal-conversion elemental analyzer (TC/EA) or elemental analyzer (EA) (STICKROD and MARSHALL, 2000) to generate and purify N_2 for continuous flow isotope ratio mass spectrometric (CF-IRMS) analyses.

Other methods include reducing NO_3^- to NH_3 using Devarda's alloy, distilling the NH_3 into H_2SO_4, adding sodium tetraphenylborate, $(C_6H_5)_4BNa$ to the distillate

and combusting the precipitated $(C_6H_5)_4BNH_4$ in an EA to produce N_2 for CF-IRMS (SAKATA, 2001). Recent analytical developments include the denitrifier method in which denitrifying bacteria convert NO_3^- to N_2O for CF-IRMS analyses of m/z 44, 45, and 46 (SIGMAN et al., 2001).

The first method developed to analyze the $\delta^{18}O$ of nitrate was derived from the technique developed by Rittenberg and Ponticorvo (1956) to measure oxygen isotope ratios of organic compounds. The modification of this technique reported by Amberger and Schmidt (1987) involves the combustion of $KNO_{3(s)}$ with $Hg(CN)_2$ at 550°C to produce CO_2 for isotopic analyses. The $\delta^{18}O$ of NO_3^- is calculated from the relative intensities of singly charged CO_2^+ ions with m/z 44 ($^{12}C^{16}O^{16}O$), 45 ($^{12}C^{16}O^{17}O$, $^{13}C^{16}O^{16}O$), and 46 ($^{12}C^{16}O^{18}O$, $^{13}O^{16}O^{17}O$, and $^{12}C^{17}O^{17}O$) relative to a working CO_2 standard. Other combustion techniques used to generate CO_2 for isotope analysis include sealed-tube thermal decomposition of $AgNO_3$ with AgCN (WASSENAAR, 1995) or graphite at 850°C (SILVA et al., 2000) and reaction of KNO_3 with guanidine hydrochloride ($NH_2C(NH)NH_2 \cdot HCl$) at 590°C (BRAUER and STRAUCH, 2000). Révész and coworkers (1997) developed a method to determine both $\delta^{15}N$ and $\delta^{18}O$ that involved heating KNO_3 with catalyzed graphite in an evacuated sealed tube at 520°C for 24 hours to produce CO_2, K_2CO_3, and N_2. The fraction of oxygen as CO_2 and K_2CO_3 and the fractionation factor between CO_2 and K_2CO_3 were constrained, and the $\delta^{18}O$ of the nitrate could be determined from the CO_2 mass-spectrometric measurements.

"On-line" techniques involve using a TC/EA to produce and purify CO for CF-IRMS analyses (KORNEXL et al., 1999). The $\delta^{18}O$ of NO_3^- is calculated from the

intensities of singly charged CO^+ ions with m/z 28 ($^{12}C^{16}O$), 29 ($^{13}C^{16}O$, $^{12}C^{17}O$), and 30 ($^{13}C^{17}O$, $^{12}O^{18}O$) relative to a CO reference gas. The denitrifier method can also be used to measure the $\delta^{18}O$ of NO_3^- (CASCIOTTI et al., 2002).

There have been significant standardization issues associated measurements of the $\delta^{18}O$ of NO_3^- over the past decade (BOHLKE et al., 2003; KORNEXL et al., 1999). Until 2003, there were two internationally distributed reference materials IAEA-N3 (also known as RM8549 (NIST) and IAEA-NO-3) and USGS-32 (also known as RM8558 (NIST)), both of which have $\delta^{18}O$ values close to atmospheric O_2. As shown by Révész and Böhlke (2002), the absence of a reference with a $\delta^{18}O$ value distinct from the $\delta^{18}O$ of atmospheric O_2 prevented researchers from addressing blanks and scale-compression issues, leading to inaccurate determinations of $\delta^{18}O$. Three KNO_3 samples were analyzed by three "off-line combustion" techniques (AMBERGER and SCHMIDT, 1987; REVESZ et al., 1997; SILVA et al., 2000) and one "on-line combustion" technique (KORNEXL et al., 1999). One sample had a $\delta^{18}O$ value near the "mid-point" of the $\delta^{18}O$ scale (approximately +21 to +25‰), while the other two samples had $\delta^{18}O$ values significantly higher and lower than the "mid-point." All four techniques yielded similar results for the KNO_3 sample with $\delta^{18}O$ near the "mid-point." However, for the KNO_3 samples with significantly lower and higher $\delta^{18}O$ values, the results for the "off-line combustion" techniques were closer to the mid-point than the values obtained by "on-line combustion." Révész and Böhlke (2002) reported that $\delta^{18}O$ scale for the "off-line combustion" techniques was compressed to 0.33 to 0.68 times the scale of "on-line combustion" technique and attributed the scale contraction to oxygen exchange between CO_2 and the glass tubes

in "off-line combustion" techniques. For the high $\delta^{18}O$ sample, which had a measured value of 54.2‰ using "on-line combustion" (assuming $\delta^{18}O$ of IAEA-NO3 = +22.7‰), the differences between the measured values for the "off-line combustion" techniques were as large as 17‰.

Published $\delta^{18}O$ values for IAEA-NO-3 include +22.7‰ (REVESZ et al., 1997), +22.9‰ (SILVA et al., 2000), +23.6‰ (MICHALSKI et al., 2002), +25.3‰ (KORNEXL et al., 1999) and +25.6‰ (BOHLKE et al., 2003). These values differ by more than reported analytical precision and are likely due to variable contraction of the $\delta^{18}O$ scale in different preparation methods (e.g., REVESZ and BOHLKE, 2002). Nitrate reference materials with widely varying $\delta^{18}O$ have only recently become available (BOHLKE et al., 2003). USGS-34 (KNO_3) was produced by the equilibration of HNO_3 with ^{18}O-depleted water, and preliminary analyses yield $\delta^{18}O$ and $\delta^{17}O$ values of -27.9‰ and -14.8‰, respectively (BOHLKE et al., 2003). USGS-35 ($NaNO_3$) was obtained by purification of nitrate ores deposits from the Atacama Desert, and preliminary results for $\delta^{18}O$ and $\delta^{17}O$ are +57.5‰ and +51.5‰, respectively (BOHLKE et al., 2003).

3.2. Stable isotope investigations of atmospheric nitrate

The isotopic composition of atmospheric NO_3^- has been of scientific interest for over half a century. The first wave of studies considered the nitrogen isotopes of precipitation NO_3^- to test and form hypotheses on atmospheric chemistry. The long-standing hypothesis that atmospheric NO_3^- was principally formed from the electrical fixation of atmospheric N_2, was challenged by several investigators, including

Hutchinson (1944; 1954), who pointed out that there was insufficient evidence linking rainwater NO_3^- concentrations to lightning events. Hoering (1957) conducted laboratory experiments on NO_3^- formed by electrical fixation and reported $\delta^{15}N$ values of +1.4‰ for nitrogen fixed between platinum electrodes and -0.5‰ for nitrogen fixed between tungsten electrodes. Hoering (1957) also analyzed NO_3^- from rain collected on the rooftop of the University of Arkansas chemistry building and reported a range of -7.2‰ to +3.4‰. Hoering's data provided evidence that electrical nitrogen fixation was not solely responsible for the production of atmospheric NO_3^-.

Meanwhile, increasing evidence showed that the primary pathway of atmospheric nitrate formation was neither electrical discharge nor the atmospheric oxidation of ammonia (e.g., ROBINSON and ROBBINS, 1970 and references therein). Nearly two decades after the first $\delta^{15}N$ measurements of precipitation NO_3^-, isotope studies on atmospheric NO_3^- resumed (FREYER, 1978; FREYER, 1978; MOORE, 1974; MOORE, 1977; WADA, 1975). The isotopic evidence supported the hypothesis that precipitation NO_3^- was the result of the "washout" of NO_x, which either dissolved directly into droplets or formed HNO_3 or aerosol NO_3^- which subsequently dissolved into rain (HEATON, 1986). Researchers also measured the $\delta^{15}N$ of atmospheric NO_2 (MOORE, 1974; MOORE, 1977), barnyard NO_2 (MOORE, 1977) automobile exhaust NO_2 (FREYER, 1978; HEATON, 1987; HEATON, 1990; MOORE, 1977), coal-fired power plant exhaust NO_2 (HEATON, 1987; 1990), gaseous HNO_3 (FREYER, 1991), cloud-water NO_3^- (GARTEN, 1992), throughfall NO_3^- collected beneath a forest canopy (GARTEN, 1992), and aerosol NO_3^- (FREYER, 1991; MOORE, 1974; MOORE, 1977). Various methods were also used to sample the dry deposited NO_3^- for the purposes of

$\delta^{15}N$ analyses, including accumulation on an inclined Perspex sheet (HEATON, 1987) and an artificial tree (GARTEN, 1996).

The next wave of investigators used stable isotopes to distinguish atmospheric NO_3^- from NO_3^- produced by non-atmospheric processes. Nitrogen isotope ratios alone were used to investigate atmospheric deposition to such ecosystems as coastal waters (FOGEL and PAERL, 1993) and forests (NADELHOFFER and FRY, 1994). Other studies capitalized from the use of nitrogen and oxygen isotope ratios, the "dual-isotope approach." Atmospheric NO_3^- (DURKA et al., 1994; VOERKELIUS, 1990) has significantly higher $\delta^{18}O$ values than NO_3^- produced by non–atmospheric processes, including synthetic production of nitrate fertilizer (AMBERGER and SCHMIDT, 1987; WASSENAAR, 1995) and nitrification in soils (MAYER et al., 2001), manure and ammonium fertilizers (WASSENAAR, 1995), and septic systems (ARAVENA et al., 1993). Oxygen isotope ratios of NO_3^- are established during nitrate formation because NO_3^- does not exchange oxygen atoms with water at pH values typical in nature (BUNTON et al., 1952; HALL and ALEXANDER, 1940; KLEIN and FRIEDEL, 1950; TITANI and GOTO, 1939). Microbial processes can significantly alter isotope ratios and interfere with efforts to discriminate between NO_3^- sources (MARIOTTI et al., 1981). Although denitrification considerably shifts the isotope ratios of residual NO_3^- towards higher $\delta^{15}N$ and $\delta^{18}O$ (ARAVENA and ROBERTSON, 1998; BOTTCHER et al., 1990; MENGIS et al., 1999), reservoirs of NO_3^- affected by denitrification (e.g., groundwater NO_3^-) typically remain distinguishable from atmospheric NO_3^- (CAMPBELL et al., 2002; SCHIFF et al., 2002; SPOELSTRA et al., 2001).

The contribution of atmospheric NO_3^- relative to non-atmospheric NO_3^-, particularly "microbial NO_3^-" formed via nitrification, can be addressed, at least qualitatively, using the "dual-isotope approach" and isotope mass balance determinations (KENDALL, 1998). Such techniques have been applied to NO_3^- studies in rivers (BATTAGLIN et al., 2001; CHANG et al., 2002; MAYER et al., 2002), tributaries in forested watersheds (BURNS and KENDALL, 2002; DURKA et al., 1994; PARDO et al., 2004; SCHIFF et al., 2002; SPOELSTRA et al., 2001; WILLIARD et al., 2001) and alpine watersheds (CAMPBELL et al., 2002), snowmelt (BURNS and KENDALL, 2002; CAMPBELL et al., 2002; KENDALL et al., 1996; OHTE et al., 2004) and desert nitrate deposits (BOHLKE et al., 1997).

A discovery by Michalski and coworkers (2003) advanced the ability to use isotopes to differentiate atmospheric and non-atmospheric NO_3^-. Whereas the $\delta^{17}O$ and $\delta^{18}O$ of nitrate formed by non-atmospheric pathways exhibit the approximate relationship $\delta^{17}O = 0.52 \times \delta^{18}O$, Michalski and others (2003) reported that this relationship was not observed in atmospheric NO_3^-. The $\Delta^{17}O$ ($\equiv \delta^{17}O - 0.52 \times \delta^{18}O$) also showed a strong seasonal pattern that could be modeled according to changes in atmospheric chemistry. The $\Delta^{17}O$ of nitrate has been used to investigate the contribution of atmospheric NO_3^- in arid ecosystems (MICHALSKI et al., 2004) and desert nitrate deposits (MICHALSKI et al., 2004).

Meanwhile, others utilized the isotopic composition of atmospheric NO_3^- to better understand the processes involved in its formation. Several researchers considered the $\delta^{15}N$ of precipitation NO_3^- to assess the relative contribution of different NO_x emitters to regional air masses (HASTINGS et al., 2003; RUSSELL et al.,

1998; XIAO and LIU, 2002). Other recent studies used the $\delta^{15}N$ of size-segregated aerosol NO_3^- (YEATMAN et al., 2001; YEATMAN et al., 2001; YEATMAN et al., 2001), the $\delta^{18}O$ of precipitation NO_3^- (HASTINGS et al., 2003), and the $\delta^{18}O$ and $\Delta^{17}O$ of aerosol NO_3^- (MICHALSKI et al., 2003) to address questions on particular atmospheric processes. Complementary studies include measurements of the $\delta^{15}N$ and $\delta^{18}O$ NO_3^- in snow and ice cores (FREYER et al., 1996; HASTINGS et al., 2004; HEATON et al., 2004) and the $\delta^{15}N$ of atmospheric NO_3^- deposition to ombrotrophic *Sphagnum* mires (BRAGAZZA et al., 2005). Comprehensive studies on the $\delta^{15}N$, $\delta^{18}O$, and $\Delta^{17}O$ of precipitation NO_3^- are in progress (ELLIOTT et al., 2004; HASTINGS et al., 2004), but there is minimal published data on the relationship between these parameters.

3.3. Summary of related findings

3.3.1. $\delta^{15}N$ of NO_x from different processes

There is evidence that different processes produce NO_x with characteristic $\delta^{15}N$ values. Conventional isotope theory (UREY, 1947) predicts that equilibrium isotope effects are small at the high temperatures required to produce thermal NO_x. Freyer (1978) and Heaton (1987), predicted that the $\delta^{15}N$ of NO_x produced from anthropogenic fuel combustion would be close to 0‰ because the $\delta^{15}N$ of atmospheric N_2 was 0‰ (by definition) and the $\delta^{15}N$ of organic nitrogen in coal ranged from -2 to +3‰. The results of Heaton (1990) did not support the hypothesis that anthropogenic NO_x was necessarily close to 0‰. When vehicle engines were operating under heavy load with high NO_x concentrations the $\delta^{15}N$ was -2‰, but

under reduced load (engine at idle), the $\delta^{15}N$ was significantly lower (-7 to -13‰). NO_x from coal-fired power stations, in contrast, exhibited a range of $\delta^{15}N$ values from +6 to +13‰ (HEATON, 1990).

Heaton (1990) explained the results on NO_x from automobile exhaust as reflecting different degrees of chemical equilibrium. Equilibrium would be kinetically limited by the high energy required to break the triple bond of N_2. If $^{14}N^{14}N$ reacted more quickly than $^{15}N^{14}N$, then the $^{15}N/^{14}N$ of NO_x would be lower than atmospheric N_2. In Heaton's experiments, under heavy load, advancing the spark ignition led to higher peak temperatures and longer reaction times, which brought the reaction closer to equilibrium (higher concentrations of NO_x). Under reduced load, there could be a greater kinetic isotope effect leading to more negative $\delta^{15}N$ values. For NO_x produced in coal-fired power stations, Heaton (1990) hypothesized that if ^{14}NO was destroyed faster than ^{15}NO then the remaining NO would be progressively enriched in ^{15}N. In coal fired power plants, the majority of organic nitrogen would be converted to fuel NO_x. While isotope fractionation is unlikely during the production of fuel NO_x, if ^{14}NO converts back to N_2 faster than ^{15}NO, then the NO_x remaining in the exhaust would have higher $\delta^{15}N$ values (HEATON, 1990).

With the exception of data from a nitric acid production plant with highly depleted $\delta^{15}N$ values (HEATON, 1987), there are no published reports of the $\delta^{15}N$ of NO_x produced by non-utility or manufacturing industries. Depending on the fuel sources and temperatures of combustion, the $\delta^{15}N$ of NO_x from industries could represent a combination of thermal and fuel NO_x. There are also no data on the $\delta^{15}N$

of NO_x from biomass burning. Since most would be fuel NO_x, it may be reasonable to assume that similar considerations explained by Heaton (1990) for power plants could apply for the $\delta^{15}N$ of NO_x from biomass burning.

The isotopic composition of microbial NO_x potentially differs from thermal or fuel NO_x. Biological processes typically favor compounds with lower $^{15}N/^{14}N$ (DELWICHE and STEYN, 1970; MARIOTTI et al., 1981), and it has been hypothesized that NO_x released from soils have low $^{15}N/^{14}N$ (HEATON, 1986; MOORE, 1977). Since the $\delta^{15}N$ of NO_x from soils has yet to be directly measured, the idea that NO_x from soils have negative $\delta^{15}N$ remains speculative.

It has been hypothesized that the $\delta^{15}N$ of NO_x produced by lightning reflects the composition of atmospheric N_2. The temperature at the core of a lightning channel can exceed 20,000°C (MALAN, 1963). During lightning, the "freeze-out" of NO_x occurs due to a rapid drop in density (GOLDENBAUM and DICKERSON, 1993) or temperature (STARK et al., 1996). The electrical discharge experiments by Hoering (1957) that were described in section 3.2 produced NO_x with $\delta^{15}N$ values close 0‰. Additional electrical discharge experiments took place in the laboratory of J. Farquhar at the University of Maryland as part of N. Bao's 2003 summer project (unpublished results). The experiments were conducted inside a glass apparatus that was filled with air (N_2, O_2, Ar, CO_2, and other trace gases) and a pool of water. An external device heated the water to produce water vapor inside the apparatus. There were five experiments during which the internal atmosphere was sparked for three, six, 12, 24, and 72 hours. At the end of the experiments, HNO_3 was collected from the apparatus,

converted to $AgNO_3$, and analyzed by mass spectrometry using the techniques described in section 4.3.

The results of these tests showed that the $\delta^{15}N$ of the NO_x varied with the number of hours of sparking (Figure 6). These results are preliminary but are included here to show that there could be a wider range of $\delta^{15}N$ produced by electrical discharge than previously reported. The experiments by Hoering (1957) and members of Farquhar's lab group used corona discharges. It should be noted that arc discharges more accurately simulate lightning (WANG et al., 1998). To date, measurements of the $\delta^{15}N$ of NO_x produced by arc discharge are not present in the literature.

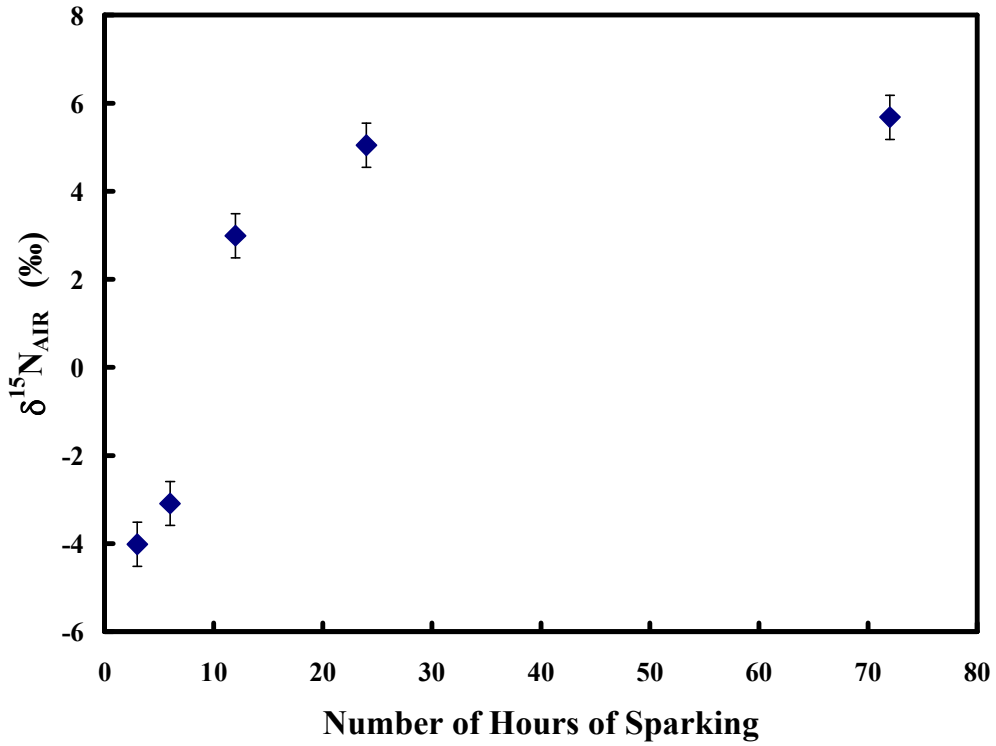

Figure 6: The $\delta^{15}N$ of nitrate scavenged from a glass apparatus used for corona discharge experiments. These tests were completed in the laboratory of J. Farquhar as part of N. Bao's 2003 summer project (unpublished data). Wet chemical treatments were conducted by K. Cooney and mass spectrometric analyses were made in the laboratory of M. Fogel at the Carnegie Institution of Washington.

3.3.2. $\delta^{15}N$ of atmospheric nitrogen compounds

Atmospheric NO_y compounds undergo complex reactions and isotope fractionation occurs during atmospheric processes, including chemical conversions, photolysis, isotope exchange, and phase changes (KAYE, 1987). Analyses of the $\delta^{15}N$ of several NO_y species and NO_3^- in dry and wet deposition show that different pools have measurably different isotope ratios (FREYER, 1991; HEATON, 1987; MOORE, 1974; 1977; YEATMAN et al., 2001; YEATMAN et al., 2001). Moore (1977) showed that $\delta^{15}N$ values for precipitation NO_3^- were significantly lower than aerosol NO_3^- and that "clean air" NO_x in Boulder, Colorado had lower $\delta^{15}N$ values than precipitation NO_3^-. The results of Freyer (1978; 1991) in Jülich, Germany agreed that $\delta^{15}N$ values are lower for precipitation NO_3^- than aerosol NO_3^-. Despite isotope fractionation between the two pools, both aerosol NO_3^- and precipitation NO_3^- in Jülich exhibited seasonal variation with higher $\delta^{15}N$ values in the winter and lower $\delta^{15}N$ values in the summer. Measurements of $HNO_{3(g)}$ in Jülich showed a narrow range of $\delta^{15}N$ values (-2 to -3‰) that was lower than aerosol NO_3^- (FREYER, 1991). Although there were too few samples to be statistically significant, $HNO_{3(g)}$ did not exhibit apparent seasonal variation.

Most measurements of the $\delta^{15}N$ of precipitation NO_3^- obtained by all methods fall in the range of -10 to +5‰ (HEATON et al., 2004). The slightly different ranges observed at individual sites are believed to be actual signatures of precipitation NO_3^- at the sites, not analytical differences. The seasonal variation in the $\delta^{15}N$ of precipitation NO_3^- observed by Freyer and coworkers (1991) in Jülich, Germany has also been identified in other locations, such as Pretoria, South Africa (HEATON,

1987). Explanations for variations in the $\delta^{15}N$ of precipitation NO_3^- include changes in the sources of precursor NO_x (e.g., RUSSELL et al., 1998) and seasonal variations in the NO_x photo-stationary state (FREYER et al., 1993).

3.3.3. $\delta^{18}O$ and $\Delta^{17}O$ of atmospheric nitrate

Precipitation nitrate measured using nitrate salt/decomposition methods exhibited relatively large ranges of $\delta^{18}O$ values. Throughfall precipitation collected beneath a forest canopy in Bavaria, Germany had a range of $\delta^{18}O$ values from +52.5 to +73.4‰ (DURKA et al., 1994; VOERKELIUS, 1990). Throughfall precipitation NO_3^- in Leading Ridge, Pennsylvania and Fernow, West Virginia had a wider range of $\delta^{18}O$ from +17 to +76‰, (WILLIARD et al., 2001). In Sault Ste. Marie, Ontario, Canada, the $\delta^{18}O$ of precipitation NO_3^- ranged from +35 to +59‰ (SPOELSTRA et al., 2001), while in Toronto, Ontario, Canada, the $\delta^{18}O$ of throughfall and precipitation NO_3^- ranged from +30 to +54‰ (SCHIFF et al., 2002). In Loch Vale, Colorado, the $\delta^{18}O$ of precipitation NO_3^- ranged from +40 to +70‰ (CAMPBELL et al., 2002), and in New Hampshire, the $\delta^{18}O$ of precipitation NO_3^- ranged from +47 to +77‰ (PARDO et al., 2004).

Rain NO_3^- from Bermuda analyzed using the denitrifier method yielded a narrower range of $\delta^{18}O$ values between +60.3 and +86.5‰ (HASTINGS et al., 2003). The $\delta^{18}O$ of snow NO_3^- from Summit Greenland analyzed using denitrifying bacteria ranged from +65.2 to 79.6‰ (HASTINGS et al., 2004). Other results obtained using the denitrifier method include precipitation NO_3^- from across the northeastern and mid-Atlantic U.S with $\delta^{18}O$ values ranging from +60 to +90‰ (ELLIOTT et al., 2004)

and precipitation NO_3^- in Princeton, NJ with $\delta^{18}O$ values ranging from +57.2 and +90.5‰ (HASTINGS et al., 2004).

The first reported $\Delta^{17}O$ measurements of atmospheric NO_3^- were on aerosols in La Jolla, CA. Prepared $AgNO_{3(s)}$ was thermally decomposed to O_2 for dual-inlet IRMS of $\Delta^{17}O$ values were calculated using the linear approximation ($\Delta^{17}O = \delta^{17}O - 0.52 \times \delta^{18}O$). The results showed a range of 20-30.8‰ (MICHALSKI et al., 2003). Reports on the $\Delta^{17}O$ of precipitation NO_3^- from Princeton, NJ determined by bacterial conversion of NO_3^- to N_2O followed by the decomposition of N_2O to O_2 similarly gave a range of +19.7 to +30.8‰ (HASTINGS et al., 2004). Both $\delta^{18}O$ and $\Delta^{17}O$ exhibit seasonal variation with the highest values in the winter and the lowest values in the summer. Seasonal variation in oxygen isotope ratios has been previously explained by changes in the primary oxidants involved in converting NO_x to atmospheric NO_3^- (HASTINGS et al., 2003; MICHALSKI et al., 2003)

4. Methods

4.1. Sample collection

Several sample collection strategies were considered and the National Atmospheric Deposition Program (NADP) operation manual (DOSSETT and BOWERSOX, 1999) was consulted prior to establishing the sampling protocol. First, rather than collecting on a daily, weekly, or monthly basis, samples were collected on a precipitation event basis, which permitted the characterization of each sample with storm tracks. Second, since collectors were only placed outside for the duration of the storms, bulk deposition collectors were used in place of sophisticated wet-deposition-only collectors. Third, rather than analyzing a few samples from several different sites, the majority of the samples were collected from a single site. A residential site in Frederick, MD was chosen as the primary collection location, because this site was not close to any point source NO_x emitters (e.g., coal-fired power stations) or high-traffic roads and was a convenient place for the frequent collection of large volumes of sample.

Precipitation samples were collected between February 2002 and May 2004 in Frederick, Maryland. Precipitation samples were collected in poly-ethylene bins (approximately 50cm by 34cm) (Figure 7) that had been washed, rinsed with deionized water and 10% hydrochloric acid, and triply rinsed with ultra-pure deionized water (the typical cleaning sequence used for the entire procedure described here). The material of the bins and the strict cleaning procedure were consistent with the NADP protocol (DOSSETT and BOWERSOX, 1999). Similar bulk

precipitation collection devices have been used for previous investigations of nitrate isotopes (e.g., HOERING, 1957; PAERL, 1985; WILLIARD et al., 2001). Several pre-cleaned collection bins were placed outside immediately before and collected directly after rain, snow, thunderstorm, and mixed precipitation events. In order to recover adequate amounts of nitrate for isotopic analyses, the preferred amount of rainwater or melted snow collected for each storm was 12-20 liters.

Figure 7: Photograph of snow collection in Frederick, Maryland on February 16, 2003 at 8:00pm. The poly-ethylene bins were approximately 34cm by 50cm. During snow storms, poly-ethylene lids were placed in between the bins. Snow on the lids was transferred into the bins at the end of the storms.

Typically, the precipitation samples were immediately transferred to clean high-density poly-ethylene (HDPE) bottles, frozen, and kept in a frozen state until

thawed and filtered prior to ion extraction. On a few occasions, the samples remained unfiltered in the covered collection bins at approximately 20°C for 24-48 hours prior to being frozen. J. Spoelstra and others (2004) recently investigated the effect of storage on nitrate concentrations and the $\delta^{18}O$ and $\delta^{15}N$ of nitrate in bulk precipitation samples. The precipitation samples collected in their experiment were divided into three aliquots. Control aliquots were immediately filtered and frozen, while filtered and unfiltered aliquots were stored in covered but not air tight bottles at 25-28°C for two weeks. The results of their investigation showed that the nitrate concentrations and $\delta^{18}O$ and $\delta^{15}N$ values for the frozen and unfrozen (filtered or unfiltered) aliquots were statistically indistinguishable.

4.2. Collection of meteorological and storm track data

Unedited meteorological data was obtained through the National Oceanic and Atmospheric Administration's (NOAA) National Climate Data Center (NCDC) for Frederick, Maryland (http://www.ncdc.noaa.gov/oa/ncdc.html). The weather station was approximately five miles from the site of precipitation collection. Data available through the NCDC included weather type (drizzle, rain, thunderstorm, vicinity thunderstorm, snow, unknown precipitation, breeze, haze, and fog), precipitation intensity (light, moderate, heavy), relative humidity, wind speed, wind direction, and precipitation totals. Data was recorded approximately every 20 minutes. If less than 0.01 inches of precipitation fell during a 20 minute time period, the quantity of precipitation records as 0 inches. As a result, simply adding the individual precipitation quantities would not yield the total amount of precipitation. The NCDC

data was used to determine the starting and ending times for precipitation events and the precipitation types.

Storm track trajectories were calculated using the National Oceanic and Atmospheric Administration's (NOAA) Hybrid Single-Particle Lagrangian Integrated Trajectory (HYSPLIT) model (http://www.arl.noaa.gov/ready/hysplit4.html). Back trajectories were calculated at 500, 1000, and 1500 meters above ground level for 24 hours. The starting times for the back trajectories were chosen as six hours prior to the starting times of the precipitation events, thus predicting the region of the air mass 30 hours prior to the precipitation event.

4.3. $AgNO_3$/decomposition method

The protocol used to extract nitrate from the water samples and prepare silver nitrate for isotopic analyses incorporated aspects of Chang et al. (1999), Silva et al. (2000) and unpublished methods used by J. Hannon and others at the USGS in Reston, Virginia. The wet chemical procedure involved filtration, anion exchange, elution of anions from the anion exchange resin, nitrate purification, conversion to silver nitrate, and freeze-drying. Isotope analyses involved separate procedures: "on-line" decomposition to N_2 and CO followed by CF-IRMS for $\delta^{15}N$ and $\delta\ ^{18}O$ and "off-line" decomposition to O_2 for dual-inlet IRMS for $\Delta^{17}O$.

4.3.1. Wet chemical techniques

The procedure used to isolate nitrate ions was similar to the methods used in early investigations of precipitation nitrate in which cation exchange resin in the H^+

form was used to collect NH_4^+, anion exchange resin in the Cl^- form was used to extract nitrate, and potassium chloride was used to elute nitrate from the resin (GARTEN, 1992; GARTEN, 1996; HOERING, 1957; MOORE, 1974; MOORE, 1977). Hoering (1957) speculated that his results could have been affected by the contamination of organic matter that was not effectively removed during the wet chemical techniques. Many researchers have discussed the presence of organic matter in their nitrate samples, and there have been numerous methods described to reduce organic contaminants (e.g., CHANG et al., 1999; HABERHAUER and BLOCHBERGER, 1999; SILVA et al., 2000; SPOELSTRA et al., 2001; WASSENAAR, 1995). The techniques chosen to minimize contamination in this study were developed by Chang and others (1999) for waters with low nitrate concentration and have been used by numerous other studies (e.g., BATTAGLIN et al., 2001; CHANG et al., 2002; PARDO et al., 2004). Despite incorporating the modifications recommended by Chang et al. (1999), there is evidence that organic contaminants were not adequately removed, as discussed later.

Three to 22 liters of each precipitation sample were filtered using GF/F type and 0.4μm polycarbonate membrane filters. Each filtered sample was transferred to a clean lowboy with a spigot and gravity dripped through a series of two columns that were packed with analytical grade resins, which were carefully treated prior to use (for more details, see Appendices A and B). The first column was loaded with AG50WX-8 cation exchange resin in the H^+ form (100-200 mesh), which was intended to protonate and/or adsorb dissolved organic carbon (DOC) (CHANG et al., 1999). The second column was filled with AG2X-8 anion exchange resin in the Cl^-

form (100-200 mesh), which was used to extract anions (e.g., nitrate and sulfate) from the precipitation samples (Chang et al. 1999). This particular anion exchange resin was chosen over AG1X-8 because it has a similar strong selectivity for nitrate but a weaker selectivity for DOC (CHANG et al., 1999).

The solution that passed through the two columns was periodically tested for the presence of nitrate using prepared colorimetric test solutions (for more details, see Appendix C). It was important to verify that the nitrate was quantitatively retained on the anion exchange column to prevent isotope fractionation (e.g., GARTEN, 1992). If the solution that passed through the column contained nitrate, the sample was discarded.

After the entire sample had passed through the columns, the AG50WX-8 resin from the cation exchange column was transferred to a clean centrifuge tube, frozen, and freeze-dried. While AG50WX-8 in the H^+ form does not contain any nitrogen, as the sample passed through the cation exchange column, precipitation NH_4^+ replaced H^+ on some of the exchange sites. Therefore, the N_2 produced by heating the AG50WX-8 resin partially filled with precipitation NH_4^+ would reflect the nitrogen isotopic composition of the precipitation NH_4^+ (LEHMANN et al., 2001). Therefore, the freeze-dried AG50WX-8 resin for each sample was saved in the freezer for possible future analyses.

Anions were then eluted from each anion exchange column using 0.25M potassium chloride solution (J. Hannon 2002, personal communication). Elution of nitrate from the AG2X-8 column was monitored by periodically analyzing drops of solution from the column for the presence of nitrate using colorimetric test solutions

(Appendix C). Typically, quantitative recovery of nitrate (and sulfate) was recovered using 145-225mL 0.25M KCl solution.

The next steps in the process involved the purification of nitrate and were derived from the techniques of Silva and colleagues (2000) and J. Hannon and coworkers (personal communication). It was determined that sulfate was quantitatively recovered within the first 50mL of 0.25 M KCl solution put through each column. This portion of the sample was acidified using 2-3 drops of 1M HCl to obtain a pH of 2-3, and 0.75 ml 0.5M $BaCl_2$ solution was added to precipitate $BaSO_{4(s)}$. After thoroughly mixing and allowing the samples to stand overnight, the $BaSO_{4(s)}$ was then removed using a 0.2μm nylon filter. The $BaSO_{4(s)}$ was carefully transferred using Millipore water from the filter into a clean glass vial, placed in a drying oven at approximately 60°C, and saved for sulfate sulfur isotope analyses (see section 4.6). The approximately 50mL of solution was added back to the rest of the sample.

Next, chloride was removed by a technique modified from J. Hannon and others at the USGS, Reston that used AG MP-50 cation exchange resin converted from the H^+ form to the Ag^+ form (for more details, see Appendix D). Each sample was added to an appropriate amount of the specially prepared resin. The cations in solution (e.g., K^+, H^+, and Ba^{+2}) replaced the Ag^+ ions retained on the resin, and the freed Ag^+ ions combined with the Cl^- ions to form $AgCl_{(s)}$. AG MP-50 has a capacity for 1.5meq/mL. When the exchange sites were predominantly filled with Ag^+, it was assumed that there were 1.5 moles of Ag^+ per milliliter resin. Since one mole of Ag^+ was required per mole of Cl^- in the sample, the amount of AG MP-50 (Ag^+) needed

could be calculated from the amount of Cl^- in each sample, which was the sum of the amounts of Cl^- from the 0.25M KCl, 0.5M $BaCl_2$, and 1M HCl solutions. Due to the cost of the AG MP-50 (Ag^+) resin, for some of the samples, only a portion of each sample was added to AG MP-50 (Ag^+) and taken through the remainder of the chemistry. For example, 75mL KCl/KNO_3 solution (plus Millipore water added during transfer steps) was added to 14mL AG MP-50 (Ag^+). Each solution was then separated from the resin/$AgCl_{(s)}$ mixture and put through a column filled with 5mL AG MP-50 (Ag^+) to maximize the exchange of the other cations for Ag^+ ions. At the end of the wet chemical method, only Ag^+ and NO_3^- should have been present in significant quantities. The result of freeze-drying the solutions should have been nearly pure $AgNO_3$ crystals. As described later, there were potentially two sources of contamination that made the silver nitrates impure.

4.3.2. Measurements of the $\delta^{15}N$ and $\delta^{18}O$ of precipitation nitrate

The $\delta^{15}N$ and $\delta^{18}O$ analyses were conducted at the Geophysical Laboratory of the Carnegie Institution of Washington, overseen by M. Fogel. Four aliquots (approximately 0.5mg) of each prepared silver nitrate were weighed into a silver capsules. Using methods derived from Kornexl, Gehre, and others (1999), each sample was dropped into a Thermal Conversion Elemental Analyzer (TC/EA), which consisted of a high temperature furnace and a gas chromatograph (GC). The furnace, heated to 1450°C, was composed of a glassy carbon tube placed inside a ceramic tube and filled with glassy carbon and graphite. The high temperature reaction of $AgNO_3$ with graphite produced mainly N_2 and CO. A stream of He carried these gases

through a gas chromatograph (GC) at 90°C and into a continuous flow isotope ratio mass spectrometer (CF-IRMS).

Although the gases were prepared according to the same TC/EA parameters, it was necessary to analyze N_2 and CO during separate runs. Duplicate samples were run for both $\delta^{15}N$ and $\delta^{18}O$. For nitrogen isotope analysis, purified N_2 was carried by He flow into the mass spectrometer, where the gas was ionized. Accelerated by a voltage potential, singly charged N_2^+ ions were separated by mass to charge ratio (m/z) and directed into Faraday cups. The $\delta^{15}N$ of nitrate was calculated from the relative intensities of singly charged N_2^+ ions with m/z of 28 ($^{14}N^{14}N$) and 29 ($^{15}N^{14}N$) compared to a working N_2 standard.

For oxygen isotope analysis, purified CO was introduced to the mass spectrometer, ionized, and separated according to m/z. The $\delta^{18}O$ of nitrate was calculated from the intensities of singly charged CO^+ ions with m/z 28 ($^{12}C^{16}O$), 29 ($^{13}C^{16}O$, $^{12}C^{17}O$), and 30 ($^{13}C^{17}O$, $^{12}O^{18}O$) relative to a CO reference gas. The $\delta^{18}O$ of IAEA-NO-3, USGS-34, and USGS-35 were measured and compared to published values to determine a calibration curve. The offset correction varied on a day-to-day basis. There are discrepancies in the literature for the $\delta^{18}O$ of these reference materials. The results reported here for TC/EA-CF-IRMS analyses are calibrated using the values recently reported by Böhlke and coworkers (BOHLKE et al., 2003): $\delta^{18}O$ (IAEA-NO-3) = +25.6‰, $\delta^{18}O$ (USGS-34) = -27.9‰, and $\delta^{18}O$ (USGS-35) = +57.5‰.

4.3.3. Determinations of the $\Delta^{17}O$ of precipitation nitrate

The techniques used to measure $\Delta^{17}O$ at the Stable Isotope Laboratory at the University of Maryland, College Park were modified from thermal decomposition methods developed at the University of California, San Diego (MICHALSKI et al., 2002). The procedure used by G. Michalski and colleagues at UCSD involved placing the silver capsules into quartz reaction tubes that were attached to a borosilicate glass line. The reaction tubes were externally heated by a ceramic resistance heater (520°C) that slid over them. In order to eliminate the potential for exchange between the sample O_2 and the quartz glass, this part of the technique was modified at UMCP.

Prepared silver nitrate (4-6mg) was weighed into silver foil capsules, and the capsules were pinched closed and folded. Each sample was loaded individually into a platinum furnace that was enclosed in a vacuum apparatus. Under vacuum conditions, the samples were heated by supplying the platinum furnace with 13 amps/1.8volts of DC current for three minutes to generate molecular oxygen by

$AgNO_3 \rightarrow ½\ O_2 + NO_2 + Ag_{(s)}$ (+ trace quantities of NO and N_2).

During the reaction, a dewar filled with liquid nitrogen was placed around the reaction chamber to minimize exchange with the glass walls. The evolved gases were then passed through a U-shaped liquid nitrogen-cooled trap to condense NO_x, and O_2 was frozen onto 5A molecular sieve substrate in a liquid nitrogen-cooled finger. After closing a valve between the cold finger and the U-trap and reaction chamber, the finger was thawed and the O_2 was frozen onto 5A molecular sieve in a second cold finger. The second cold finger filled with molecular sieve was thawed to room

temperature and the purified O_2 was introduced into the sample bellows of a Delta Plus gas source mass spectrometer. Meanwhile, a standard gas was introduced into the standard bellows.

The sample and standard gases alternated being introduced through a capillary to the ion source, where the gases were ionized and accelerated by a voltage potential. The ion beams were separated by a magnet according to m/z and collected by an array of Faraday collectors. The intensities of the O_2^+ ion beams with m/z ratios of 32 ($^{16}O^{16}O$), 33 ($^{17}O^{16}O$), and 34 ($^{18}O^{16}O$, $^{17}O^{17}O$) were measured, and the 34/32 and 33/32 ratios were determined. The average of the isotope ratios determined for each sample gas was compared to the isotope ratios of the standard gas to determine the $\delta^{17}O$ and $\delta^{18}O$ of the samples relative to the standard gas. The $\Delta^{17}O$ was then calculated using the equation $\Delta^{17}O = \delta^{17}O - 1000 * ((1 + \delta^{18}O/1000)^{0.52} - 1)$.

Several additional steps were included in the $\Delta^{17}O$ protocol to maximize accuracy and precision. Each time the reaction chamber was open to load a new sample, the seal was re-greased to ensure that maximum vacuum conditions would be produced. Once the decomposition line had been evacuated to 5mtorr by a mechanical pump, several traps were cooled to liquid nitrogen temperatures and the line continued to be evacuated by a diffusion pump. During the evacuation of the line, the cold fingers filled with molecular sieve were wrapped with heating tape and heated to 220°C for one hour. This protocol removed water from the surfaces and minimized the potential for a memory effect.

4.3.4. Quality assurance tests

J. Hannon of the USGS, Reston discovered an issue associated with the use of AG MP-50(Ag^+) to remove chloride from the samples and produce $AgNO_3$ (2003 personal communication). The method used by J. Hannon differed slightly from the procedure described above. Columns filled with AG 50W X8 (H^+) were not used prior to the anion exchange columns; AG 1X anion exchange resin was used in place of AG 2X; and the final step involved the use of AG 50W X8 (K^+) to produce KNO_3 instead of AG MP-50 (Ag^+) to produce $AgNO_3$. When the standards USGS-34 (KNO_3, $\delta^{18}O$ = -27.9‰) and USGS-35 ($NaNO_3$, $\delta^{18}O$ = +57.5‰) were dissolved in deionized water, put through the wet chemical procedure, and isotopically analyzed, the $\delta^{18}O$ values for USGS-34 were higher and the $\delta^{18}O$ values for USGS-35 were lower than the published values. There was also a greater difference in the measured $\delta^{18}O$ values when less nitrate salt was dissolved, processed, and analyzed. There were no observed differences in the measured $\delta^{15}N$ values. In addition, when deionized water was put through the chemical procedure (blank experiment), the freeze-dried result was a fluffy tan colored solid. The solid was analyzed using an elemental analyzer and had the following composition: 15%S, 27%C, and 0.15%N. J. Hannon concluded that a small, constant amount of AG MP-50 resin, which has a matrix of styrene divinylbenzene with a sulfonic acid functional group ($R\text{-}SO_3^-$), was being leached into the sample during the chloride removal step. Donna Hardy of Bio-Rad's Technical Support Group verified the potential for the sulfonic acid functional group to leach from the resin (personal communication).

To address these issues at the University of Maryland, standards were put through the wet chemical procedure. Two aliquots of the USGS-34 standard and two aliquots of USGS-35 standard were dissolved in 75mL of 0.25M KCl solution, added to14mL of the prepared AG MP-50 (Ag^+) resin, dripped through a 5mL column of AG MP-50 (Ag^+) resin, freeze-dried, and analyzed. A blank experiment was also conducted in which 75mL of the 0.25M KCl solution was taken through the identical procedure as the samples.

To test for the presence of organic matter, the prepared silver nitrates, including dissolved standards and the precipitation nitrate samples, were analyzed for % carbon and C/N using an elemental analyzer coupled to CF-IRMS in the laboratory of M. Fogel at the Carnegie Institution of Washington. The presence of carbon would provide evidence of organic matter in the silver nitrates. Dissolved organic matter generally contains 40% oxygen. Thus, the presence of organic compounds would indicate a likely source of non-nitrate oxygen contaminating the samples.

4.4. Denitrifier method

Several samples were analyzed using a technique that uses denitrifying bacteria to prepare N_2O for isotopic analyses (CASCIOTTI et al., 2002; SIGMAN et al., 2001). The analyses were overseen by J. Kaiser. The techniques used to revive freeze-dried denitrifying bacteria, *Pseudomonas aureofaciens,* prepare a nutrient broth, and inoculate the broth were conducted by G. Cane at Princeton University. After growing for six days, the bacteria were ready to harvest. The medium was tested for the presence of nitrite because nitrite indicates the bacterial culture is not

usable. The prepared solution was divided into 40mL tubes and centrifuged. The medium was then concentrated 10-fold and 0.1ML of 6.0 M ammonium sulfate, $(NH_4)_2SO_4$ was added. Then, 2mL of concentrated bacteria were pipetted into 20mL vials, which were sealed and purged for six hours by bubbling He through the vials. The appropriate amount of precipitation samples to contribute 15 nanomoles of N was added to each bottle. The vials were then incubated overnight. The next day, 0.1mL of 10N sodium hydroxide, NaOH, was injected into each bottle to end the biological reaction. The N_2O produced by the bacteria were injected into a gas-bench for purification and concentration prior to mass-spectrometric analyses of m/z 44, 45, and 46. From $^{45}N_2O/^{44}N_2O$ and $^{46}N_2O/^{44}N_2O$, it was possible to calculate the $\delta^{15}N$ and $\delta^{18}O$ of nitrate (CASCIOTTI et al., 2002; SIGMAN et al., 2001).

4.5. Measurements of ion concentrations

Nitrate/nitrite concentrations in the precipitation samples were analyzed in the laboratory of D. Sigman at Princeton University. An auto-sampler was used to inject 100μL of the water samples into an acidic medium containing vanadium III heated to 80-90°C. Nitrite and nitrate were reduced to NO, which was carried by a stream of He to a chemi-luminescence NO_x analyzer (BRAMAN and HENDRIX, 1989). The measurement of standard solutions ranging from 1.79 to 60.35μM permitted the calibration of peak area versus concentration. Periodic measurement of the standard solutions throughout the run verified the consistency of the system. Reproducibility was better than 0.2μM (1σ), which was typical for this apparatus (HASTINGS et al., 2003).

Nitrate and sulfate concentrations were determined using ion chromatography (IC) in the Environmental Engineering Laboratory at the University of Maryland, overseen by A. Davis. Hunho Kim and Houng Li assisted with the operation of the Dionex DX-100 ion chromatograph. Calibration solutions were prepared from chloride, nitrate, and sulfate stock solutions of known concentrations. The intermittent analysis of check standards showed that sulfate concentration data was reproducible during all IC runs within 5μM (1σ). Two batches of nitrate concentration data had precision better than 5μM (1σ). However, the last batch of nitrate concentration data, which included a large number of samples, was inaccurate because nitrate and chloride were eluted at the same time from the aging column.

Ammonium concentrations were measured at Geophysical Laboratory of the Carnegie Institution of Washington managed M. Fogel using conventional phenol hypochlorite colorimetric techniques (SOLORZANO, 1969). A pipette was used to transfer 0.7mL of each sample into snap cap sample vials. An oxidizing solution was prepared by adding four parts alkaline solution (100g sodium citrate and 5g NaOH in 500mL pure water) to one part 1.5 N hypochlorite solution (bleach). First, 0.1 mL phenol solution (20g phenol in 200mL 95% v/v ethyl alcohol) was added and the mixture was vortexed. Then, 0.1 nitroprusside solution (1g sodium nitroprusside in 200mL pure water) was added to the sample tubes and the solution was mixed. Next, 0.25mL of the oxidizing solution was added and the mixture was vortexed prior to covering the sample tubes with aluminum foil and allowing the solutions to incubate for at least one hour. The solutions turned varying shades of blue, and optical densities of the solutions were measured using a spectrophotometer (670nm).

Standard solutions of known NH_4^+ concentrations were used to construct a calibration curve so that the NH_4^+ concentrations of the samples could be calculated from the absorbance data.

4.6. Determinations of the $\delta^{34}S$ of precipitation sulfate

Analyses of the $\delta^{34}S$ of precipitation sulfate were overseen by D. Ernest and A.J. Kaufman at the Stable Isotope Laboratory of the University of Maryland College Park. Approximately 0.5mg of dried $BaSO_4$ crystals were weighed into tin capsules. The capsules were dropped into an Elemental Analyzer to produce SO_2 for continuous flow mass spectrometric analyses. Most of the samples were run in duplicate. Duplicate NBS-127 sulfate standards were analyzed before and after each set of six samples to calculate the 1 σ reproducibility, which was typically better than 0.5‰, and the offset from the sulfur isotope reference, VCDT, which is based on a troilite (FeS) from Canon Diablo meteorite, CDT (KROUSE and COPLEN, 1997). Sulfur isotope ratios are reported relative to VCDT in delta notation.

$$\delta^{34}S = \left(\frac{\left({}^{34}S / {}^{32}S \right)_{\text{sample}}}{\left({}^{34}S / {}^{32}S \right)_{VCDT}} - 1 \right) \times 1000\,‰$$

5. Results

5.1. Meteorological and storm track data

Data from the National Climate Data Center revealed that a variety of storms were sampled (Table 1). The samples are organized and numbered in order of the date of sample collection. The start and end times for the precipitation events showed that the storms varied in length from a few hours to greater than a day. Precipitation types included rain (RA), snow (SN), thunderstorm (TS), vicinity thunderstorm (VCTS), and unknown or mixed precipitation (UP).

Storm track data determined using the NOAA HYSPLIT model showed that air masses approached Frederick, Maryland from several different directions (Table 1). The three-dimensional model results for storms are included in Appendix E. For some of the storms, air masses at 500m, 1000m, and 1500m above ground level moved towards Frederick in the same direction. For other storms, air masses at different elevations entered the region from different directions.

The storm track data did not exhibit a strong seasonal pattern. For each season, air masses moved into the area from several different directions. For example, for the storms sampled in Spring 2003, dominant directions of air mass movement included from the west (W), south (S), east (E), northeast (NE), west northwest (WNW), and southwest (SW).

Table 1: Precipitation collection, meteorological, and storm track data. Meteorological data was obtained from the National Climate Data Center. Abbreviations for precipitation types are rain (RA), snow (SN), thunderstorm (TS), vicinity thunderstorm (VCTS), and unknown or mixed precipitation (UP). Storm track data was determined using the NOAA HYSPLIT model. Abbreviations for directions of air mass movement include from the west (W), East (E), North (N), South (S). In some cases, these letters are combined to give more detailed information. For example, NW indicates from the northwest, and WNW indicates from the west northwest (more from the west than from the north). The table is continued on the following two pages.

Sample # by date	Precip Start Time (Eastern US)	Precip End Time (Eastern US)	Precip Types	Portion of the storm collected	Back Trajectory Start Time (UTC)	Direction of Air Mass Movement
1	2/6/03 20:01	2/7/03 7:41	SN	entire	2/6/03 19:00	W
2	2/15/03 1:22	2/15/03 15:02	SN	entire	2/15/03 14:00	W
3	2/27/03 6:41	2/28/03 7:41	SN	entire	2/27/03 6:00	E (500m), SE (1000m), and W (1500m)
4	3/13/03 18:04	3/13/03 21:20	RA, VCTS	entire	3/13/03 17:00	WSW
5	4/7/03 2:40	4/7/03 20:01	RA, SN, UP	from 4-7-03 11:15 to end	4/7/03 2:00	WNW
6	5/8/03 8:45	5/8/03 13:20	RA, TS	entire	5/8/03 7:00	W
7	5/15/03 16:05	5/18/03 13:45	RA, TS, VCTS	entire	5/15/03 14:00	S
8	5/15/03 16:05	5/18/03 13:45	RA, TS, VCTS	from beginning to 5-16-03 9:15	5/15/03 14:00	S
9	5/15/03 16:05	5/18/03 13:45	RA	from 5-16-03 9:15 to end	5/16/03 7:00	S
10	5/20/03 21:03	5/21/03 15:44	RA	entire	5/20/03 19:00	E, S
11	5/23/03 12:05	5/25/03 0:44	RA, TS	entire	5/23/03 10:00	NE (500m, 1000m), local S (1500m)
12	6/8/03 22:03	6/9/03 0:40	RA	entire	6/8/03 20:00	WNW (500m), SW (1000m, 1500m)
13	6/12/03 15:20	6/12/03 22:02	RA, TS, VCTS	entire	6/12/03 13:00	SW
14	6/13/03 13:41	6/13/03 20:20	RA, TS, VCTS	entire	6/13/03 12:00	SW

Table 1 (continued)

Sample # by date	Precip Start Time (Eastern US)	Precip End Time (Eastern US)	Precip Types	Portion of the storm collected	Back Trajectory Start Time (UTC)	Direction of Air Mass Movement
15	7/3/03 12:43	7/4/03 15:41	RA, TS, VCTS	entire (one storm 7-3-03 from 12:43 to 14:41 and another storm 7-4-03 from 13:41 to 15:41)	7/3/03 11:00	S
16	7/6/03 19:02	7/7/03 14:42	RA, TS, VCTS	entire (one storm 7-6-03 from 19:02 to 22:22 and another storm 7-7-03 14:03 to 14:42)	7/6/03 17:00	W
17	7/9/03 7:42	7/9/03 17:03	RA, TS, VCTS	entire	7/9/03 6:00	W
18	7/22/03 18:01	7/22/03 2:20	RA, TS, VCTS	entire	7/22/03 16:00	SW
19	8/12/03 15:43	8/12/03 17:42	RA, TS	entire	8/12/03 13:00	local NW
20	9/1/03 14:20	9/1/03 19:40	RA, TS, VCTS	entire	9/1/03 12:00	SW
21	9/3/03 20:03	9/4/03 14:01	RA, TS, VCTS	entire	9/3/03 18:00	SW
22	9/15/03 16:45	9/15/03 17:21	RA, TS, VCTS	entire	9/15/03 15:00	SW
23	9/18/03 9:22	9/19/03 15:41	RA	from beginning to 9-18-03 18:00	9/18/03 7:00	NE (500m, 1000m), E(1500m)
24	9/18/03 9:22	9/19/03 15:41	RA	from 9-18-03 at 18:00 to 9-18-03 at 22:00	9/18/03 16:00	E
25	9/18/03 9:22	9/19/03 15:41	RA	from 9-18-03 22:00 to end	9/18/03 20:00	E
26	9/22/03 15:21	9/23/03 6:25	RA, TS, VCTS	entire	9/22/03 13:00	SE
27	9/25/03 17:21	9/25/03 20:23	RA, TS, VCTS	entire	9/25/03 15:00	WSW
28	9/27/03 21:44	9/28/03 6:42	RA, TS, VCTS	entire	9/27/03 20:00	S
29	11/5/03 5:41	11/5/03 21:41	RA	entire	11/5/03 5:00	S
30	11/6/03 6:21	11/6/03 18:40	RA	entire	11/6/03 5:00	WSW

Table 1 (continued)

Sample # by date	Precip Start Time (Eastern US)	Precip End Time (Eastern US)	Precip Types	Portion of the storm collected	Back Trajectory Start Time (UTC)	Direction of Air Mass Movement
31	11/11/03 10:01	11/12/03 20:41	RA	entire	11/11/03 9:00	W
32	11/24/03 16:01	11/24/03 21:41	RA	entire	11/24/03 15:00	S
33	11/28/03 5:01	11/28/03 19:40	RA	entire	11/28/03 4:00	SSW
34	12/4/03 21:40	12/6/05 10:01	RA, SN, UP	entire	12/4/03 21:00	S (500m), SW (100m, 1500m)
35	12/10/03 13:21	12/11/03 8:19	RA, UP	entire	12/10/03 12:00	S
36	12/14/03 3:20	12/24/03 13:39	RA, SN, UP	entire (First storm 12-14-03 from 3:20 to 19:20, second storm 12-17-03 from 4:19 to 14:02, and third storm 12-24-03 from 00:20 to 13:39)	12/14/03 2:00	NW
37	1/5/04 7:40	1/5/04 14:02	RA	entire	1/5/04 6:00	SW
38	1/23/04 21:02	1/26/04 22:40	SN	entire	1/23/04 20:00	NW
39	2/3/04 6:40	2/3/04 14:20	RA, SN, UP	entire	2/3/04 6:00	E,S
40	2/5/04 20:40	2/6/04 19:20	RA, SN, UP	entire	2/5/04 19:00	NW
41	3/5/04 21:40	3/6/04 15:42	RA, TS, VCTS	entire	3/5/04 20:00	SW
42	3/18/04 18:20	3/19/04 9:40	RA, SN, VCTS	entire	3/18/04 17:00	W
43	3/31/04 21:42	4/3/04 12:41	RA, VCTS	entire	3/31/04 21:00	NE (500m), SW (1000m, 1500m)
44	4/12/04 5:20	4/13/04 18:40	RA, VCTS	entire	4/12/04 4:00	local NE
45	4/23/04 16:40	4/23/04 23:21	RA	entire	4/23/04 16:00	WSW
46	5/1/04 20:20	5/3/04 19:40	RA	entire	5/1/04 18:00	SSW

5.2. $AgNO_3$/decomposition method data

5.2.1. Standards analyzed by $AgNO_3$/decomposition methods

The results of the experiments of dissolved standards taken through the wet chemical procedure showed that $\delta^{15}N$ values were not affected by the wet chemical procedure, while $\delta^{18}O$ values of the processed standards were significantly lower than the standards taken directly from their vials (Table 2). The results of the blank experiment produced 0.6mg of a dark brown solid. Analyses of %C content using the elemental analyzer revealed the presence of carbon. The dissolved standards had been contaminated by an oxygen containing compound during the analytical procedure.

Table 2: Data obtained for the standard solutions put through the wet chemical procedure. The standard USGS-34 has published values of $\delta^{18}O$ = -27.5‰ and $\delta^{15}N$ = -1.87‰. USGS-35 has published values of $\delta^{18}O$ = +57.5‰ and $\delta^{15}N$ = +2.86‰.

Standard	**Freeze-Dried Sample Description**	**mmol NO_3 used**	**mmol NO_3 recov.**	**% yield mmol NO_3**	**$\delta^{15}N_{AIR}$ (‰) ±0.5 (1σ)**	**$\delta^{18}O_{VSMOW}$ (‰) ±0.5 (1σ)**	**$\Delta^{17}O$ (‰) ±0.05 (1σ)**	**% C ±0.05**
USGS-34 (KNO3)	white	0.251	0.233	92.8%	-1.5	-26.1	0.86	0.25
USGS-34 (KNO3)	white, grayish brown tinge	0.049	0.052	104.7%	-1.8	-21.6	0.55	1.82
USGS-35 (NaNO3)	white, slightly tan	0.249	0.221	88.7%	2.9	56.7	21.60	0.26
USGS-35 (NaNO3)	white, slightly tan	0.055	0.052	93.7%	2.5	55.3	21.23	1.45

The measured $\delta^{18}O$ values represented the precipitation samples plus the analytical blank. The following mass-balance calculation was used to determine the magnitude and isotopic composition of the analytical blank (HAYES, 2004). (N terms represent molar quantities, δ represents $\delta^{18}O$, Σ represents the sample prepared for analysis, s represents the sample, and b represents the blank.)

$$N_\Sigma \delta_\Sigma = N_s \delta_s + N_b \delta_b$$

The substitution of $N_\Sigma - N_b$ for N_s and the rearrangement of the equation gave the following equation in the form of $y = mx + b$.

$$\delta_\Sigma = \delta_s - N_b(\delta_s - \delta_b)/ N_\Sigma$$

If the results of multiple analyses were plotted for δ_Σ vs. $1/ N_\Sigma$, the intercept would be δ_s. In the case of the standard experiments, the values of δ_s were known. Therefore, for both the USGS-34 and USGS-35 experiments, it was possible to plot the measured $\delta^{18}O$ values for each prepared aliquot versus the inverse values of the molar quantities obtained with the published values of the standards as the intercepts. The molar quantities of oxygen were calculated by dividing the masses of the prepared samples by the molar mass of $AgNO_3$ 169.91g/mol and multiplying by three moles oxygen for every one mole of $AgNO_3$. Since the samples were not pure silver nitrate, this calculation introduces some uncertainty. A linear regression was performed on the data for each standard, and the intersection of the two lines yielded the $\delta^{18}O$ of the blank and molar quantity of oxygen from the blank. The blank consisted of 0.015mmol oxygen and had a $\delta^{18}O$ of 34.6‰.

5.2.2. Observations on prepared silver nitrates

Three observations provided evidence that the prepared silver nitrates were impure. First, whereas silver nitrate crystals should be colorless, the prepared silver nitrates exhibited colors ranging from white to very dark brown (Table 3). Second, whereas pure silver nitrate should have a molar ratio of nitrogen to oxygen of 0.33, the N/O of the prepared silver nitrates ranged from 0.16 to 0.31 (Table 3). Molar ratios were calculated from the weight percent nitrogen and oxygen data obtained using the thermal conversion elemental analyzer and continuous flow mass spectrometer. Third, whereas pure silver nitrate does not contain carbon, the prepared silver nitrates contained 0.97 to 3.03%C (Table 3). Since organic matter typically contains approximately 40% oxygen, the presence of carbon provides evidence for the presence of an oxygen-containing contaminant in the prepared silver nitrates.

The silver nitrates prepared from precipitation samples contained more carbon than could be attributed to the analytical blank. In addition to the organic compounds added during the wet chemical procedure, there was likely a second source of carbon (and oxygen) in the prepared silver nitrates. The %C results for the standard experiments (Table 2) showed that carbon content is roughly proportion to the moles of sample. In the experiments in which more than 0.2mmoles of nitrate salts were dissolved, the prepared silver nitrates had approximately 0.25% carbon. In the experiments in which only approximately 0.05mmoles of nitrate salts were dissolved, the prepared silver nitrates still had less than 2% carbon. For several of the precipitation nitrate samples that yielded more than 0.2mmoles, the %C values were significantly larger than 0.25% (Table 3), providing evidence of a second oxygen-containing contaminant, which is described in more detail in section 6.1.

Table 3: Observations on the silver nitrates prepared from precipitation samples. Weight percent nitrogen and oxygen data was determined during separate runs using the thermal conversion elemental analyzer and continuous flow mass spectrometry. Molar N/O values were calculated using the weight percent data with an overall uncertainty of 0.08.

Sample # by date	Precip Start Date	$AgNO_{3(s)}$ (mmol)	Freeze-Dried Sample Description	Wt% N (TC/EA)	Wt% O (TC/EA)	N/O ±0.08	Wt% C (EA) ±0.05%
1	2/06/03	0.036	dark brown, sticky		29.08		
2	2/15/03	0.177	med-dark brown granular	8.33	29.67	0.25	2.93
4	3/13/03	0.190	med-dark brown	9.07	26.10	0.30	
5	4/07/03	0.163	med-dark brown	9.51	27.19	0.31	
7	5/15/03	0.523	med-dark brown granular	6.09	27.11	0.20	
8	5/15/03	0.357	med-dark brown, fluffy	8.77	29.87	0.26	2.32
9	5/16/03	0.164	dark brown	9.24	27.60	0.29	
11	5/23/03	0.385	med-dark brown, fluffy	8.92	29.17	0.27	1.70
14	6/13/03	0.077	medium brown	8.21	28.46	0.25	
15	7/03/03	0.298	golden tan	4.80	25.47	0.16	2.22
18	7/22/03	0.058	dark brown	6.09	31.22	0.17	
19	8/12/03	0.039	dark brown, sticky	7.18	27.66	0.23	
20	9/01/03	0.037	dark brown, sticky	5.99	29.36	0.18	
22	9/15/03	0.076	slightly tan, fluffy	5.26	23.25	0.20	
23	9/18/03	0.034	tan, fluffy	7.65	27.80	0.24	
26	9/22/03	0.046	vanilla tan		29.88		
32	11/24/03	0.042	grayish tan	7.95	27.95	0.25	
34	12/04/03	0.130	white	8.74	26.97	0.28	
35	12/10/03	0.062	dark	7.30	25.59	0.25	
37	1/05/04	0.105	white, powdery	9.08	26.23	0.30	
38	1/23/04	0.245	white, fluffy	8.96	26.84	0.29	0.97
40	2/05/04	0.067	white	7.84	26.63	0.26	
41	3/05/04	0.132	caramel, granular	7.79	26.29	0.26	
42	3/18/04	0.164	white, fluffy	8.49	25.45	0.29	
43	3/31/04	0.498	grayish tan	6.94	24.77	0.25	
44	4/12/04	0.147	caramel	6.67	23.95	0.24	3.03

5.2.3. Samples analyzed by $AgNO_3$/decomposition methods

The $\delta^{15}N$ values for Frederick, Maryland precipitation nitrate obtained using the $AgNO_3$/decomposition method ranged from -5.1±0.5‰ to +5.9±0.5‰ (Table 4). Contributions of nitrogen from the analytical blank were negligible, and therefore no blank correction was necessary. The highest $\delta^{15}N$ values occurred in the winter and the lowest $\delta^{15}N$ values occurred in the summer.

Table 4: Precipitation nitrate isotope ratios obtained using the $AgNO_3$/decomposition method. It was unnecessary to apply a blank correction to the $\delta^{15}N$ data. There was an analytical blank correction applied to $\delta^{18}O$ and $\Delta^{17}O$ to account for oxygen-containing contaminants in the prepared silver nitrates.

Sample # by date	Precipitation Start Date	$\delta^{15}N_{AIR}$ (‰) ±0.5 (1σ)	$\delta^{18}O_{VSMOW}$ (‰) ±0.5 (1σ)	"Analytical Blank Corrected" $\delta^{18}O_{VSMOW}$ (‰) ±0.5 (1σ)	$\Delta^{17}O$ (‰) ±0.05 (1σ)	"Analytical Blank Corrected" $\Delta^{17}O$ (‰) ±0.05 (1σ)
1	2/06/03		69.1	74.5		
2	2/15/03	3.3	80.2	81.5	30.12	30.98
4	3/13/03	2.3	79.5	81.9	30.10	31.71
5	4/07/03	-1.2	74.2	77.1	26.47	28.37
7	5/15/03	-3.0	53.1	53.3	16.59	16.75
8	5/15/03	-3.9	67.1	68.2	23.00	23.77
9	5/16/03	-0.9	64.5	66.8	23.54	25.36
11	5/23/03	1.7	74.4	75.5	21.93	22.54
14	6/13/03	-2.9	55.5	57.0	17.81	19.02
15	7/03/03	-3.5	42.5	42.6	15.08	15.33
18	7/22/03	-5.1	50.6	52.1		
19	8/12/03	-5.0	57.9	61.3		
20	9/01/03	-3.2	48.8	51.0		
22	9/15/03	-0.3	42.3	42.8		
23	9/18/03	0.5	62.6	67.4		
26	9/22/03		61.9	65.2	20.96	23.47
32	11/24/03	4.5	73.8	79.0		
34	12/04/03	2.7	77.7	79.4		
35	12/10/03	0.9	56.1	57.9		
37	1/05/04	5.4	50.7	51.5		
38	1/23/04	5.9	48.6	48.9	17.28	17.63
40	2/05/04	-0.2	75.7	78.9		
41	3/05/04	2.5	65.4	66.6	19.46	20.21
42	3/18/04	2.7	80.3	81.7	28.96	29.85
43	3/31/04	1.7	64.8	65.1		19.30
44	4/12/04	-0.3	59.8	60.7		

The oxygen isotope data from the $AgNO_3$/decomposition method required an analytical blank correction. As described in section 5.2.1., there was approximately 0.015 moles of an oxygen-containing contaminant added during the wet chemical procedure. The $\delta^{18}O$ of the contaminant was determined to be 34.6‰, and the $\Delta^{17}O$ was assumed to be zero. Table 4 shows the $\delta^{18}O$ and $\Delta^{17}O$ of precipitation nitrate obtained using the $AgNO_3$/decomposition method before and after the analytical blank correction. The $\delta^{18}O$ of precipitation nitrate ranged from +42.6±0.5‰ to +81.9±0.5‰ and the $\Delta^{17}O$ of precipitation nitrate ranged from +15.33±0.05‰ to +31.71±0.05‰ using the $AgNO_3$/decomposition method. The highest $\delta^{18}O$ and $\Delta^{17}O$ values occurred in the winter and the lowest $\delta^{18}O$ and $\Delta^{17}O$ occurred in the summer, but there was significant within-season variation.

5.3. Denitrifier method data

Analysis of precipitation nitrate samples using the denitrifier method yielded results of 3.6±0.2‰ to +7.1±0.2‰ for $\delta^{15}N$ (Table 5). The $\delta^{18}O$ of precipitation nitrate obtained using the denitrifier method ranged from +61.6±0.3‰ to +86.8±0.3‰ (Table 5). Both $\delta^{15}N$ and $\delta^{18}O$ exhibited a strong seasonal pattern with the highest values in the winter and the lowest values in the summer, and intermediate values in the spring and autumn. There was minimal within-season variation in the $\delta^{15}N$ and $\delta^{18}O$ data from the denitrifier method.

Table 5: Precipitation nitrate isotope ratios obtained using the denitrifier method.

Sample # by date	Precipitation Start Date	$\delta^{15}N_{AIR}$ (‰) ±0.2	$\delta^{18}O_{VSMOW}$ (‰) ±0.3
1	02/06/03	0.65	86.81
2	02/15/03	2.91	85.55
8	05/15/03	-3.63	69.98
10	05/20/03	-1.82	77.63
12	06/08/03	-3.02	64.58
13	06/12/03	-0.51	64.69
14	06/13/03	-0.87	61.57
15	07/03/03	-2.07	71.14
17	07/09/03	-0.06	73.70
18	07/22/03	-2.59	66.21
19	08/12/03	-2.21	64.78
20	09/01/03	-0.56	66.46
22	09/15/03	-0.11	70.56
23	09/18/03	1.11	74.84
30	11/06/03	7.05	77.42
34	12/04/03	4.58	73.24
36	12/14/03	5.48	79.57
39	02/03/04	3.99	80.59
42	03/18/04	3.12	81.27
44	04/12/04	1.50	79.44
46	05/01/04	1.99	64.63

5.4. Ion concentration data

There were large ranges of ammonium, sulfate, and nitrate+nitrite concentrations for the Frederick precipitation samples (Table 6). Ammonium concentrations ranged from 8±5μM to 205±5μM. Sulfate concentrations ranged from 7±5μM to 75±5μM, and nitrate + nitrite concentrations ranged from 2.1±0.2μM to 173.6±0.2μM. There were no strong linear relationships between ammonium, sulfate, or nitrate+nitrite concentrations and date. Although precipitation samples with high nitrate+nitrite concentrations generally also had high ammonium and sulfate concentrations, there were no significant linear correlations between the different

concentrations. Furthermore, there was no apparent relationship between concentration data and nitrate isotope ratios.

Table 6: Ion concentration data and the $\delta^{34}S$ of precipitation sulfate.

Sample # by date	Precipitation Start Date	$[NH_4^+]$ (μM) ±5 (color)	$[SO_4^-]$ (μM) ±5 (IC)	$[NO_3^-]$ (μM) ±5 (IC)	$[NO_3^-]$ + [NO3-] (μM) ±0.2 (NO_x box)	$\delta^{34}S$ ±0.5 (‰)
1	02/07/03	10	1		15.7	6.6
2	02/15/03	30	4		37.4	6.4
3	02/28/03		5	16		6.1
4	03/13/03		50	67		5.8
5	04/07/03		75	60		5.1
6	05/08/03	11	9		2.1	5.0
7	05/18/03		46	36		5.5
8	05/18/03	34	47	39	37.4	5.5
9	05/18/03		53	32		5.0
10	05/21/03	205	72		172.6	
11	05/25/03		38	34		5.4
12	06/09/03	30	7		20.9	
13	06/12/03	30	11		28.3	5.4
14	06/13/03	65	19		42.6	5.0
15	07/04/03	107	28		36.5	7.6
16	07/07/03	39	19		16.7	5.9
17	07/09/03	36	9		36.4	
18	07/22/03	25	6		18.5	4.4
19	08/12/03	29	10		111.6	5.7
20	09/01/03	24	4		7.7	6.3
21	09/04/03	22	13		47.6	5.2
22	09/15/03	55	20		29.2	5.5
23	09/19/03	30	3		9.7	8.4
24	09/19/03	14	2		4.7	8.5
25	09/19/03	14	3		5.6	12.3
26	09/23/03	9	4		5.6	4.9
27	09/25/03	15	9		18.1	5.0
28	09/28/03	43	16		129.8	6.4
29	11/05/03	43	6		2.1	5.8
30	11/06/03	24	15		57.7	5.7
31	11/12/03	9	4		nd	6.0
32	11/24/03	8	6		nd	6.8
33	11/28/03	56	13		27.4	6.9
34	12/06/05	20	4		18.3	7.1
35	12/11/03	13	7		8.1	6.9
36	12/24/03	23	16		40.0	6.8
37	01/05/04	57	37		96.9	5.3

Table 6 (continued)

Sample # by date	Precipitation Start Date	$[NH_4^+]$ (μM) ±5 (color)	$[SO_4^-]$ (μM) ±5 (IC)	$[NO_3^-]$ (μM) ±5 (IC)	$[NO_3^-]$ + [NO3-] (μM) ±0.2 (NO_x box)	$\delta^{34}S$ (‰)	1σ for $\delta^{34}S$ (‰)
38	01/26/04	19	7		10.8	6.0	0.1
39	02/03/04	12	5		15.5	7.4	0.5
40	02/06/04	20	9		11.2	5.7	0.5
41	03/06/04	21.8	6.25		21.8	4.96	0.52
42	03/19/04	79.8	23.74		110.8	5.68	0.34
43	04/03/04	31.8	9.58		47.6	6.95	0.5
44	04/13/04	35	0.97		28.3	5.65	0.27
45	04/23/04	150.5	6.95		49.9	4.51	0.27
46	05/03/04	41.3	5.62		9.7		

5.5. $\delta^{34}S$ of precipitation sulfate

With the exception of three samples collected during Hurricane Isabel in September 2003, the $\delta^{34}S$ of precipitation sulfate ranged from 4.4±0.3‰ to 7.6±0.4‰ (Table 6). The mean $\delta^{34}S$ value for Frederick, Maryland precipitation sulfate during the sampling period was 5.8‰ ±0.8‰ (1σ for the sample measurements). The $\delta^{34}S$ values for the three Isabel samples in order of the storm's progression were 8.4±0.5‰, 8.5±0.5‰, and 12.3±0.5‰. The higher $\delta^{34}S$ values of the hurricane samples could be the result of increased oceanic contributions. Whereas the $\delta^{15}N$ of precipitation nitrate varied seasonally, the $\delta^{34}S$ of precipitation sulfate remained relatively constant. There was no correlation between $\delta^{34}S$ and sulfate concentrations or $\delta^{34}S$ and $\delta^{15}N$.

6. Discussion

6.1. Comparison of the $AgNO_3$/decomposition and denitrifier methods

Many authors have discussed the possibility or presence of dissolved organic matter in the nitrate salts used for decomposition analyses (e.g., KENDALL, 1998). Recently, Heaton and coworkers (2004) reported that organic contaminants in silver nitrates prepared from arctic snow samples led to decreases in measured $\delta^{18}O$ values and used C/N and N/O data to determine the extent of organic contamination. Here, we present a method assessment based on a comparison of precipitation nitrate isotope measurements obtained by the $AgNO_3$/decomposition and denitrifier methods.

Previous comparisons of nitrate salt/decomposition and the denitrifier method identified a tendency for the denitrifier method to overestimate $\delta^{15}N$ by as much as 1-2‰ for nitrates with non-zero $\Delta^{17}O$ (COPLEN et al., 2004). In this study, we took $\Delta^{17}O$ into consideration in our data reduction and re-evaluated the $\delta^{15}N$ of the denitrifier and $AgNO_3$/decomposition methods. We also considered whether dissolved organic nitrogen compounds interfered with $\delta^{15}N$ measurements.

There were significant differences between the $\delta^{15}N$ values obtained using the $AgNO_3$/decomposition and denitrifier methods. In general, measurements of $\delta^{15}N$ using the denitrifier method were higher than those obtained using the $AgNO_3$/decomposition method. In some cases, the difference between the two methods was greater than -2.5‰. There was a linear relationship between the $\delta^{15}N$

values obtained using the $AgNO_3$/decomposition and denitrifier methods ($r^2 \approx 0.9$) (Figure 8).

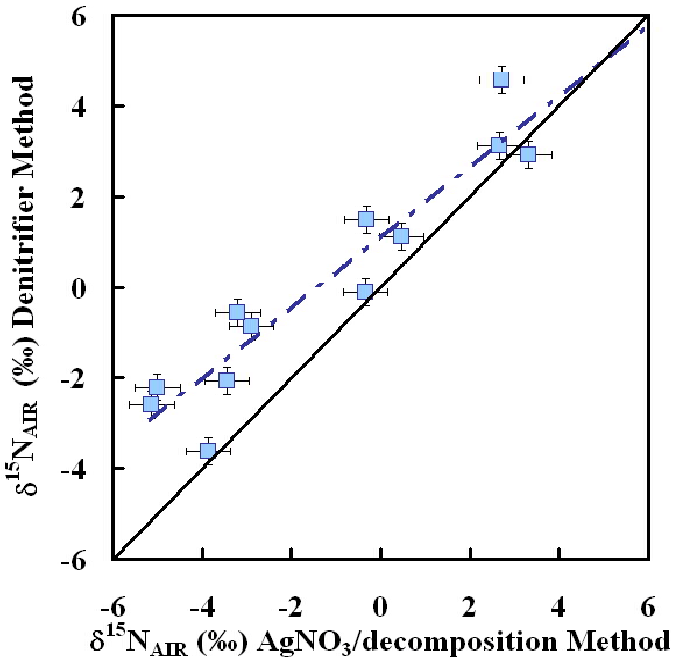

Figure 8: $\delta^{15}N$ versus $\delta^{15}N$ obtained using the $AgNO_3$/decomposition and denitrifier techniques. Error bars represent 1σ mass spectrometric reproducibility of nitrate standards. Data from the $AgNO_3$/decomposition method are averages of duplicate analyses. The solid line is the 1:1 line, and the dashed line shows the linear regression of the data ($y=0.79x+1.09$, $r^2=0.89$).

The $\delta^{15}N$ of the prepared silver nitrates may have been affected by organic nitrogen. While the organic contaminant from the analytical procedure had negligible amounts of nitrogen, organic nitrogen from the precipitation itself may have affected $\delta^{15}N$ values. Heaton et al. (2004) reported that increased organic contamination, determined by measured C/N ratios, coincided with slightly higher $\delta^{15}N$ values. In their study, the $\delta^{15}N$ values of arctic snow NO_3^- exhibited a range from -18 to -7‰, which is significantly lower than the range of $\delta^{15}N$ values for Maryland precipitation nitrate. Thus, the magnitude and direction of the effect of organic contaminants on

the $\delta^{15}N$ of Maryland precipitation NO_3^- would not necessarily be the same. In order for organic contaminants to cause $\delta^{15}N$ measurements to be lower than the actual $\delta^{15}N$ of Maryland precipitation NO_3^-, the $\delta^{15}N$ of the organic contaminant would have to be lower than -4‰. The observed differences in $\delta^{15}N$ may also be the result of a scale contraction in the denitrifier method results.

Although both the $AgNO_3$/decomposition and denitrifier methods measure the $\delta^{18}O$ of nitrate standards accurately and precisely (CASCIOTTI et al., 2002), previous studies reveal there may be differences between atmospheric nitrate measurements obtained by these techniques. The $\delta^{18}O$ of atmospheric nitrate measured by nitrate salt/ decomposition methods ranges from +17 to +77‰, whereas the $\delta^{18}O$ of atmospheric nitrate measured by denitrifier ranges from +57 to +90‰. The lower and mid-range values of the nitrate salt/decomposition methods may be the result of organic compounds with lower $\delta^{18}O$ values contaminating prepared nitrate salts (KENDALL, 1998). To date, there have been no published comparisons of the isotope ratios of atmospheric nitrate measured by the $AgNO_3$/decomposition and the denitrifier methods. Analyzing precipitation nitrate from Frederick, Maryland by both methods provided a unique test for the effect of organic contaminants on isotope ratio measurements.

There were large and inconsistent differences between the $\delta^{18}O$ measurements obtained using the $AgNO_3$/ decomposition and denitrifier methods. In general, the $\delta^{18}O$ values from the denitrifier method were significantly higher than from the $AgNO_3$/decomposition method. The differences between the two methods were inconsistent, and some of the differences between measurements were nearly 30‰.

There was not a strong linear correlation (0.41) between the $\delta^{18}O$ values measured by the two methods (Figure 9).

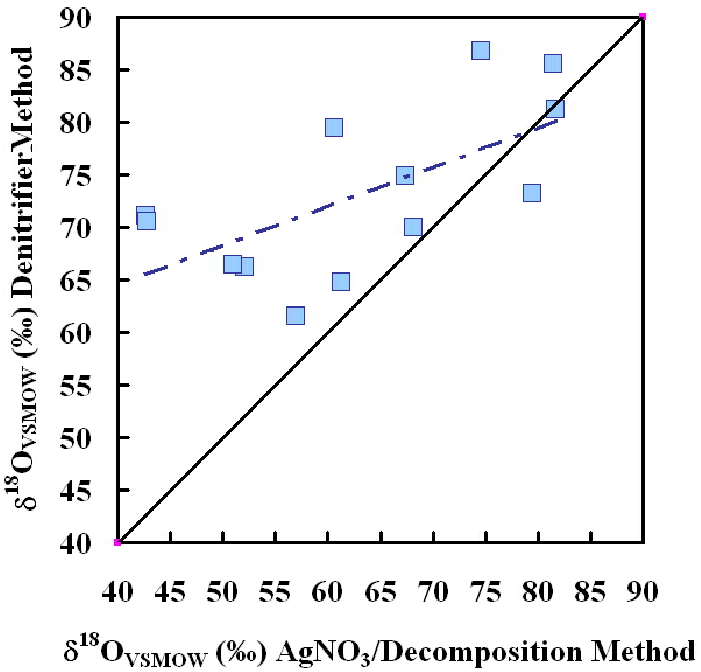

Figure 9: $\delta^{18}O$ versus $\delta^{18}O$ obtained using the $AgNO_3$/decomposition and denitrifier techniques. Error bars represent 1σ mass spectrometric reproducibility of nitrate standards. The data obtained using the $AgNO_3$/decomposition method are averages of duplicate analyses. The solid line is the 1:1 line, and the dashed line shows the linear regression of the data ($y=0.37x+49.63$, $r^2=0.41$).

The most plausible explanation for the differences between the $\delta^{18}O$ obtained using the two techniques is the effect of organic contamination on the $\delta^{18}O$ results from the $AgNO_3$/decomposition method. "On-line" combustion methods accurately measured the $\delta^{18}O$ of the total oxygen in the samples introduced to the TC/EA. When impure samples were analyzed, the results were actually the weighted sums of the contaminants and the precipitation NO_3^-.

Heaton and coworkers (2004) considered the deviation of N/O of the prepared silver nitrates from the N/O of pure silver nitrate (0.33) in order to correct $\delta^{18}O$

values. The prepared silver nitrates were a mix of snow nitrate and an organic contaminant. Heaton and coworkers used +25‰ as the value for the organic end-member, which was the $\delta^{18}O$ of "brown organic particles" present in their prepared silver nitrates. On a plot of $\delta^{18}O$ of silver nitrates versus measured N/O, they extrapolated from an organic end-member through sample measurements to N/O of 0.33 to determine the $\delta^{18}O$ of uncontaminated arctic snow nitrate. Uncorrected $\delta^{18}O$ values ranged from +42.1 to +70.8‰, while the corrected $\delta^{18}O$ values ranged from approximately +60 to +85‰ (HEATON et al., 2004). The correction method of Heaton and others (2004) was applied to the data set for Frederick precipitation NO_3^- samples (Figure 10).

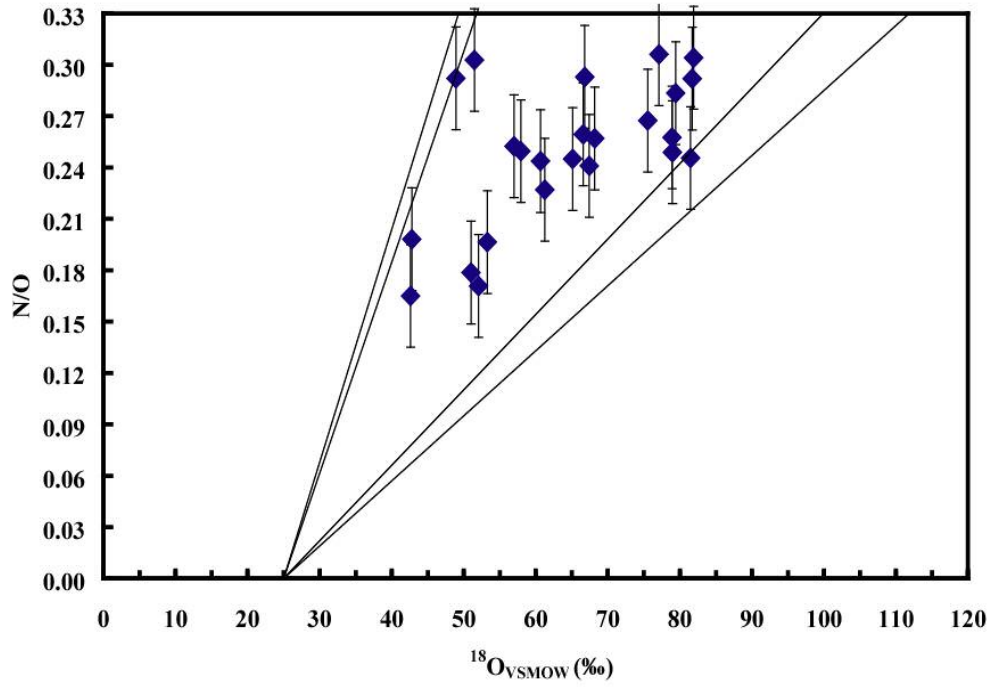

Figure 10: Data correction method used by Heaton et al. (2004) applied to Frederick, Maryland precipitation samples. Error bars for N/O are 0.08 (1σ) and were calculated as described in the text. Error bars for $\delta^{18}O$, which represent the 1σ reproducibility of standards, are smaller than the data symbols.

The corrected range of $\delta^{18}O$ values was +52‰ to +101‰ with uncertainties related to the precision of N/O. Heaton and coworkers (2004) did not include error bars on their N/O or describe ways to address uncertainties associated with their correction method. In our study, N and O were measured during separate runs using the TC/EA and continuous flow mass spectrometry. We determined the uncertainty of N/O by dividing randomly selected mole% N values of nitrate standards (calculated from measured wt% O values) by randomly selected mole% O values of nitrate standards (calculated from measured wt % O values). One standard deviation of the calculated N/O values was 0.08. The uncertainty on the "corrected range" of $\delta^{18}O$ values was determined by extrapolating through the error bars to N/O of 0.33. Considering the uncertainties of N/O, the range of $\delta^{18}O$ values is from +50 to +113‰. This calculated range is significantly wider than the range measured for $\delta^{18}O$ using the denitrifier method.

6.2. Negligible effect of scavenging processes on isotope ratios

When considering the isotopic composition of precipitation NO_3^-, which is only a portion of the total NO_3^- deposited from the atmosphere, there are additional variables to consider. Reactive nitrogen compounds are constantly being removed from air masses via dry deposition. Recent studies on the $\delta^{15}N$ of size-segregated aerosol NO_3^- (YEATMAN et al., 2001; YEATMAN et al., 2001; YEATMAN et al., 2001) have also taken into consideration the report by Spokes and coworkers (2000) that dry deposition and precipitation selectively removes coarse-mode aerosol NO_3^-. Furthermore, as Eriksson (1959) first emphasized, precipitation does not

quantitatively remove NO_y from the atmosphere, and isotope fractionation likely occurs during scavenging. Heaton (1987) showed that the amount of recent rainfall had an effect on the $\delta^{15}N$ of precipitation NO_3^-. Precipitation NO_3^- from storms that followed periods of heavy precipitation exhibited lower $\delta^{15}N$ values than precipitation NO_3^- from events that occurred after periods of lighter precipitation. Within storm variations in the $\delta^{15}N$ of precipitation NO_3^- have also been reported (HEATON, 1987; MOORE, 1974). While the results of Moore (1974) were not straightforward, Heaton (1987) found that during the course of a rain event, there was an increase in the $\delta^{15}N$ of precipitation NO_3^-. In addition, a study in Guiyang, China (XIAO and LIU, 2002) showed that mean $\delta^{15}N$ values for light rainfalls were significantly lower than the mean $\delta^{15}N$ for heavy rainfalls, although the causes for this difference were unclear.

If in- and below-cloud scavenging processes have a major effect on isotope ratios, then there may be a relationship between the amounts of precipitation and the $\delta^{15}N$, $\delta^{18}O$, and $\Delta^{17}O$ values. There may also be a relationship between the amounts of precipitation recently fallen and the isotope ratios. Concentration data may also provide information useful for assessing the role of scavenging processes. Scavenging processes may contribute to a relationship between ion concentrations, but there are numerous factors that influence concentrations that likely affect different ions in variable ways. Heavy precipitation events may yield lower ion concentrations than light precipitation. The time between precipitation events may also influence ion concentrations because wet periods minimize the build up of trace gases and aerosols and because less frequent washout during dry periods leads to higher ion concentrations in individual precipitation events. Rates of dry deposition, which are

influenced by many factors, may also affect ion concentrations in precipitation because they control the background atmospheric NO_y levels.

Although the role of below cloud scavenging processes is difficult to asses, there is no evidence that scavenging processes have a major effect on isotope ratios. The lack of correlation between concentration data and between concentration and isotope ratios supports the hypothesis that scavenging processes were unlikely the primary control on isotopic compositions.

Previous studies considered the effect of recent rainfall on nitrogen isotope ratios. Heaton (1987) showed that $\delta^{15}N$ values were influenced by the amount of recent rainfall. It was not possible to evaluate our data using amounts of recent rainfall because quantitative rainfall totals were unavailable from nearby weather stations (see section 4.2). For the most part, the sampling period for the Frederick, Maryland study was characterized by frequent rain events. It would be interesting to compare this set of samples to samples collected during drier sampling periods.

There was one instance in which we were able to evaluate isotopic changes during a storm. For the storm collected from 5-15-03 to 5-18-03, there were separate collections of the first part of the storm and the second part of the storm. Precipitation nitrate from the second part of the storm had a higher $\delta^{15}N$ value than the first part of the storm. The observation of higher $\delta^{15}N$ values as the storm progressed were consistent with the trend observed by Heaton (1987). One explanation for lower $\delta^{15}N$ values later in the storm may be that precipitation removes coarse-fraction aerosol NO_3^-, which tend to have lower $\delta^{15}N$ values (closer to precipitation NO_3^-), more readily than fine-fraction aerosol NO_3^-, which generally

have higher $\delta^{15}N$ values (FREYER, 1991). As storms progress, there is less coarse-fraction aerosol NO_3^- remaining in the atmosphere. With less coarse-fraction aerosol NO_3^- contributing to precipitation NO_3^-, the $\delta^{15}N$ values of precipitation NO_3^- decrease. Other causes for this effect may be due to isotope fractionation associated with the dissolution of NO_y species into rain droplets.

6.3. Influences on the $\delta^{15}N$ of precipitation nitrate

Both the $AgNO_3$/decomposition and denitrifier methods revealed seasonal variation in the $\delta^{15}N$ of precipitation nitrate from Frederick, Maryland (Figure 11). Values in the winter were significantly higher than values in summer.

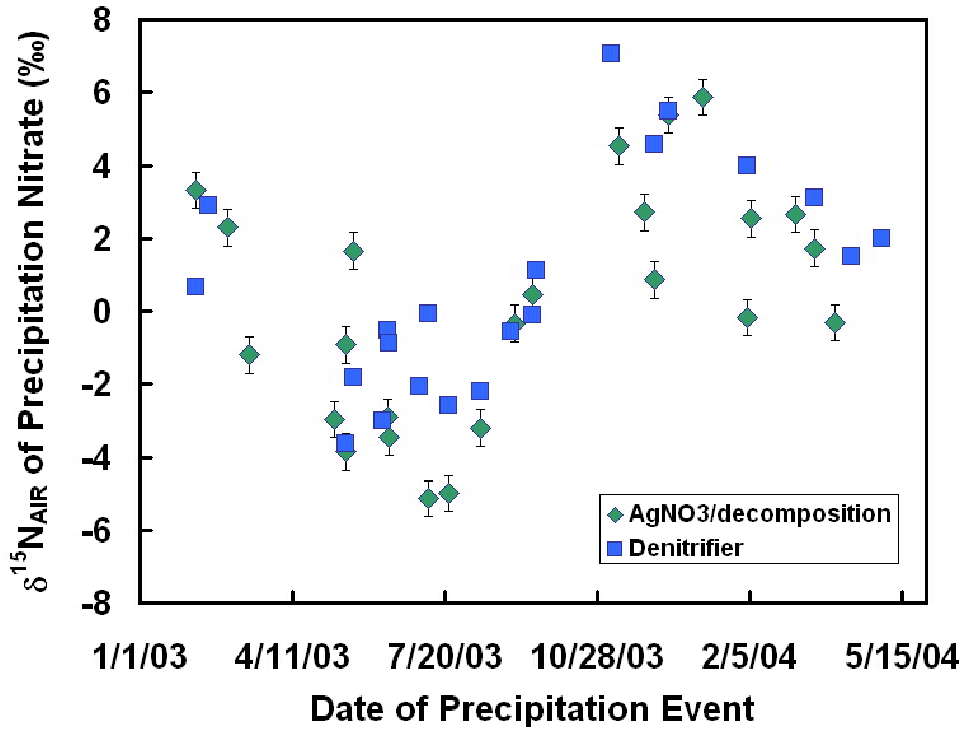

Figure 11: The $\delta^{15}N$ of precipitation nitrate versus date for the $AgNO_3$/decomposition and denitrifier methods. Error bars represent the 1σ reproducibility of nitrate standards, and error bars for the denitrifier method are smaller than the data symbols. The data for the $AgNO_3$/ decomposition method are averages of duplicate analyses.

The $\delta^{15}N$ of precipitation nitrate may reflect the $\delta^{15}N$ of precursor NO_x and/or nitrogen isotope fractionation processes. If the $\delta^{15}N$ of precursor NO_x is the major factor determining the $\delta^{15}N$ of atmospheric NO_3^-, then the seasonal variation may be due to changes in the dominant NO_x formation processes. There may also be a relationship between the $\delta^{15}N$ of precipitation nitrate and storm track data. A seasonal pattern in air mass movements could possibly be the cause for the seasonal variations in $\delta^{15}N$. In addition, if the precursor NO_x and SO_x come from similar sources and if sources are key in understanding the isotopic compositions of precipitation nitrate and sulfate, then there may also be a relationship between the $\delta^{15}N$ of nitrate and the $\delta^{34}S$ of sulfate in the precipitation. On the other hand, if there are no seasonal patterns in NO_x sources or storm track data, then the $\delta^{15}N$ of NO_x of precipitation nitrate may vary seasonally as a result of seasonal changes in atmospheric chemistry that affect nitrogen isotope fractionation.

6.3.1. Effect of precursor NO_x on the $\delta^{15}N$ of precipitation nitrate

If the majority of NO_x is deposited in the region where the NO_x was produced, then the $\delta^{15}N$ of atmospheric nitrate would reflect the $\delta^{15}N$ of the precursor NO_x. Since there is evidence that NO_x produced by different processes have characteristic $\delta^{15}N$ ranges (HEATON, 1987; 1990), the $\delta^{15}N$ of atmospheric NO_3^- could provide information about the relative significance of different NO_x sources (HASTINGS et al., 2003; RUSSELL et al., 1998). While NO_x produced by different processes may also have different oxygen isotope ratios (KENDALL, 1998), the $\delta^{18}O$ and $\Delta^{17}O$ of atmospheric NO_3^- most likely do not reveal the signature of the precursor NO_x

because oxygen atoms are transferred back and forth from O_3 during NO_x cycling (HASTINGS et al., 2003; MICHALSKI et al., 2003).

The $\delta^{15}N$ of total NO_x introduced to a particular air mass ($\delta^{15}N_T$) can be represented as the weighted sum of the $\delta^{15}N$ of NO_x by the major producers, including automobiles ($\delta^{15}N_a$), power plants ($\delta^{15}N_{pp}$), non-utility industries ($\delta^{15}N_i$), biomass burning ($\delta^{15}N_{bb}$), microbial production ($\delta^{15}N_{mp}$), and lightning ($\delta^{15}N_l$), by

$$\delta^{15}N_T \times N_T \approx \delta^{15}N_a \times N_a + \delta^{15}N_{pp} \times N_{pp} + \delta^{15}N_i \times N_i + \delta^{15}N_{bb} \times N_{bb} + \delta^{15}N_{mp} \times N_{mp} + \delta^{15}N_l \times N_l,$$

where N is the number of moles of NO_x or the fraction of the total NO_x.

According to the Maryland Department of the Environment (M.D.E., 2002-2005), approximately 46% of NO_x in the Baltimore area in the summer of 1990 was produced by internal combustion engines in "off-road" and "on-road" mobile sources, and 38% was generated by power plants. Manufacturing industries accounted for roughly 8% of the NO_x and the remaining 8% was attributed to unlisted sources. The mass balance calculation for Maryland precipitation nitrate using these estimates can be written as

$$\delta^{15}N_T \approx \delta^{15}N_a \times 0.46 + \delta^{15}N_{pp} \times 0.38 + \delta^{15}N_i \times 0.08 + \delta^{15}N_{\text{unlisted sources}} \times 0.08$$

Different processes may produce NO_x with characteristic nitrogen isotope compositions (section 3.3.1). In summary, measurements of automobile exhaust range from –13‰ to +2‰, while data on coal-fired power plant exhaust ranges from +5 to +13‰. Hoering (1957) provided evidence that the $\delta^{15}N$ of electrical discharge and possibly lightning NO_x is near 0‰, and researchers have speculated that the $\delta^{15}N$ of microbial NO_x is negative and potentially lower than -15‰ (e.g., Moore, 1977). Assuming that $\delta^{15}N_i$ exhibits the same range as power plants and that the majority of

the uncharacterized 8% exhibits a $\delta^{15}N$ of 0‰ (e.g., lightning), then roughly half of the NO_x would have the composition of the NO_x of mobile sources and half would have the composition of power plants. The total $\delta^{15}N$ during the summer would be an average of the $\delta^{15}N_a$ (-13 to +2) and $\delta^{15}N_{pp}$ (+6 to +13‰), which would be -3.5‰ using the lowest values in the ranges and +7.5 using the highest values in the ranges.

In Maryland and the surrounding regions, production of NO_x by utilities remains relatively constant throughout the year because residents rely on power plants to generate electricity for heating and air conditioning. In general, NO_x from mobile sources is highest during the summer and lowest during the winter. Typically, increased thunderstorm activity during the summer leads to more NO_x produced by lightning. Microbial NO_x may also be higher in the spring and summer due to increased biological activity. Since the $\delta^{15}N$ values typical of NO_x from mobile sources, lightning, and biological activity are all lower than the $\delta^{15}N$ values of power plants, the total $\delta^{15}N$ of NO_x introduced to air masses may be lower in the summer than the winter due to seasonal changes in NO_x formation processes.

6.3.2. Comparison of the $\delta^{15}N$ of nitrate and storm track data

The movement of air masses can transport NO_x away from the sites of NO_x generation. Therefore, the $\delta^{15}N$ of precipitation nitrate may not reflect the $\delta^{15}N$ of NO_x produced in that region, but rather the NO_x produced in the region where the air mass presided the day before. Using reported ranges for the $\delta^{15}N$ of NO_x produced by the major formation processes and estimates, previous studies have qualitatively determined the relative contributions of NO_x sources to different regions. In

particular, investigators have hypothesized that if the $\delta^{15}N$ of precursor NO_x is the main control on the $\delta^{15}N$ of atmospheric NO_3^-, there would likely be a relationship between the $\delta^{15}N$ of precipitation NO_3^- and the source regions for the storm's air masses. For individual storm events, the location of the air masses can be traced back to their locations on the previous days using models, such as the NOAA Air Resources Laboratory HYSPLIT model.

An investigation of N deposition to Lewes, Delaware considered the relationship between air source regions and the concentration and $\delta^{15}N$ of precipitation NO_3^- (RUSSELL et al., 1998). Of the five dominate directions of air transport to the region, the largest fluxes of NO_3^- were attributed to air masses from the south. These southerly air masses were slow moving and were associated with large amounts of precipitation. The next largest fluxes were from the northwest, followed by the west and then the southwest. The lowest fluxes were from easterly air masses, most likely because of relatively low emissions over the ocean. The median $\delta^{15}N$ values for the different clusters were not statistically different and ranged from -1.3 to +0.5‰ with an overall range of $\delta^{15}N$ values from -4.0 to +4.4‰. The authors concluded that fossil fuel combustion represented the greatest source of NO_x. Higher NO_3^- concentrations during the spring were attributed to increased inputs from soil emissions, which were possibly related to agricultural activities. Although there was not a statistically significant difference, the median $\delta^{15}N$ value was also lower for spring than the other seasons, which could represent a microbial NO_x source characterized by negative $\delta^{15}N$.

Other studies have observed an effect of seasonal patterns in the movement of air masses on the $\delta^{15}N$ of atmospheric NO_3^-. Hastings and coworkers (2003) interpreted their observed seasonal variation in $\delta^{15}N$ of Bermuda rain NO_3^- using storm track data. In the cool season (mean $\delta^{15}N$ = -5.9‰), the majority of air masses that contributed to Bermuda's storms were transported from the North American continent. The lower $\delta^{15}N$ of cool season precipitation NO_3^- were explained by higher contributions of NO_x from anthropogenic emissions, particularly automobiles with negative $\delta^{15}N$ values. During the warm season (mean $\delta^{15}N$ = -2.1‰), many of Bermuda's air masses originated over the oceans. The mean $\delta^{15}N$ value closer to 0‰ was attributed to higher contributions of lightning-derived NO_x. Yeatman and colleagues (2001) also showed that there was a difference between the mean $\delta^{15}N$ of aerosol NO_3^- at a coastal site in Weybourne, England depending on whether the air masses originated in northern UK (+15±3‰) or southern UK (10±3‰). Higher $\delta^{15}N$ in air masses from northern UK were attributed to more NO_x from industrial activity.

For Frederick, Maryland samples, the observed variation in the $\delta^{15}N$ of precipitation nitrate could not be explained using storm track data alone. Whereas there was a seasonal pattern in the $\delta^{15}N$ values (Figure 11), there was a significant amount of within-season variation in the storm track data (Table 1).

6.3.3. Comparison of the $\delta^{15}N$ of nitrate to the $\delta^{34}S$ of sulfate

Whereas the $\delta^{15}N$ of precipitation nitrate varied seasonally, the $\delta^{34}S$ of precipitation sulfate remained relatively constant throughout the sampling period (Figure 12). Atmospheric sulfate is the result of the atmospheric oxidation of SO_2.

Similar to the $\delta^{15}N$ of atmospheric NO_3^-, the $\delta^{34}S$ of SO_2 may reflect the isotopic composition of the gaseous precursor or atmospheric fractionation processes. The $\delta^{34}S$ of sulfate may reflect the relative contributions of atmospheric sulfur compounds from coal combustion, biogenic emissions, and ocean sources (Xiao and Liu 2002).

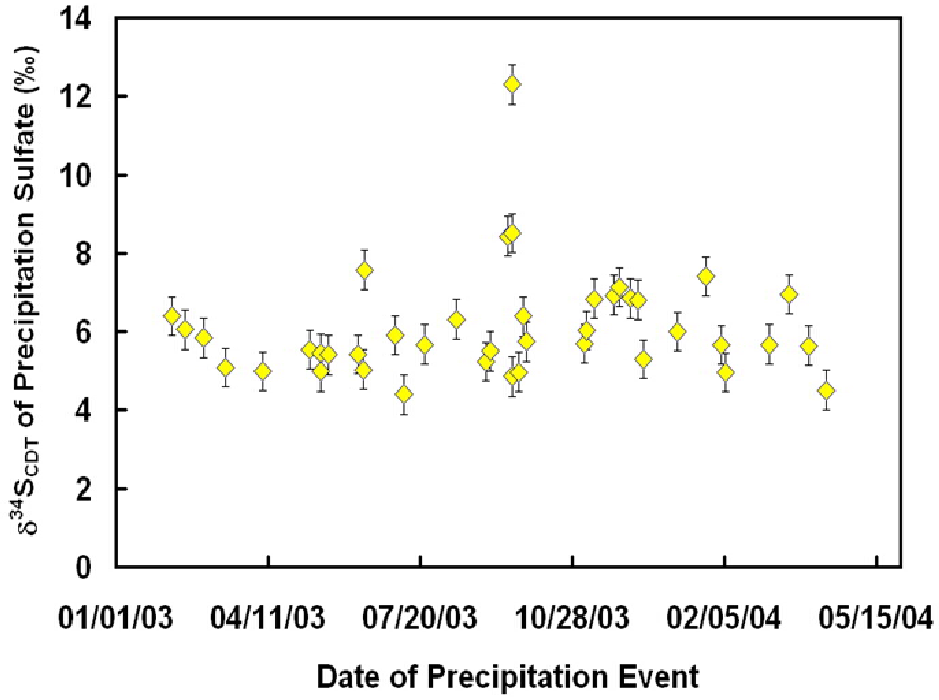

.

Figure 12: The $\delta^{34}S$ of Frederick, MD precipitation sulfate versus time obtained using an elemental analyzer coupled to a continuous flow isotope ratio mass spectrometer. Error bars represent 1σ mass spectrometric reproducibility of NBS-127 sulfate standard. Typically, two standards were measured before and after every set of six samples. The $\delta^{34}S$ data are averages of duplicate analyses.

The three samples that had $\delta^{34}S$ values higher than 8‰ were from Hurricane Isabel in September 2003 and were collected in a time series. The higher $\delta^{34}S$ values could be associated with the hurricane samples containing more sulfur derived from ocean sources, which may have higher $\delta^{34}S$ values than coal combustion or biogenic emissions (Xiao and Liu 2002). As the storm progressed the $\delta^{34}S$ of precipitation

sulfate increased. The direction of the isotope effect observed in sulfur isotope ratios as the storm progressed was the same as the isotope effect in the nitrogen isotope ratios of nitrate during the May 15-18th storm described previously.

There was no correlation between the $\delta^{15}N$ of nitrate and the $\delta^{34}S$ of sulfate in Frederick precipitation. If the processes that produced NO_x and SO_x varied seasonally and if their isotopic compositions were determined by formation processes, there would likely have been a relationship between nitrate and sulfate isotope ratios. Lack of correlation between the $\delta^{15}N$ of nitrate and storm track and the $\delta^{15}N$ of nitrate and the $\delta^{34}S$ of sulfate provides evidence that precursor NO_x is not the only relevant parameter influencing $\delta^{15}N$ values.

6.3.4. Influence of isotope fractionation on the $\delta^{15}N$ of nitrate

Although the observed seasonal variation in Frederick, Maryland precipitation nitrate may be the result of changes in the contributions from different NO_x producers, such as automobiles, power plants, and lightning channels, there is evidence that the seasonal changes in NO_x chemistry affect atmospheric nitrogen isotope fractionation. The seasonal variation observed in the $\delta^{15}N$ was similar to the patterns shown in previous investigations. Figure 13 shows mean seasonal $\delta^{15}N$ values plotted along with data taken from the literature. With the exceptions of the data reported by Hastings et al. (2003) and Russell et al. (1998), the highest $\delta^{15}N$ values were measured in winter atmospheric nitrate and the lowest $\delta^{15}N$ values were measured in summer atmospheric nitrate at all of the locations.

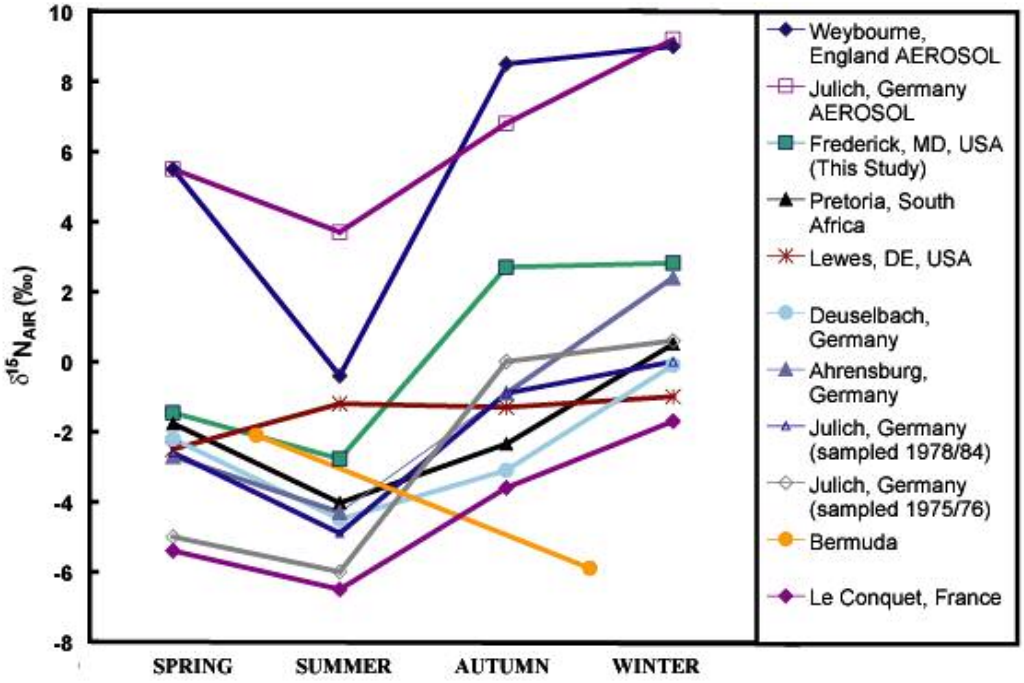

Figure 13: Comparison of seasonal $\delta^{15}N$ variation in Frederick precipitation nitrate to observations of previous studies. Unless indicated as "AEROSOL," the measurements are of precipitation nitrate. Data on Weybourne, England (Yeatman et al. 2001), Frederick, MD (this study) Pretoria, South Africa (Heaton, 1987), and Julich, Deuselbach, and Ahrensburg, Germany, and Le Conquet, France (Freyer, 1991) are mean seasonal values. Data on Lewes, DE (Russell et. al 1998) are median seasonal values. Bermuda rain data (Hastings et al. 1003) are mean values for the warm and cool seasons.

The seasonal pattern observed in Frederick, Maryland has also been identified at number of international locations, including Ahrensburg and Deuselbach, Germany and Le Conquet, France in the northern hemisphere (FREYER, 1991) and Pretoria, South Africa in the southern hemisphere (HEATON, 1987). At the time of the studies, Pretoria had significantly less industry and more lightning than Jülich. The finding that both regions exhibited the same seasonal signature despite largely different NO_x sources provides support for an explanation related to seasonal changes in atmospheric chemistry. The seasonal pattern of the highest $\delta^{15}N$ values in the winter

and the lowest $\delta^{15}N$ values in the summer was also observed in aerosol NO_3^- from the coastal site of Weybourne, England (YEATMAN et al., 2001).

Freyer and others (1993) postulated that seasonal changes in the photochemical steady-state conditions of NO and NO_2 or NO_x oxidation pathways were responsible for the variation in the $\delta^{15}N$ of aerosol and precipitation NO_3^-. Within minutes of entering the atmosphere during the day, NO reaches chemical equilibrium with NO_2 due to rapid NO_2 photolysis and reaction of NO with O_3 to regenerate NO_2. There are seasonal changes in atmospheric chemistry that affect the NO_x photochemical stationary state. During the summer, higher O_3/NO_x ratios cause the majority of NO_x to be in the form of NO_2, while lower O_3/NO_x ratios in the summer result in higher concentrations of atmospheric NO.

Freyer and coworkers (1993) measured NO_x ($NO+NO_2$), NO_2, and O_3 concentrations and the $\delta^{15}N$ of NO_x and NO_2 in Jülich, Germany during 1988-1991. The absolute values for the $\delta^{15}N$ of NO_2 were 4-6‰ lower than aerosol NO_3^- and 2-4‰ higher than precipitation NO_3^- determined in Jülich during earlier sampling periods (1975/1976 and 1979/1984) (FREYER, 1991). There was a linear relationship between daily NO_2/NO_x and $\delta^{15}N$ ($r^2=0.94$) with lower NO_2/NO_x and higher $\delta^{15}N$ in the winter and higher NO_2/NO_x and lower $\delta^{15}N$ in the summer. The hypothesis offered by Freyer and others (1993) involved the exchange reactions between NO and NO_2 shown below, where *k*+ and *k*- are rate constants.

Since only one N atom is

$$^{15}NO + {}^{14}NO_2 \xrightarrow{k+} {}^{14}NO + {}^{15}NO_2$$
$$^{14}NO + {}^{15}NO_2 \xrightarrow{k-} {}^{15}NO + {}^{14}NO_2$$

being exchanged the equilibrium constant, K_{eq}, and equilibrium fractionation factor α_{eq} are the same for this reaction.

$$K_{eq} = \frac{k+}{k-} = \frac{[^{14}NO][^{15}NO_2]}{[^{15}NO][^{14}NO_2]} = \alpha_{eq} = \frac{\beta(NO_2)}{\beta(NO)}$$

Using the β-factors tabulated by Richet et al. (1977), the α_{eq} for this exchange reaction is 1.044 at 0°C. Freyer and coworkers (1993) assumed that oxidation of NO to NO_2 by HO_2 and RO_x is minor relative to oxidation by O_3. During the summer, most NO is oxidized to NO_2 by O_3 due to high O_3 concentrations and the $\delta^{15}N$ of NO_2 reflects the $\delta^{15}N$ of NO_x. During the winter, NO and NO_2 coexist because O_3 concentrations are insufficient to completely oxidize NO to NO_2. As a result of equilibrium isotope exchange, the $\delta^{15}N$ of NO_2 increases as the $\delta^{15}N$ of NO decreases. Then, NO_2 with higher $\delta^{15}N$ values undergoes further transformations that result in aerosol and precipitation NO_3^- with higher $\delta^{15}N$ values than the precursor pool of NO_x. The remaining NO may get transported away from the region of NO_x formation.

6.4. Influences on the $\delta^{18}O$ and $\Delta^{17}O$ of precipitation nitrate

While there are differences between the $AgNO_3$/decomposition and denitrifier methods, the $\delta^{18}O$ of precipitation nitrate obtained using both methods exhibited seasonal variation with higher $\delta^{18}O$ in the winter and lower $\delta^{18}O$ in the summer (Figure 14). There is more within-season variation in the $AgNO_3$/decomposition results, most likely as a result of the inconsistent effects of organic contamination.

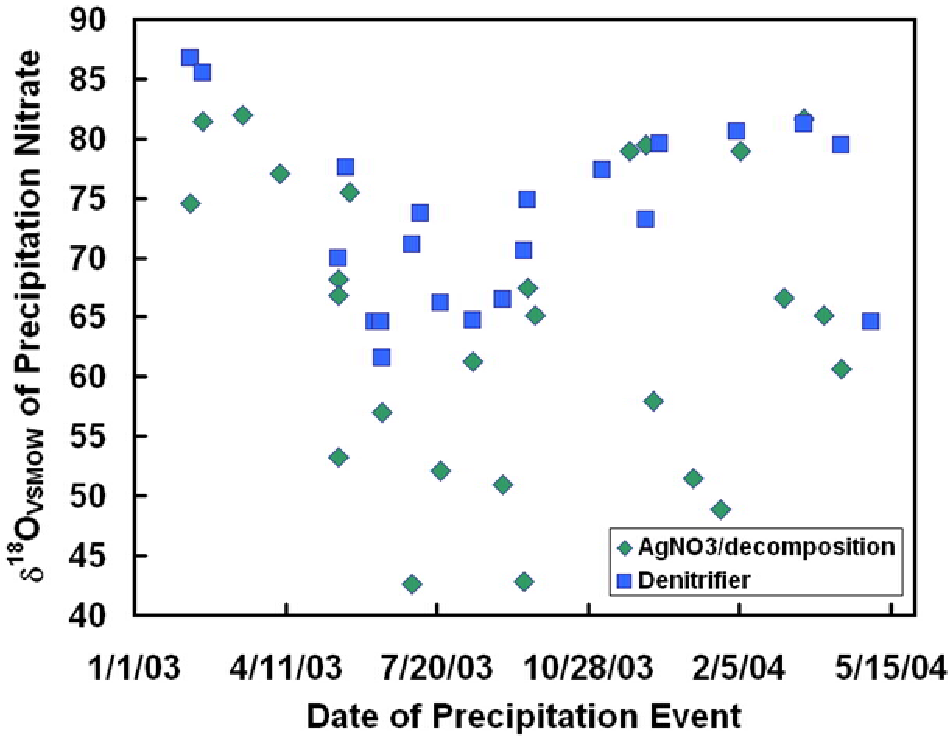

Figure 14: A plot of $\delta^{18}O$ versus date for two independent methods. Error bars representing the 1σ reproducibility of nitrate standards are smaller than the data symbols. The data for the $AgNO_3$/ decomposition method are averages of duplicate analyses.

The seasonal variation observed in the $\delta^{18}O$ of Frederick precipitation nitrate samples was consistent with the results of previous investigations. Analyses of throughfall NO_3^- in Bavaria Germany showed that the lowest $\delta^{18}O$ values occur in the summer (DURKA et al., 1994; VOERKELIUS, 1990). Data on throughfall and precipitation NO_3^- in Leading Ridge, Pennsylvania and Fernow, West Virginia also varied seasonally with the highest $\delta^{18}O$ values in winter samples and the lowest values in summer samples. (WILLIARD et al., 2001). Slightly different ranges for rain NO_3^- (+40 to +65‰) and snow NO_3^- (+50 to +70) appeared in data from Loch Vale, Colorado (CAMPBELL et al., 2002), and the mean $\delta^{18}O$ for rain NO_3^- (+58‰) was

significantly different than the mean $\delta^{18}O$ for snow NO_3^- (+67‰) in New Hampshire (PARDO et al., 2004). Bermuda rain NO_3^- also showed seasonal variation with warm season samples averaging +68.6‰ and cool season samples averaging +79.6‰ (HASTINGS et al., 2003). At Summit Greenland, the mean $\delta^{18}O$ of summer samples was +69.8‰, while the mean $\delta^{18}O$ of winter samples was +77.5‰ (HASTINGS et al., 2004).

The $\Delta^{17}O$ of precipitation nitrate in Frederick, Maryland also revealed a trend of higher values in the winter and lower values in the summer (Figure 15), which is the seasonal pattern reported by Michalski and coworkers (2003) for aerosol nitrate from La Jolla, CA. The range of $\Delta^{17}O$ values for this study (+15.3±0.05‰ to +31.7±0.05‰) is wider than the range reported by Michalski et al. (2003) of +15.3 to +30.1‰, which may be the result of the effect organic contamination on $\Delta^{17}O$.

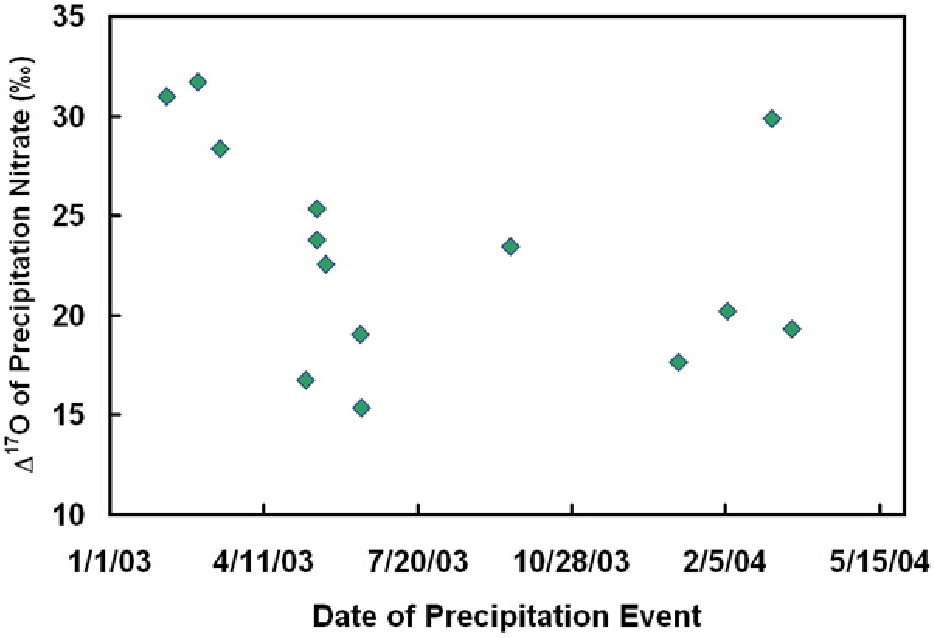

Figure 15: $\Delta^{17}O$ of Frederick, MD precipitation NO_3^- versus time. Error bars representing 1σ reproducibility of standards are smaller than the data symbols

Michalski and others (2003) successfully reproduced their $\Delta^{17}O$ measurements of aerosol nitrate using a $\Delta^{17}O$ isotope fractionation model that was coupled to a photochemical box model for the polluted marine boundary layer (PMBL). They showed that atmospheric NO_3^- exhibited positive $\Delta^{17}O$ values because of the transfer of oxygen atoms from ozone (O_3). The $\Delta^{17}O$ of atmospheric NO_3^- depends on the number of oxygen atoms derived from tropospheric O_3, which has $\Delta^{17}O$ as high as 35‰ (Krankowsky et al. 1995), compared to the $\Delta^{17}O$ of other atmospheric oxidants, such as the peroxy radical (HO_2), organic peroxy radicals (RO_x), hydroxyl radical (OH), and H_2O, which are close to zero. The qualitative observations made for Frederick, MD precipitation oxygen isotopes were consistent with their model.

Seasonal variations in the $\delta^{18}O$ and $\Delta^{17}O$ of atmospheric NO_3^- were likely the result of different proportions of the three major nitrate production pathways (Figure 16). The pathways with greater contributions of oxygen atoms from ozone result in atmospheric nitrate with higher $\delta^{18}O$ and $\Delta^{17}O$ values. While some NO gets oxidized to NO_2 by the oxidants the peroxy radical (HO_2) or organic peroxy radicals (RO_x), generally the oxygen atoms in NO_2 are from O_3. In pathway #1, the third oxygen atom is derived from they hydroxyl radical (OH), which has a $\Delta^{17}O$ close to zero. Therefore, only 2/3 of the oxygen atoms in nitrate are derived from ozone. In the case of pathway #2, all six of the oxygen atoms can possibly be from O_3. In the case of pathway #3, as much as 5/6 of the oxygen atoms in atmospheric nitrate can be derived from O_3, with only 1/6 derived from H_2O.

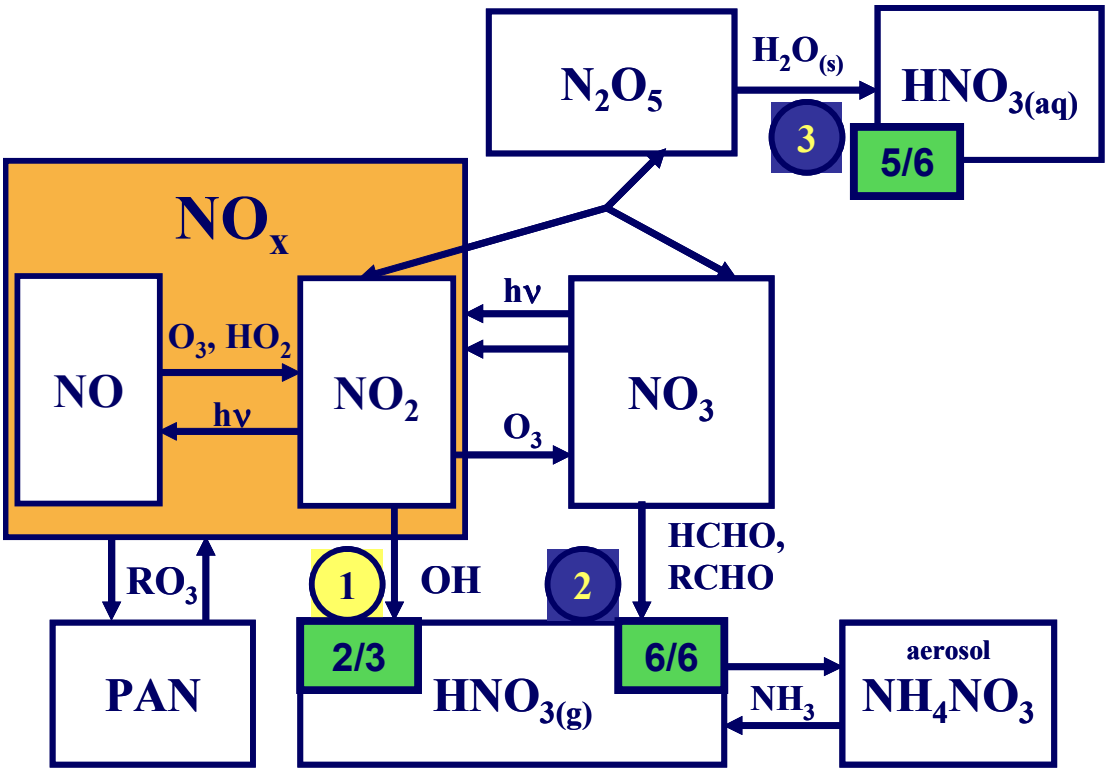

Figure 16: Atmospheric reaction pathway with estimates of the maximum number of oxygen atoms transferred from ozone to atmospheric nitrate. Pathway #1, which dominates daylight (and summer) chemistry results in nitrate with a maximum of 2/3 oxygen atoms from ozone (lower $\delta^{18}O$ and $\Delta^{17}O$ values). Pathways #2 and #3 become more important during nighttime (and winter) chemistry and produce nitrate with a maximum of 3/3 and 5/6 oxygen atoms from ozone, respectively (higher lower $\delta^{18}O$ and $\Delta^{17}O$ values).

The oxygen isotope observations made for Frederick precipitation nitrate can be explained by seasonal changes in NO_x oxidation chemistry. Since the majority of nitric acid forms by pathway #1 in the summer, the $\delta^{18}O$ and $\Delta^{17}O$ of precipitation nitrate are lower. In the winter, higher contributions of nitric acid formation by pathways #2 and #2 lead to increased $\delta^{18}O$ and $\Delta^{17}O$ values.

7. Conclusions

The comparison of the $AgNO_3$/decomposition and denitrifier methods showed that the results of the decomposition method were affected by the presence of organic contaminants in the prepared silver nitrates. Some of the organic contaminants were added during the analytical procedure. Contamination likely occurred as a result of sulfonic acid leaching from the silver resin used to remove chloride and produce $AgNO_3$. Incomplete removal of organic compounds from the precipitation itself added to the contamination issues. Researchers using the $AgNO_3$/decomposition method in the future should develop a method of removing organic contaminants prior to freeze-drying the prepared $AgNO_3$ solutions or devise an approach to correct measurements for organic contamination. Some of the advantages to using the denitrifier method in future studies include smaller sample size requirements and the absence of issues associated with organic contamination.

Precipitation nitrate exhibited the highest $\delta^{15}N$, $\delta^{18}O$, and $\Delta^{17}O$ values in the winter and the lowest values in the summer. Source regions of air masses were not primarily responsible for the observed isotope variations. While $\delta^{15}N$, $\delta^{18}O$, and $\Delta^{17}O$ varied seasonally, storm track data for the Frederick storm events showed that the geographical origins of the air masses varied within seasons. Below cloud scavenging processes were also unlikely the major determinants of isotope ratios. There were no observable relationships between isotope ratios and concentration data as there would be if isotope ratios were primarily determined by nitrate removal rates via dry or wet deposition.

Whereas the $\delta^{34}S$ of precipitation sulfate remained constant with the exception of hurricane samples, the $\delta^{15}N$ of precipitation nitrate varied seasonally, and there was no relationship between the $\delta^{15}N$ of precipitation nitrate and the $\delta^{34}S$ of precipitation sulfate. If the isotopic composition of precursor NO_x and SO_2 were the major determinants of the $\delta^{15}N$ of precipitation nitrate and the $\delta^{34}S$ of precipitation sulfate, and if processes contributed similar proportions of the total atmospheric NO_x and SO_2, then there would be a relationship between these parameters.

The most likely causes for the observed variations in $\delta^{15}N$, $\delta^{18}O$, and $\Delta^{17}O$ were seasonal variations in atmospheric chemistry that influenced nitrogen isotope fractionation processes and the dominant oxidation pathways of nitrate formation. The nitrogen isotope ratios of precipitation nitrate from Frederick, Maryland exhibited the same seasonal pattern as precipitation nitrate from Jülich, Germany (FREYER, 1978; FREYER, 1991) and Pretoria, South Africa (Heaton, 1987) and aerosol nitrate from Weybourne, England (Yeatman et al. 2001). Nitrate in snow and winter rain samples had the highest $\delta^{15}N$ values, while summer rain samples had the lowest $\delta^{15}N$ values. These observations were consistent with the model of Freyer and coworkers (1993), which showed that the $\delta^{15}N$ of NO_2 increased with decreasing atmospheric NO_2/NO_x ratios. Equilibrium isotope exchange between NO and NO_2 during the winter resulted in higher $\delta^{18}O$ values in NO_2 and thus precipitation NO_3^-. Rapid conversion of NO to NO_2 during the summer minimized the effect of equilibrium isotope exchange.

The $\delta^{18}O$ and $\Delta^{17}O$ of Maryland precipitation nitrate showed the same pattern as previous studies (HASTINGS et al., 2003, MICHALSKI et al., 2003). Oxygen isotope

ratios were primarily affected by seasonal changes in the predominant pathways of nitrate formation. The $\delta^{18}O$ and $\Delta^{17}O$ of atmospheric nitrate depends on the proportion of oxygen atoms from O_3, which has significantly higher $\delta^{18}O$ and $\Delta^{17}O$ values than other atmospheric oxidants.

This study provides evidence that atmospheric fractionation processes are relevant in understanding atmospheric NO_3^- isotope ratios. Atmospheric fractionation networks can increase our understanding of atmospheric chemistry in addition to mechanisms of isotope exchange. Increased knowledge about variations in atmospheric NO_3^- as a result of these fractionation networks can also improve our ability to trace atmospheric NO_3^- through watersheds.

Appendix A

The following procedure was used to treat the anion exchange resin AG2X-8 (Cl^- form, 100-200 mesh), purchased from Biorad, prior to use. These methods were adopted from the procedure used by J. Hannon's at the USGS, Reston for anion exchange resin AG1X-8).

1. Weigh out 150g of AG2X-8 into a clean 600mL beaker.
2. Rinse the resin using Millipore water.
    a. Add Millipore water to the resin (150g of AG2X-8 occupies approximately 200mL).
    b. Add approximately 250mL additional Millipore water.
    c. Stir the resin/water mixture.
    d. After allowing the resin to settle for five minutes, pour off the Millipore water and any resin still suspended.
    e. Repeat steps b-e six times.
3. Transfer the resin to a 2.5cm diameter by 50cm column with a clean stop cock attached to the end of the column.
4. Gravity drip 2000mL 1.0 M NaOH through the column (the resin turns a darker orange color as it converts from the Cl^- form to the OH^- form).
5. Gravity drip 1000mL Millipore water through the column.
6. Gravity drip 1000mL 2.0 M HCl (e.g., 168mL concentrated HCl diluted to one liter using Millipore water) through the column to convert the resin back to the Cl^- form. During this step, heat is released and air bubbles form.

7. Shake column gently to release the air bubbles formed during step 6.
8. Gravity drip 2000mL Millipore water through the column.
9. Gravity drip 450mL methanol through the column.
10. Transfer the resin from the column to a clean beaker and allow the resin to air dry at room temperature for approximately one week.
11. Transfer the resin to a clean bottle and store dry.
12. When ready to extract ions from a sample, fill a 1.0cm diameter glass column with a clean stop cock attached to the end of the column with an appropriate amount of AG2X-8 resin:
    a. Estimate the amount of resin needed to accommodate the anions in the sample using concentration data (if available) and the volume of sample being passed through the column (AG2X-8 can accommodate 1200meq per mL resin). Use approximately twice the amount of resin calculated. If no concentration data is available, assume maximum concentration values.
    b. Pipette 1mL of water into a 1.0cm diameter glass column, and mark the outside of the column to indicate the resin bed height that corresponds to 1mL. Continue pipetting particular volumes of water into the column and marking the outside of the column with the corresponding resin bed heights until the column is marked up to 6mL
    c. Use a metal spatula (cleaned with ethanol) to transfer several milliliters of the dry resin to a small clean bottle.
    d. Add Millipore water to the bottle with the dry resin.

e. Fill the marked column halfway with Millipore water.

f. Use a 1-5mL pipette to transfer the appropriate amount of AG2X-8 resin from the bottle to the column. (Pipetting the resin into a column filled with water will decrease the formation of gas bubbles in the resin bed.)

Appendix B

The following procedure was used to treat the cation exchange resin AG50WX-8 (H^+ form, 100-200 mesh), purchased from Biorad, prior to use.

1. Weigh out 150g of AG50WX-8 into a clean 600mL beaker.
2. Rinse the resin using Millipore water.
    a. Add Millipore water to the resin.
    b. Add approximately 250mL additional Millipore water.
    c. Stir the resin/water mixture.
    d. After allowing the resin to settle for one minute, pour off the Millipore water and any resin still suspended.
    e. Repeat steps b-e three times.
3. Transfer the resin to a 2.5cm diameter by 50cm column with a clean stop cock attached to the end of the column.
4. Gravity drip 4L of 4M HCl through the resin packed column at a rate of 50-100 drips per minute.
5. Gravity drip 1L of 1M HCl through the column.
6. Transfer the resin from the column to a clean bottle, storing the resin in 1M HCl.
7. When ready to run the sample through a cation exchange column, fill a 1.5cm diameter glass column with a clean stop cock attached to the end of the column with an appropriate amount of AG50WX-8 resin:

a. Pipette 1mL of water into a 1.5cm diameter glass column with a clean stop cock attached to the end of the column, and mark the outside of the column to indicate the resin bed height that corresponds to 1mL. Continue pipetting particular volumes of water into the column and marking the outside of the column with the corresponding resin bed heights until the column is marked up to 5mL.
b. Fill the marked column halfway with Millipore water.
c. Use a 1-5mL pipette to transfer 5mL AG50WX-8 resin from the storage bottle to the column. (Pipetting the resin into a column filled with water will decrease the formation of gas bubbles in the resin bed.)
d. Gravity drip approximately 250mL Millipore water through the packed column until the pH of the solution coming through the column is 6.0.

Appendix C

The following procedures were used to prepare colorimetric test solutions and to identify the presence of nitrate/nitrite.

1. Prepare the nitrate reducing solution:
    a. Prepare hydrazine sulfate solution:
        i. Dissolve 13.75 g hydrazine sulfate in Millipore water.
        ii. Dilute solution to 500mL using Millipore water.
    b. Prepare $CuSO_4$ solution:
        i. Dissolve 4.00 g $CuSO_4$ in Millipore water.
        ii. Dilute solution to 1000mL using Millipore water.
    c. Prepare the final solution:
        i. Combine 1.35mL hydrazine sulfate solution and 0.80mL $CuSO_4$ solution.
        ii. Dilute solution to 100mL with Millipore water.
    d. The hydrazine sulfate solution and $CuSO_4$ solutions can be used for up to one year, while a new batch of the final solution should be prepared every month.
2. Prepare 0.3M NaOH solution.
3. Prepare the nitrite coloring solution:
    a. Dissolve 1.0 g sulfanilamide in 10mL concentrated HCl.
    b. Carefully add the sulfanilamide in HCl solution to 75mL Millipore water.

c. Add 50 mg N-(1-naphthyl) ethylenediamine dihydrochloride to the solution.

d. Dilute the solution to 100mL with Millipore water.

4. Test for the Presence of nitrate/nitrite.

    a. To one of the slots in a porcelain plate, add two drops of Millipore water.

    b. To another slot in the porcelain plate, add two drops of a sample solution.

    c. Add one drop of nitrate reducing solution and one drop of 0.3M NaOH solution to the Millipore water and sample solution in the porcelain plate.

    d. After waiting for 20 minutes, add two drops of nitrite coloring solution to the Millipore water and sample solution.

    e. After waiting for two minutes, compare the colors of the Millipore water and the sample solution.

        i. If both solutions are a very pale pink, the concentration of nitrate/nitrite in the sample solution is below detection.

        ii. If the Millipore water is very pale pink and the sample solution is significantly darker pink, nitrate/nitrite is present in the sample solution.

        iii. Sample solutions will vary in shades of pink with solutions of higher nitrate/nitrite concentration being darker.

Appendix D

The following procedure was used to convert the AG MP-50 (H^+) resin, purchased from Biorad, to the Ag^+ form (modified from a personal communication with J. Hannon). Although the resin was prepared in batches as described below, the various batches were homogenized and stored in a single amber colored bottle.

1. Weigh out approximately 60g AG MP-50 (H^+) and add to a clean 600-mL beaker.
2. Add approximately 250mL of Millipore water to the resin and stir for two minutes.
3. After allowing three minutes for the resin to settle to the bottom of the beaker, pour out the rinse water and the resin that remains suspended.
4. Repeat steps 2-3 ten times, or until the rinse water appears clear.
5. Transfer the resin using Millipore water to a 2.5 cm diameter glass column.
6. Prepare 0.44M $AgNO_{3(aq)}$ (e.g., 15g $AgNO_{3(s)}$ for every 200mL Millipore water).
7. Gravity drip 0.44M $AgNO_{3(aq)}$ through the packed column and observe changes (e.g., color) as Ag^+ replaces H^+ on the exchange sites of the resin.
8. Verify the conversion of the resin from the H^+ form to the Ag^+ form:
    a. At first, the solution passing through the column will have a pH of 0-1 (verify using pH paper), and will not contain silver ions (verify by collecting several milliliters of the solution in a clean test tube and

adding a few drops of HCl; AgCl precipitate will form in the presence of Ag^+ ions).

b. As the exchange sites fill with Ag^+ ions, the pH of the solution coming through the column will increase and silver ions will become present.

c. When the pH of the solution coming through the column is greater than 4, conversion to the Ag^+ form is complete. (On average, 550mL 0.44M $AgNO_{3(aq)}$ is required to convert 60g AG MP-50 from the H^+ form to the Ag^+ form.)

9. Rinse the resin thoroughly using several liters of Millipore water. (On average, 6L of Millipore water is rinsed through the column.)

a. Mix the resin periodically.

b. Check for the presence of nitrate using colorimetric test solutions (for more details, see Appendix C).

c. Verify that there is no nitrate present in the water coming through the column and transfer the prepared resin to an amber colored bottle.

Appendix E

Strom track data for sample 1

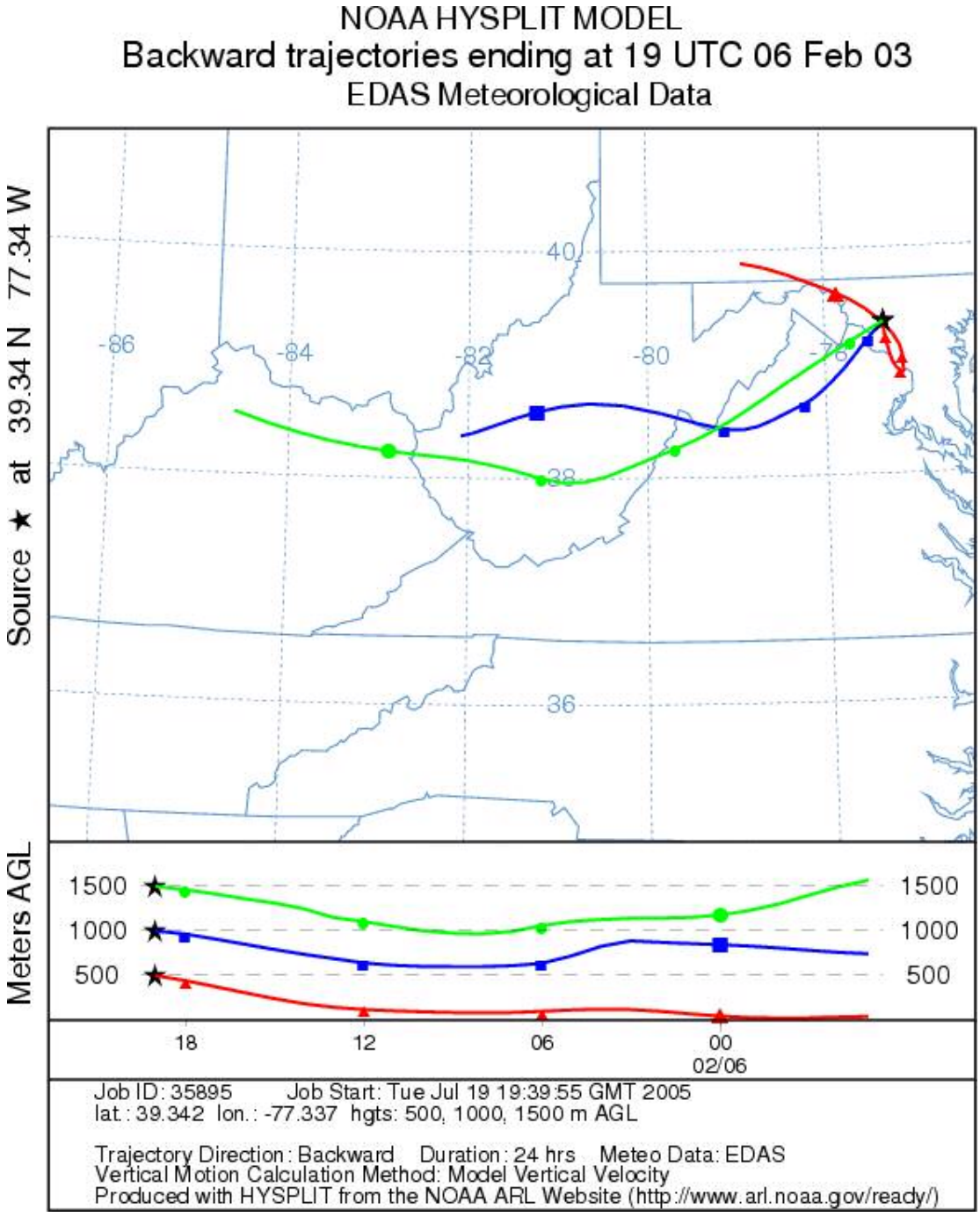

Strom track data for sample 2

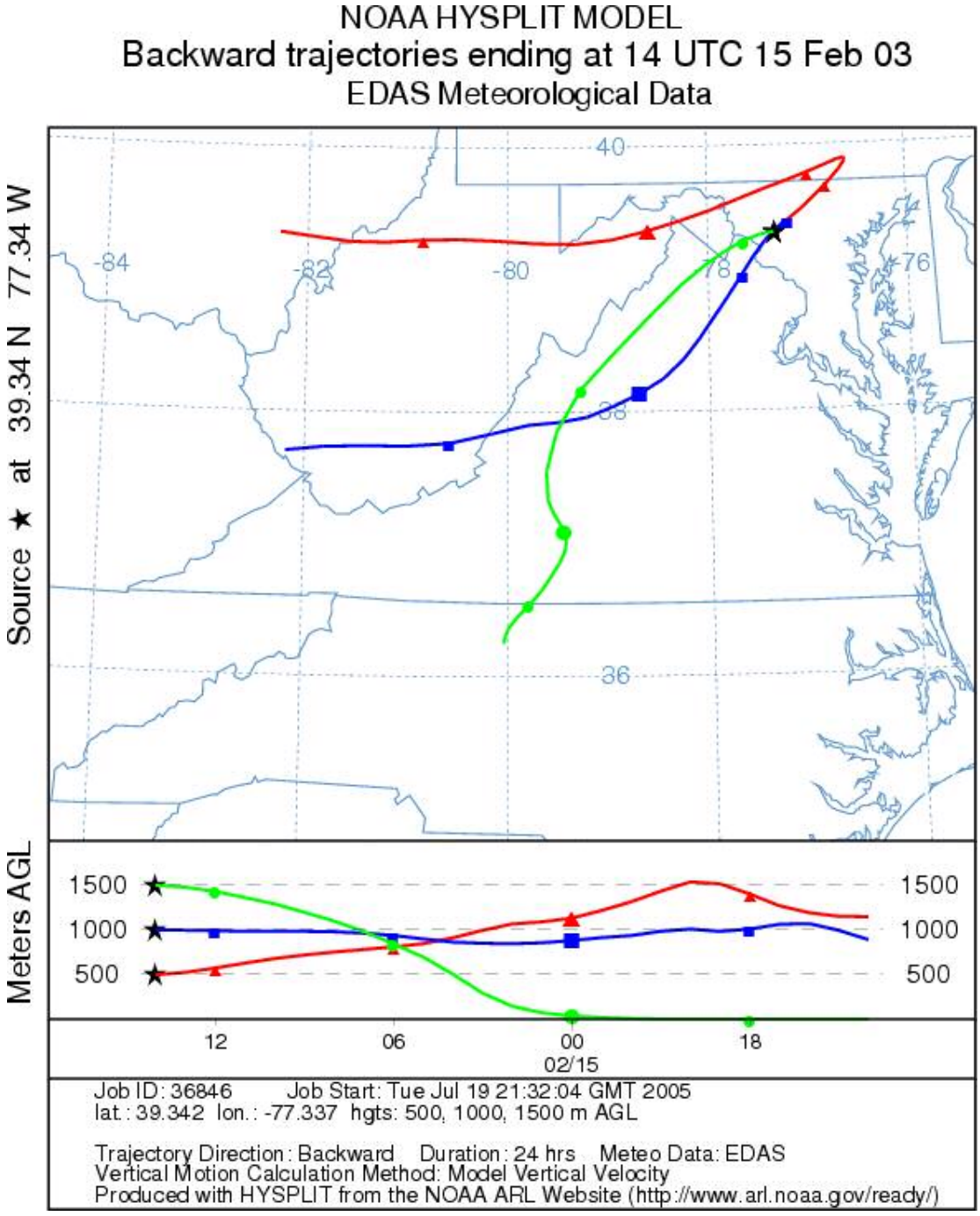

Strom track data for sample 3

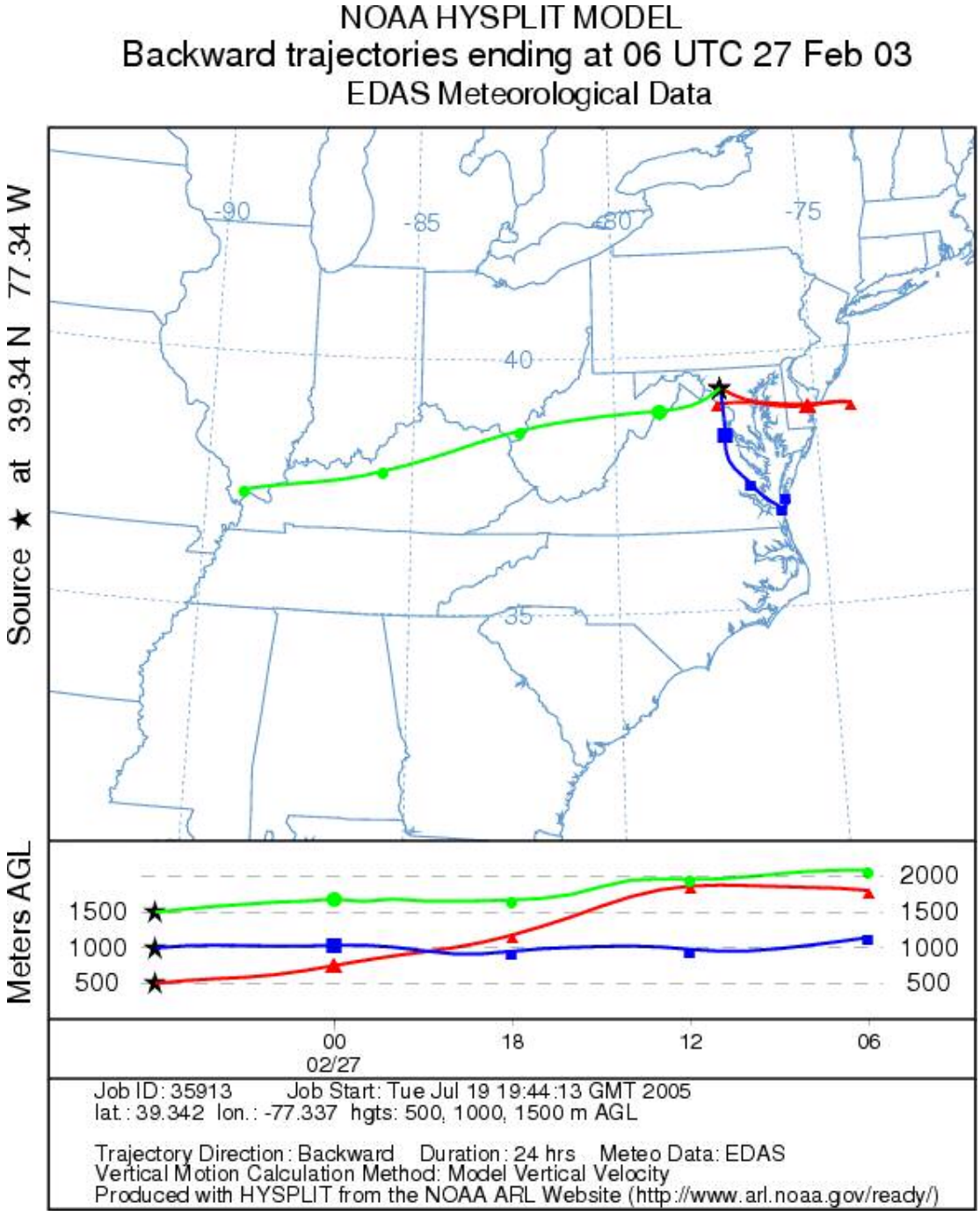

Strom track data for sample 4

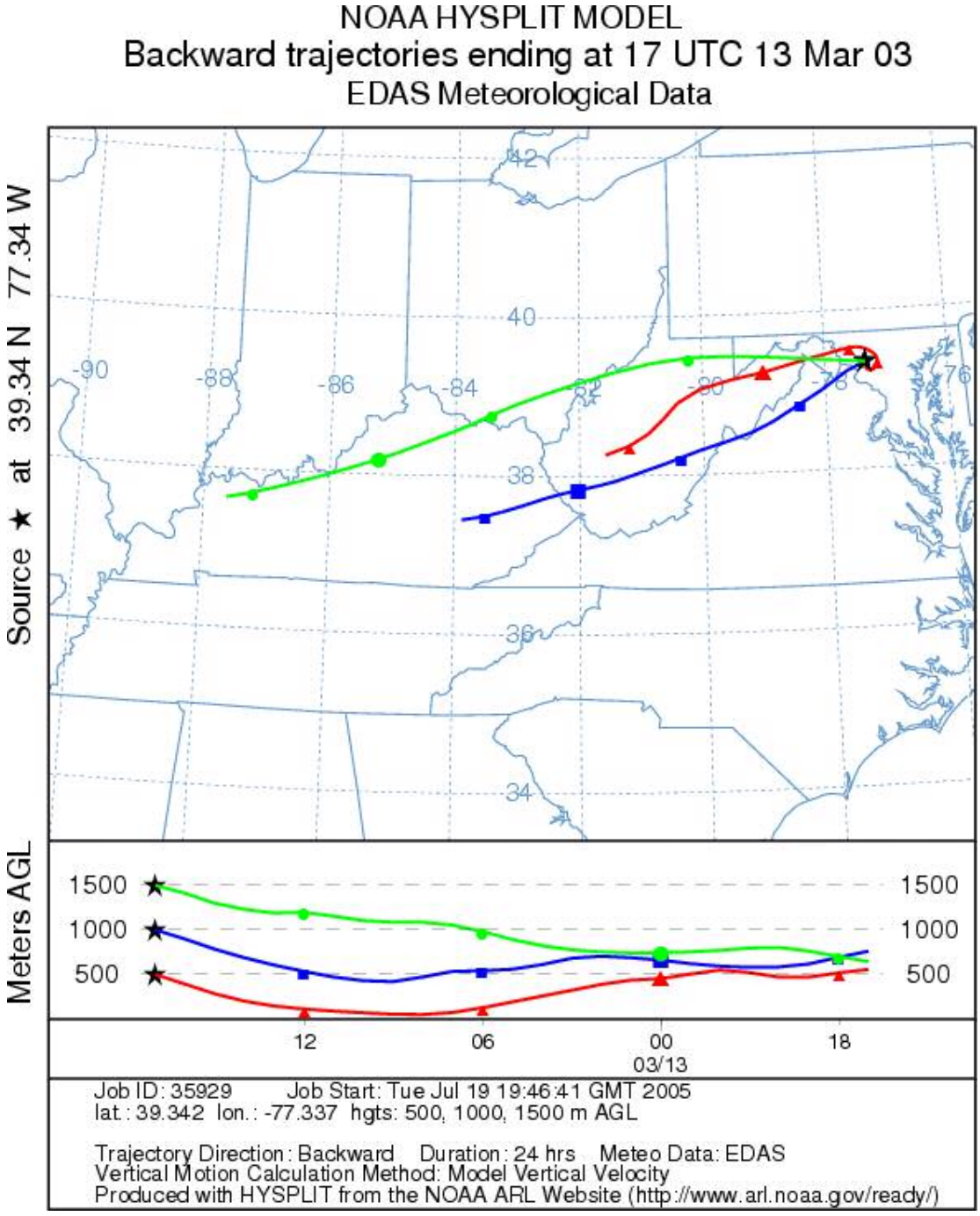

Strom track data for sample 5

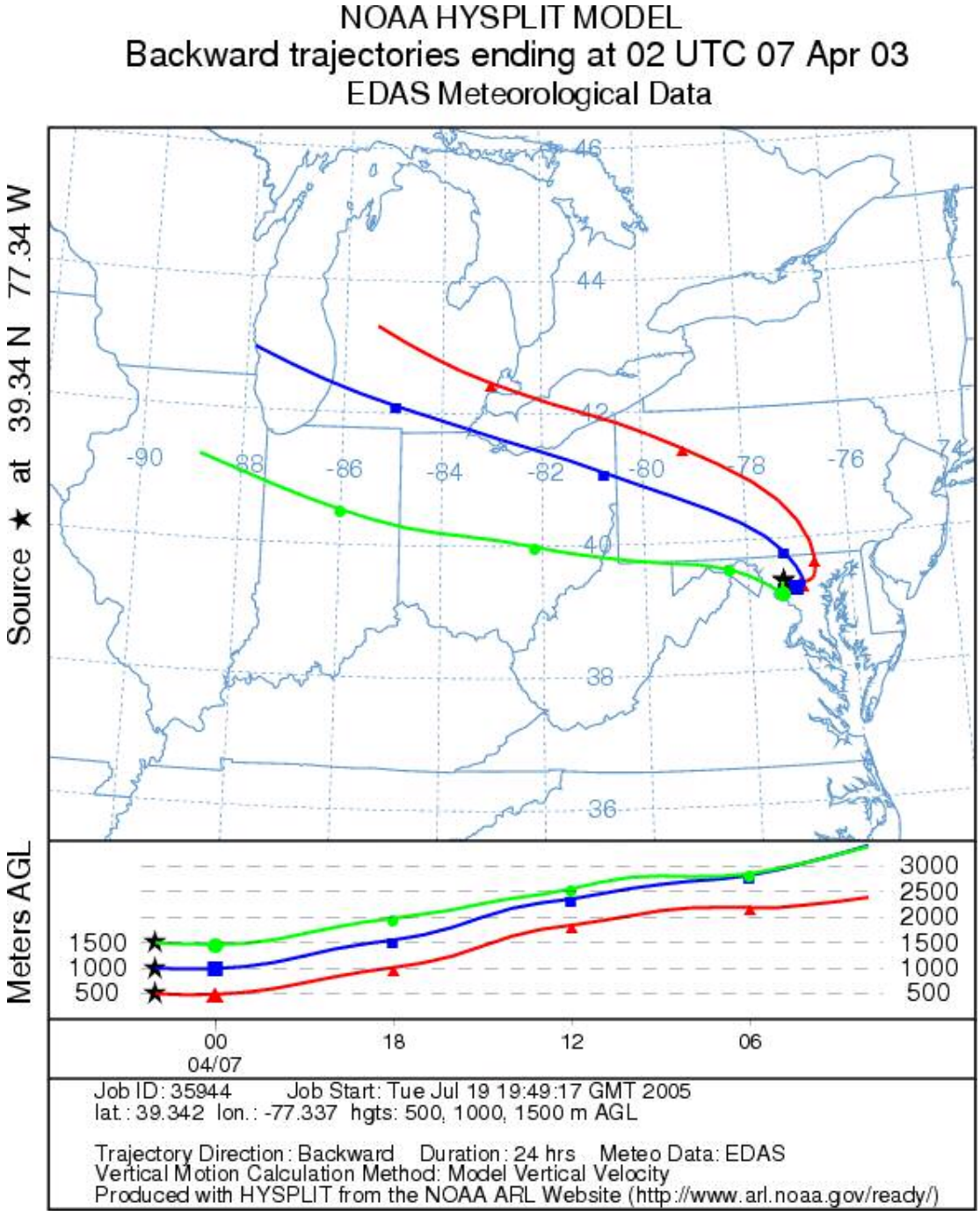

Strom track data for sample 6

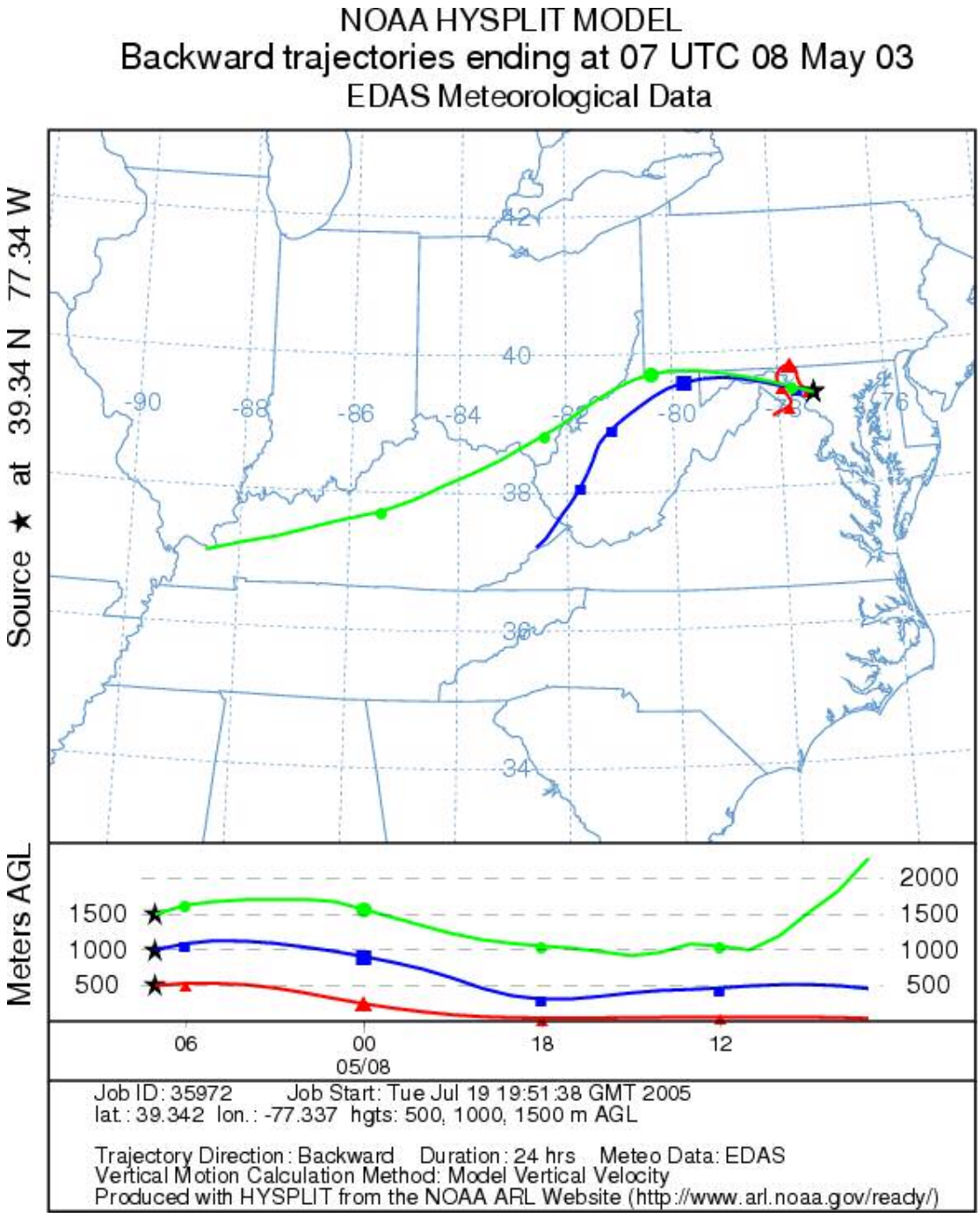

Strom track data for samples 7 and 8

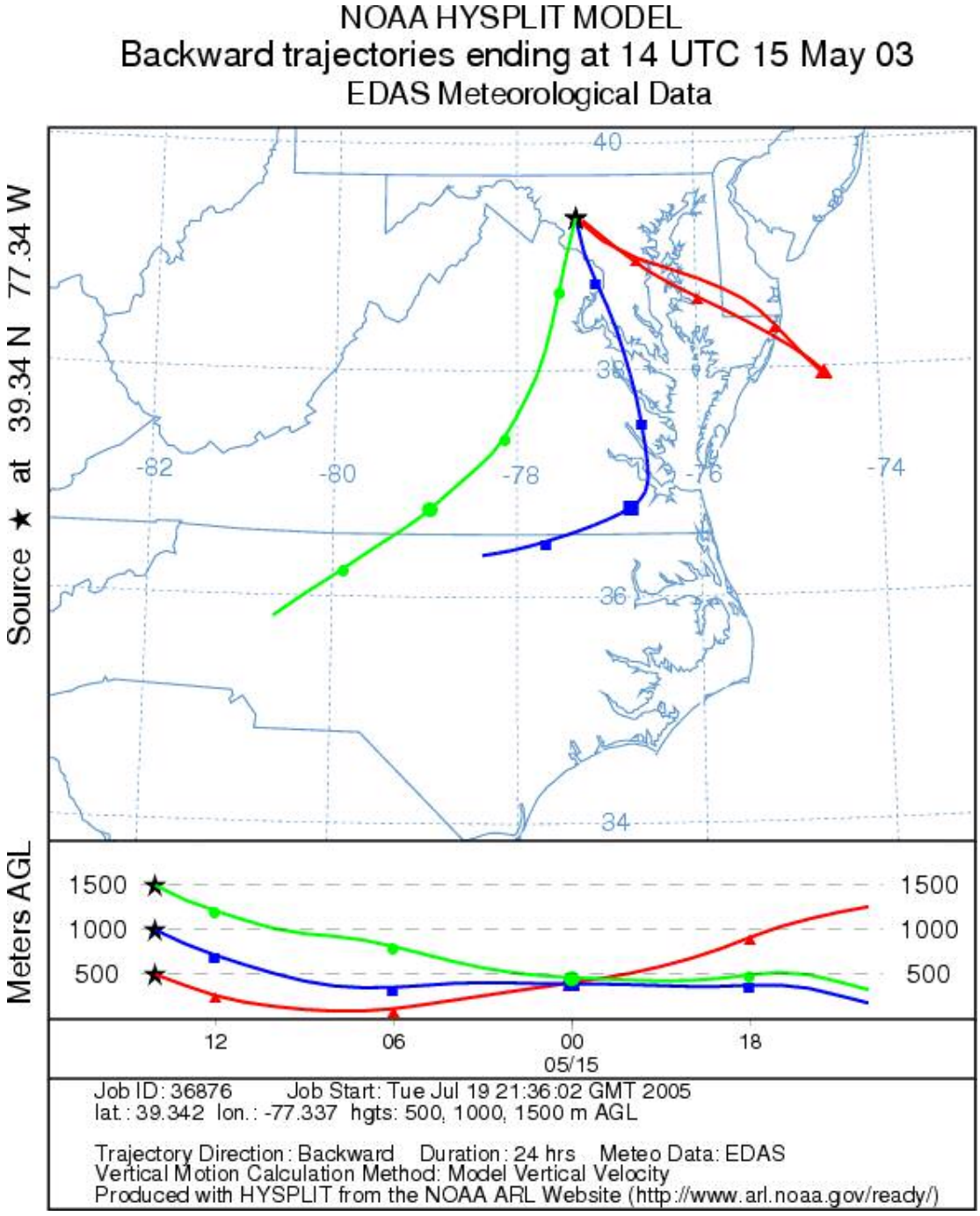

Strom track data for sample 9

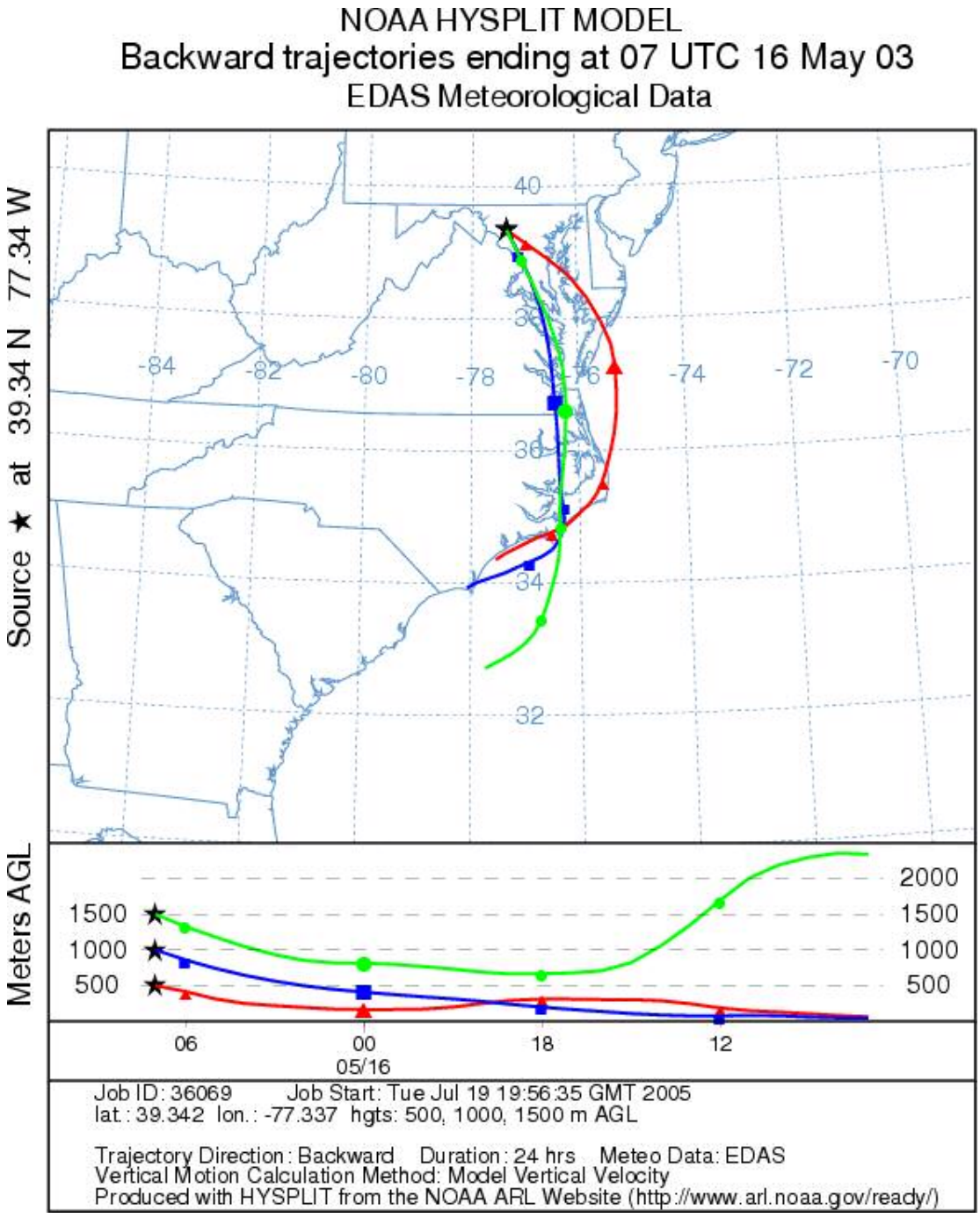

Strom track data for sample 10

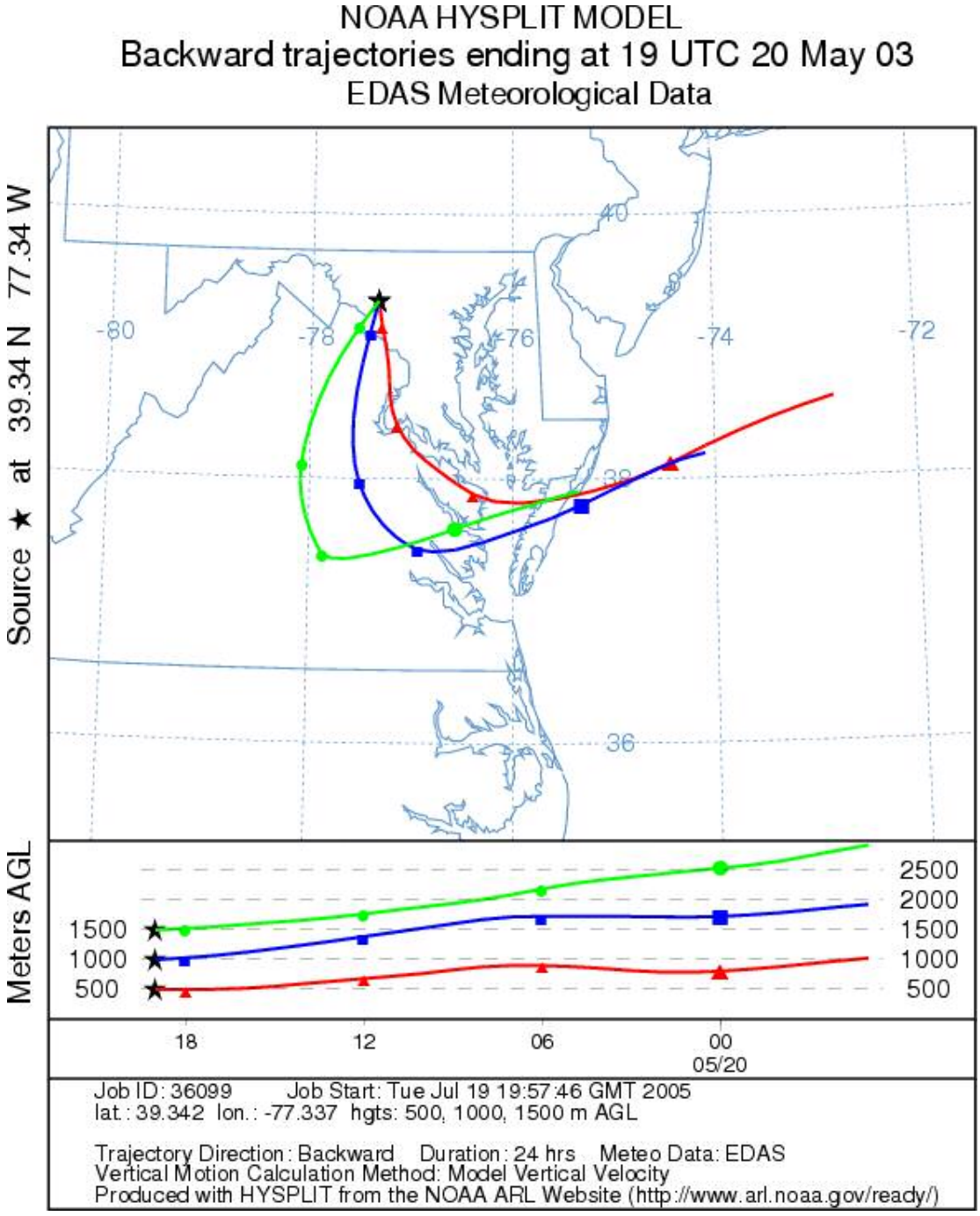

Strom track data for sample 11

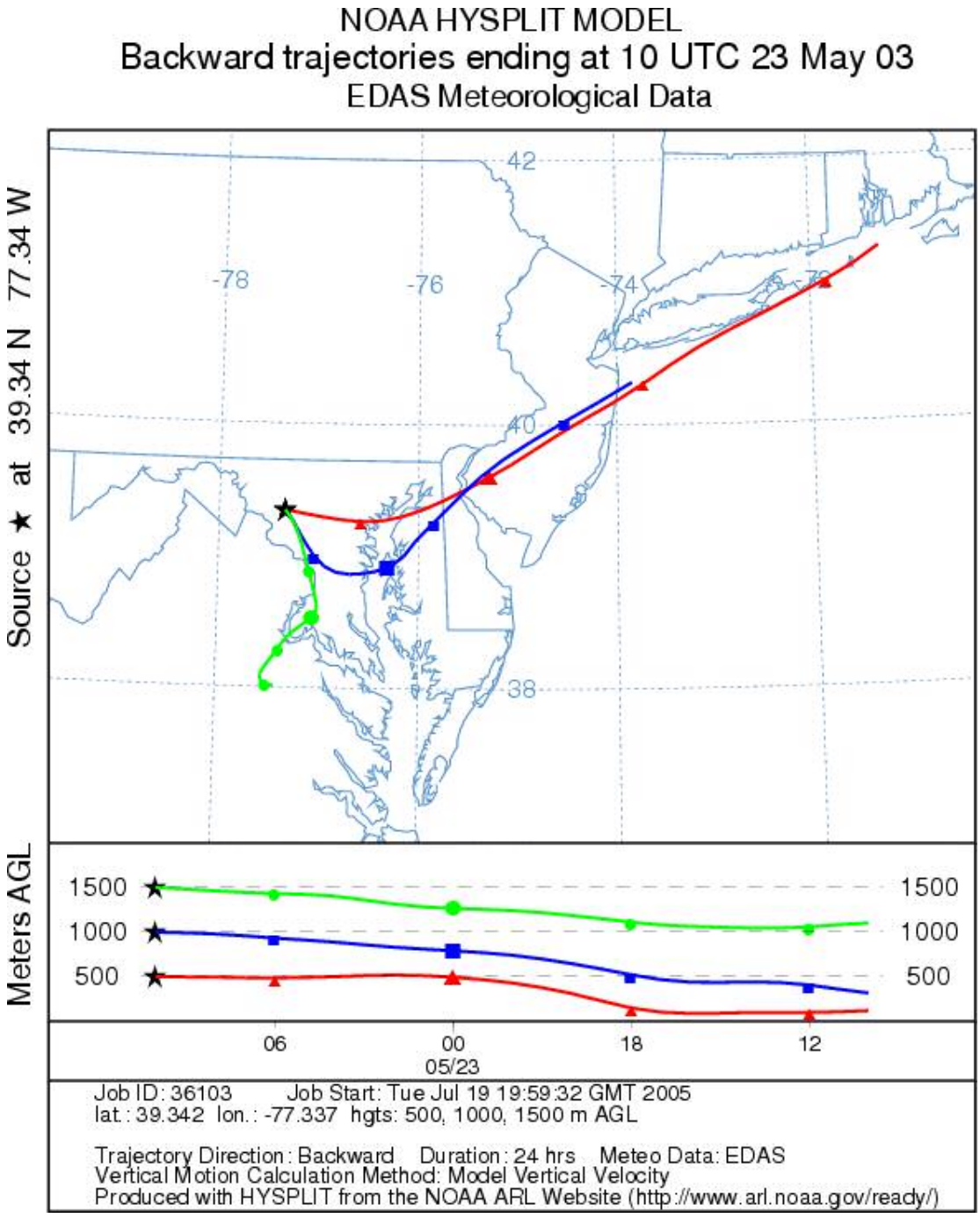

Strom track data for sample 12

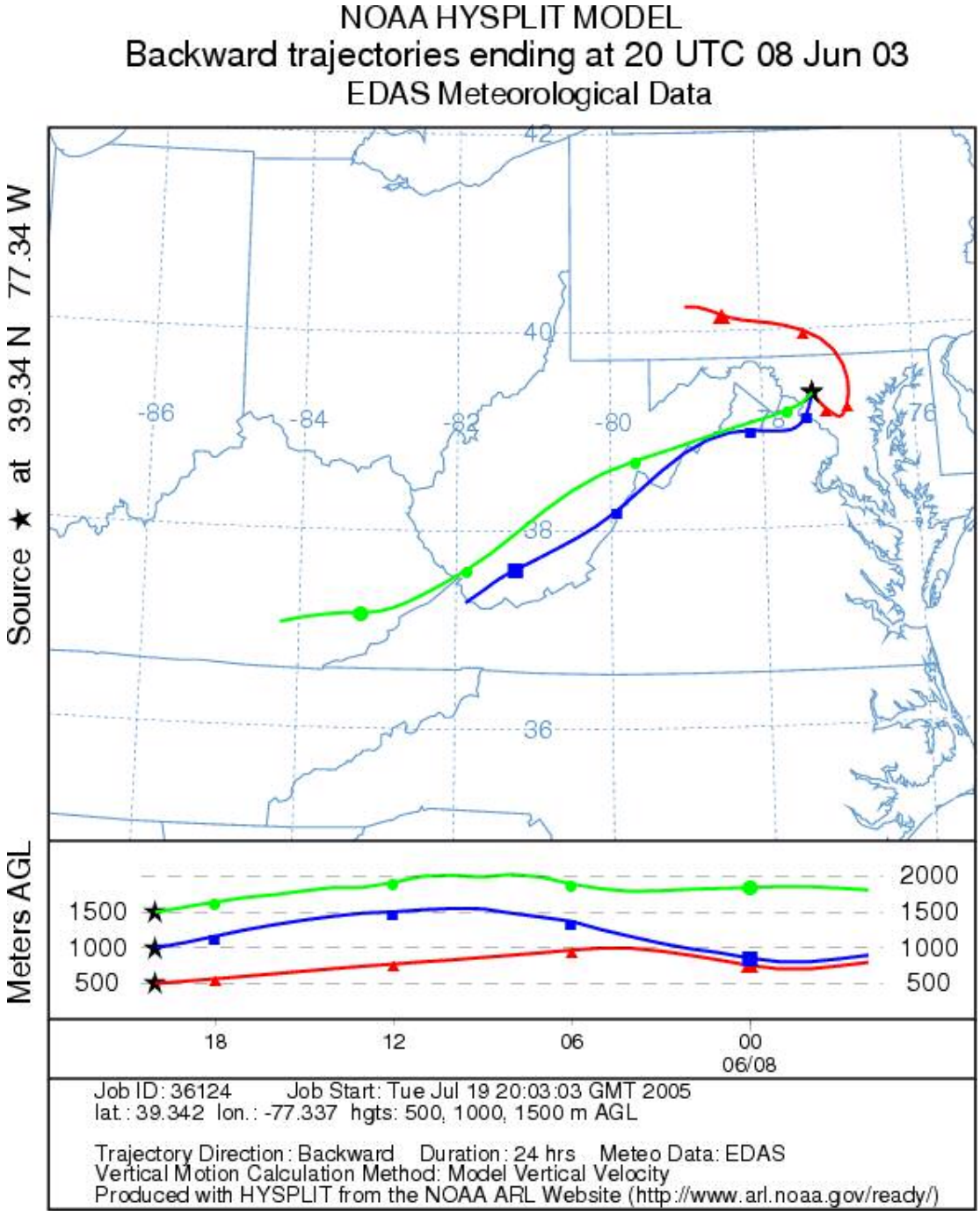

Strom track data for sample 13

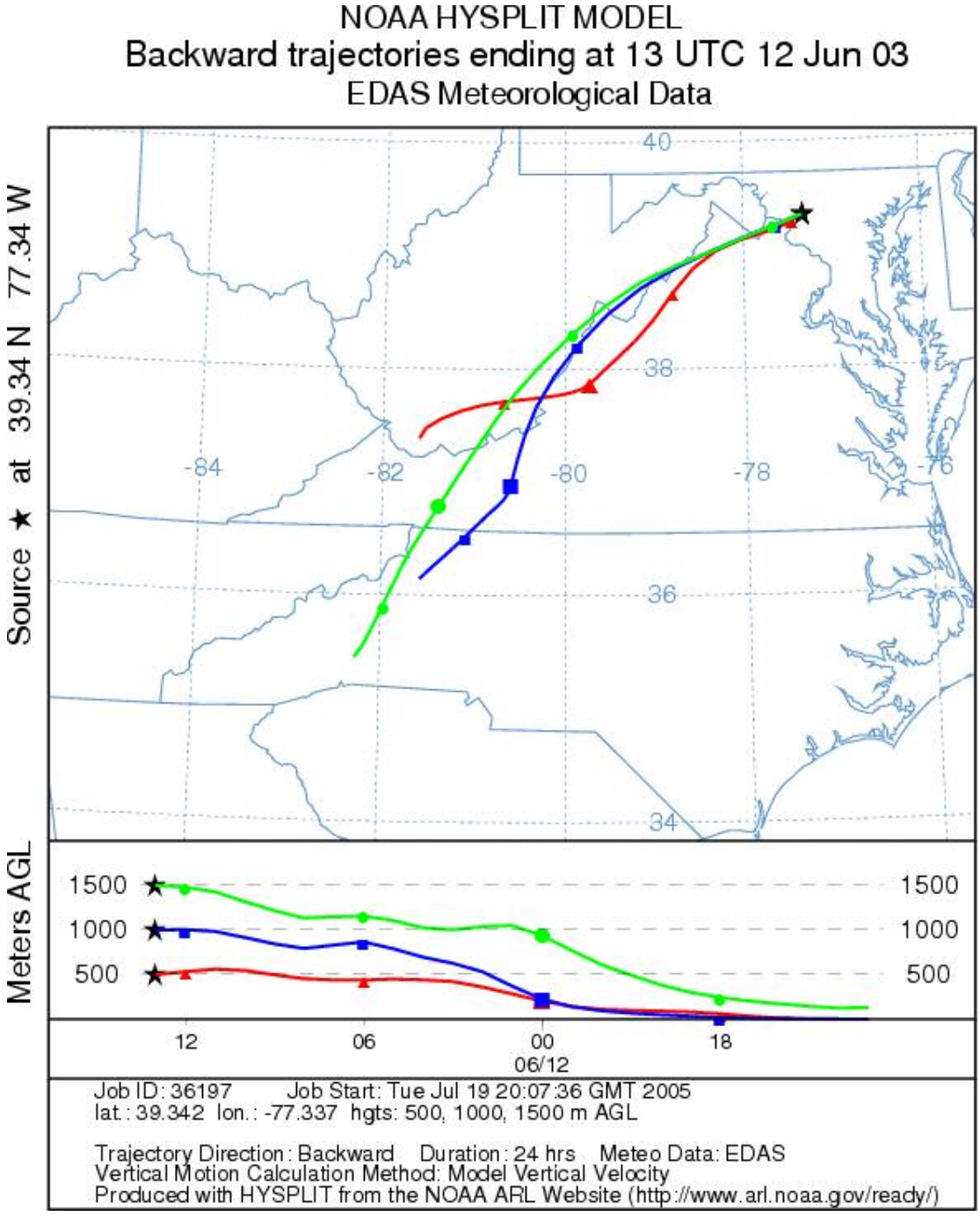

Strom track data for sample 14

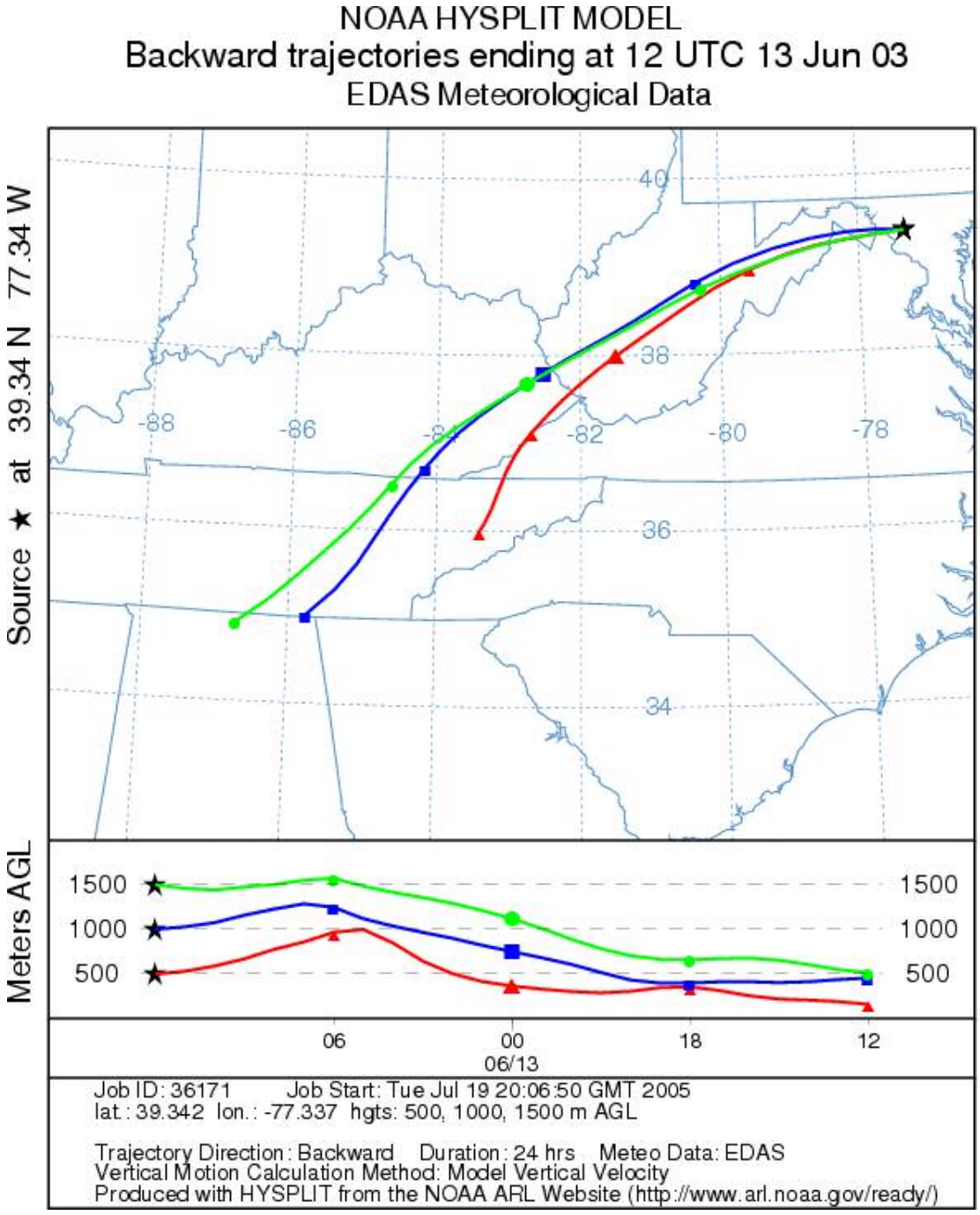

Strom track data for sample 15

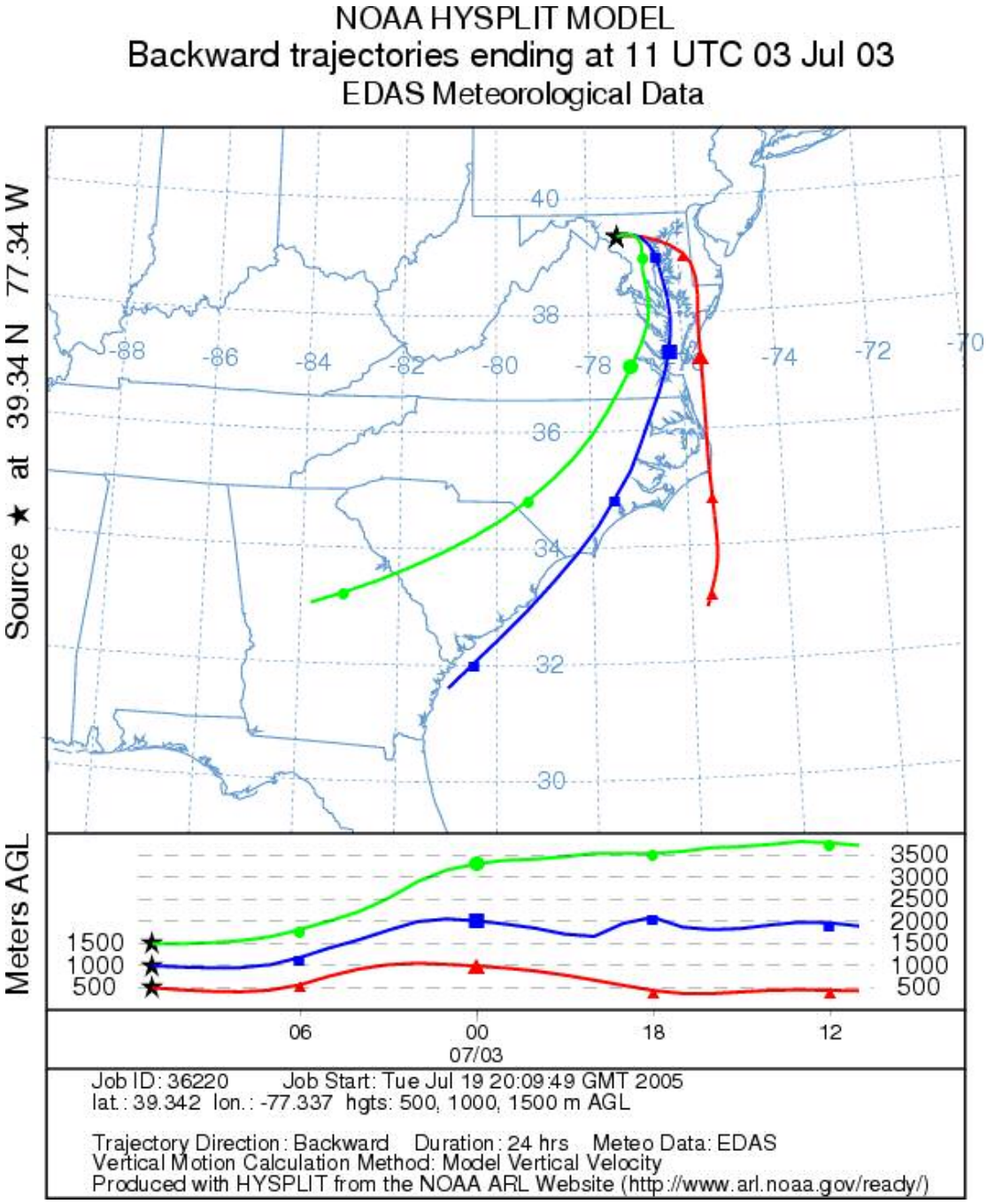

Strom track data for sample 16

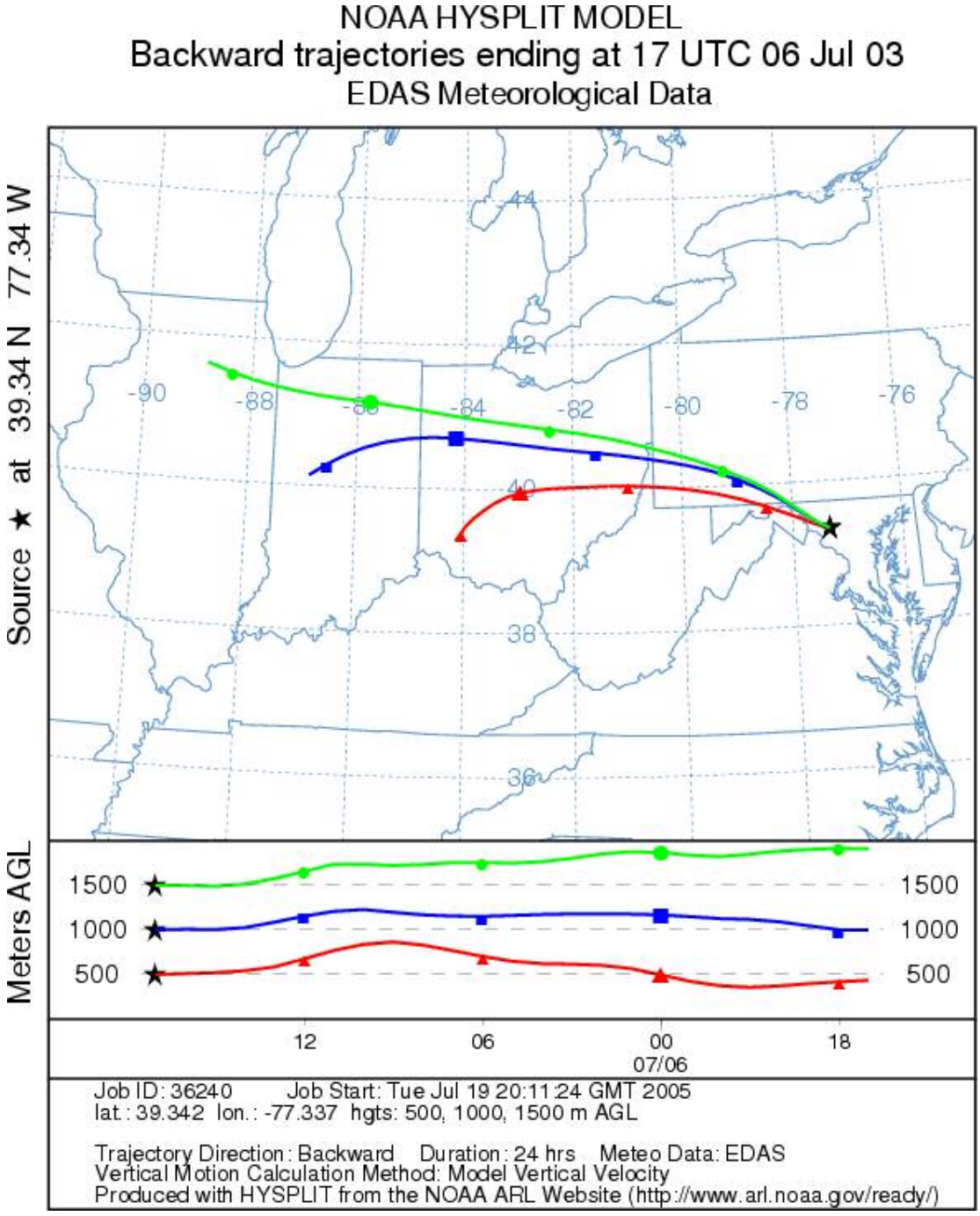

Strom track data for sample 17

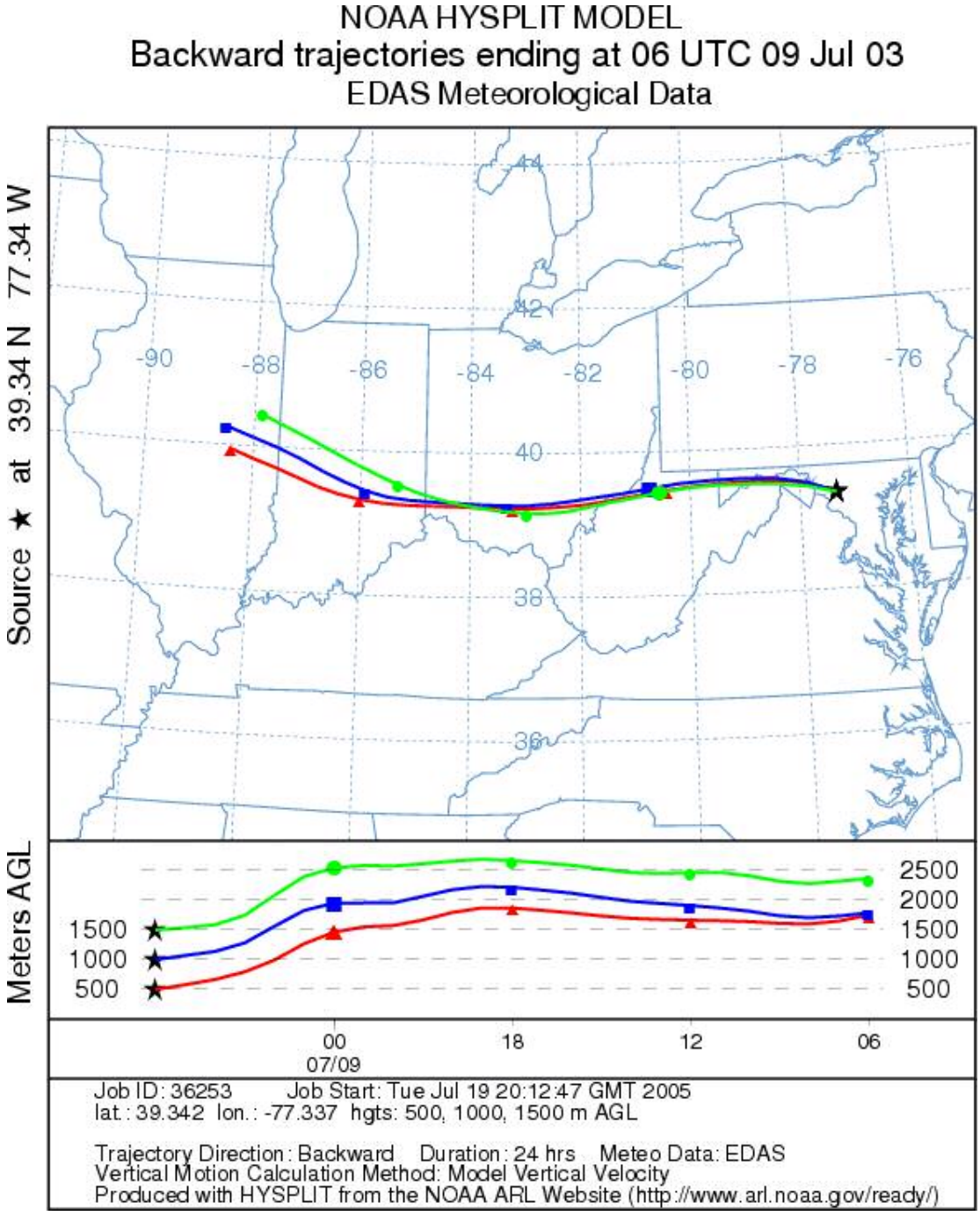

Strom track data for sample 18

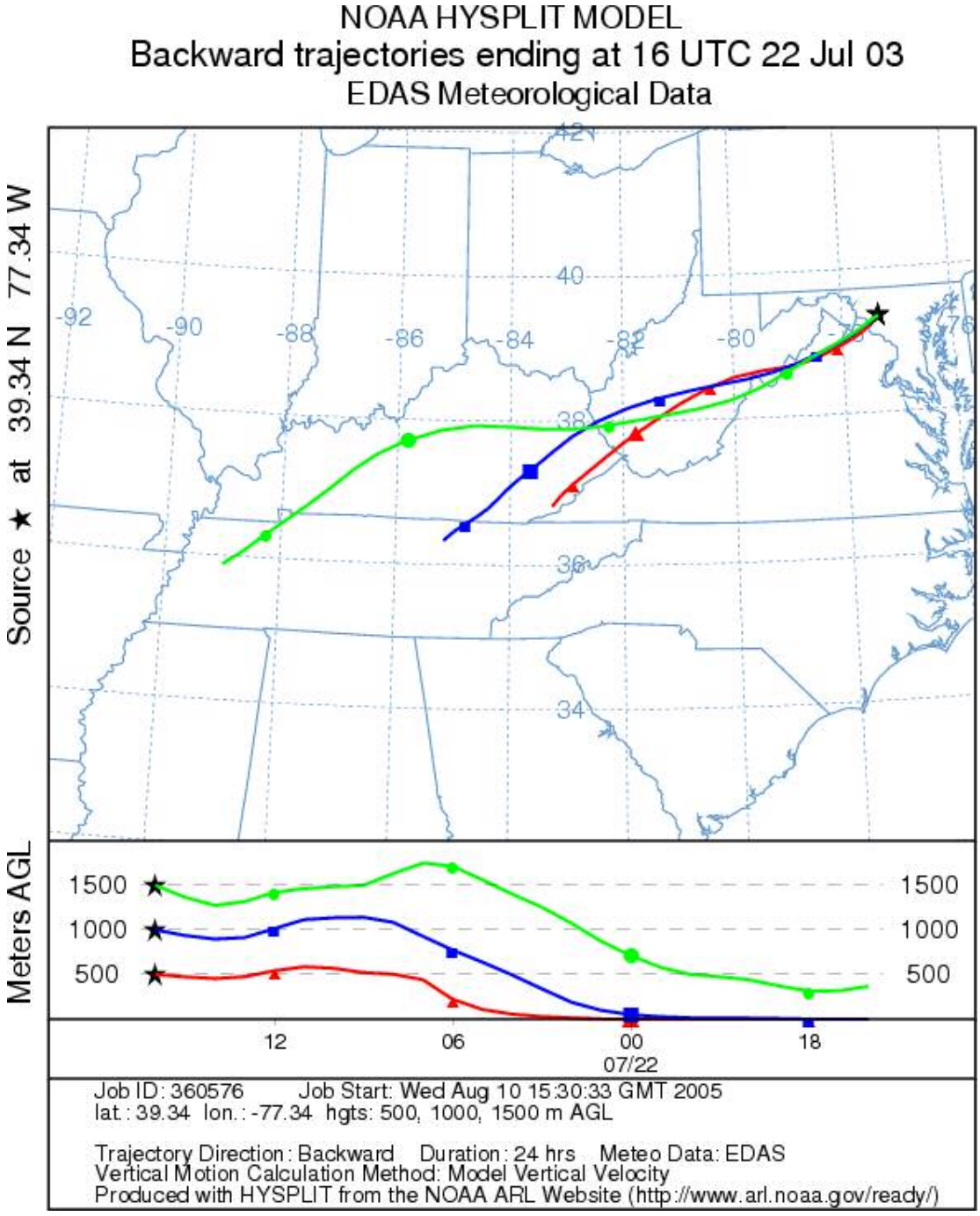

Strom track data for sample 19

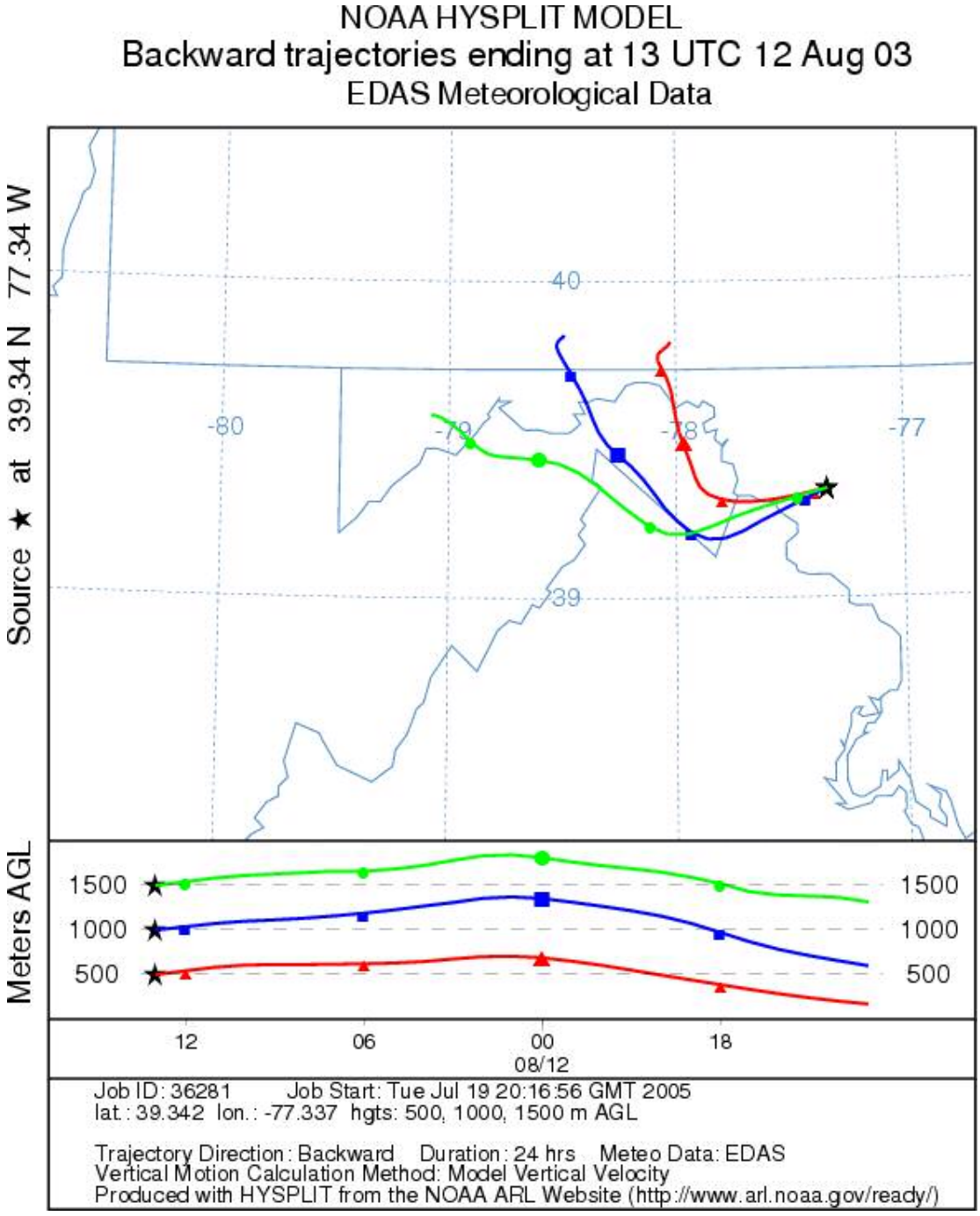

Strom track data for sample 20

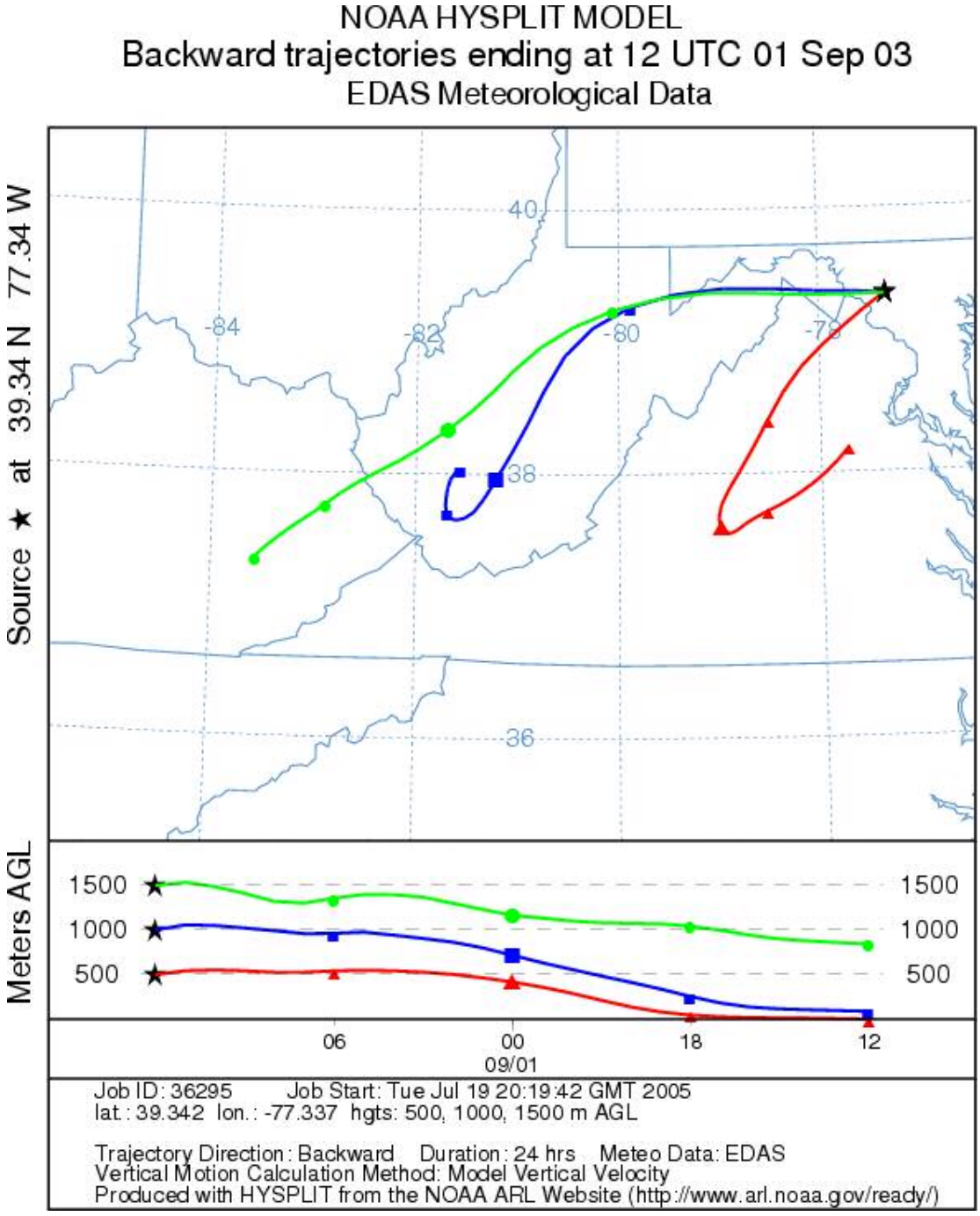

Strom track data for sample 21

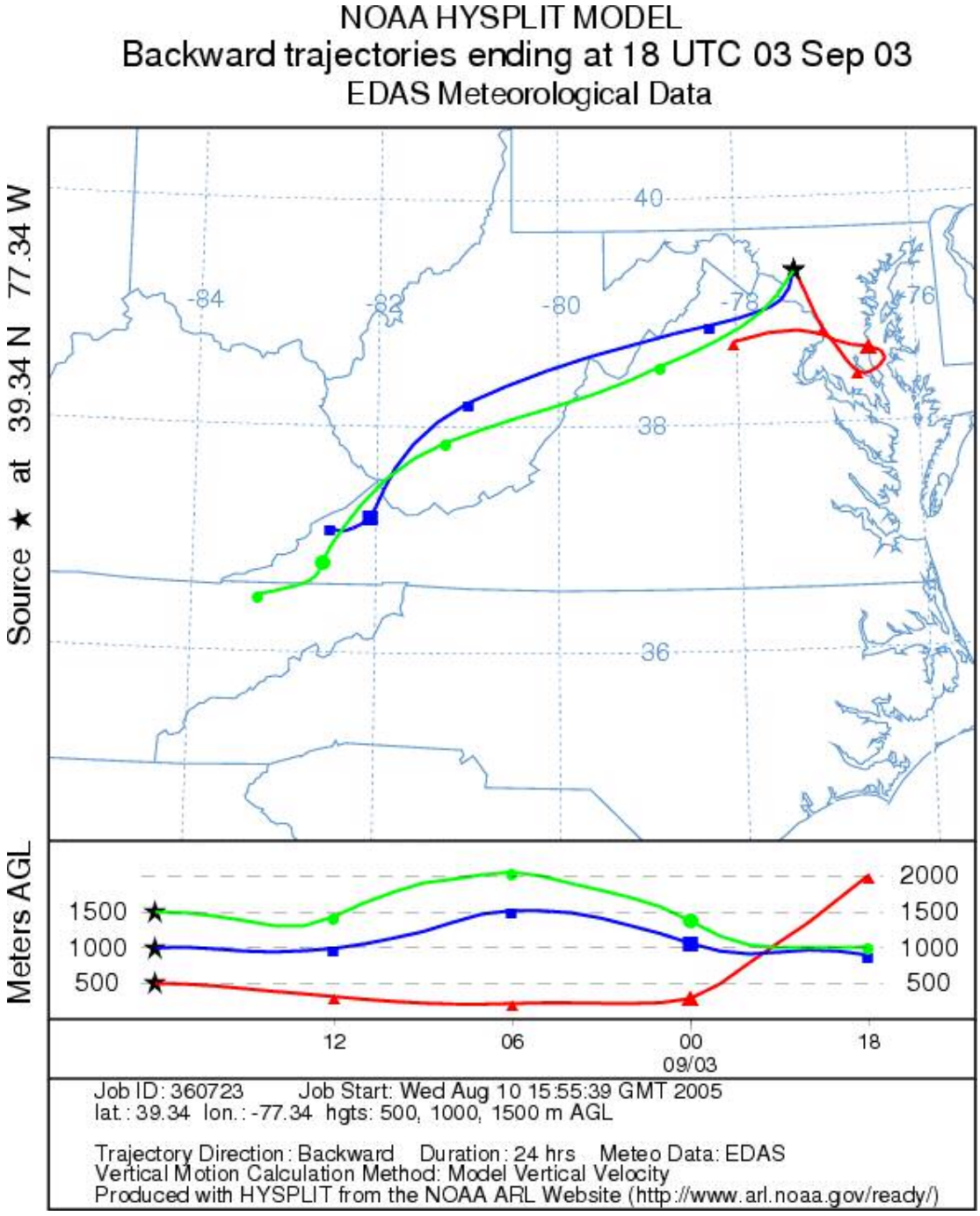

Strom track data for sample 22

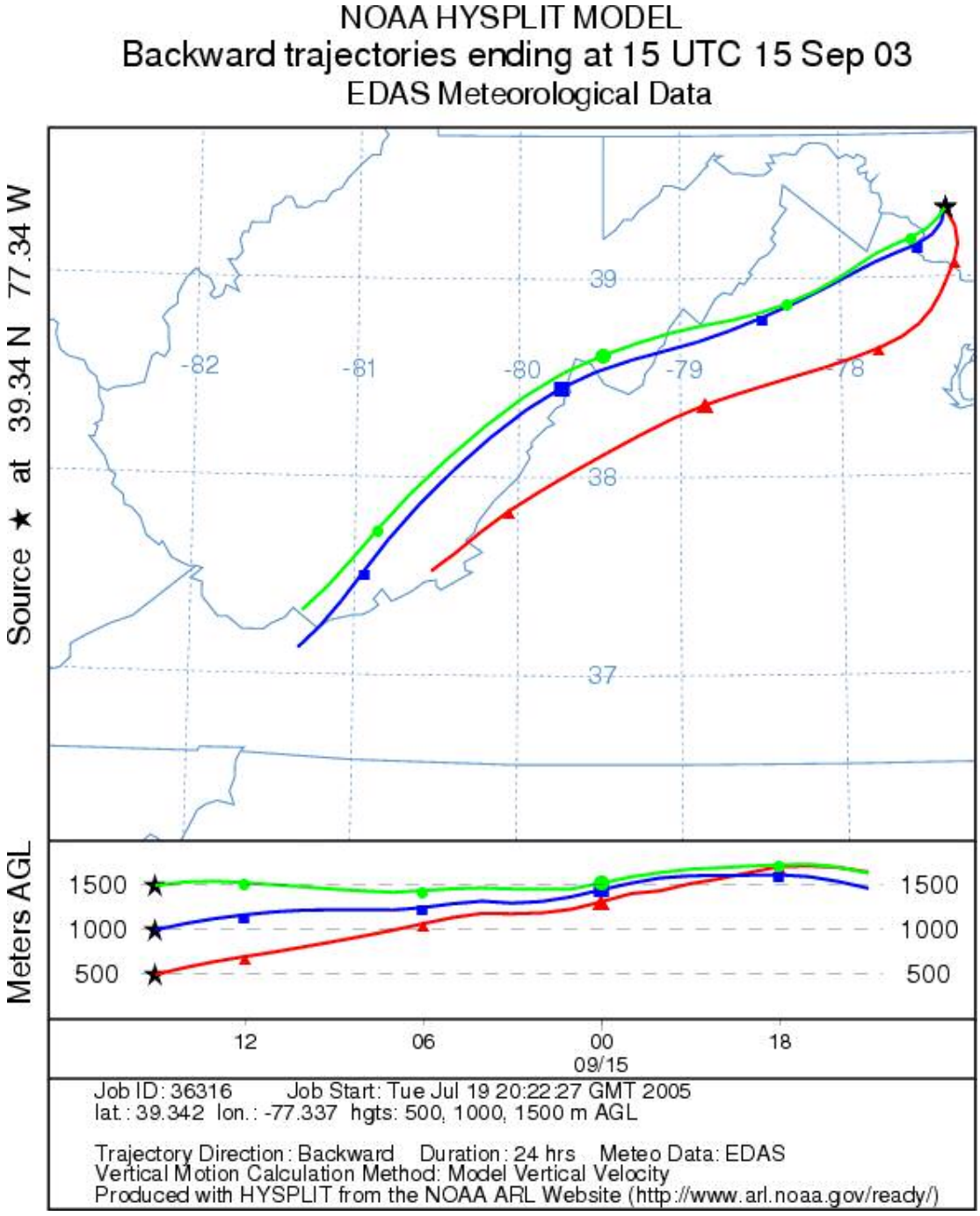

Strom track data for sample 23

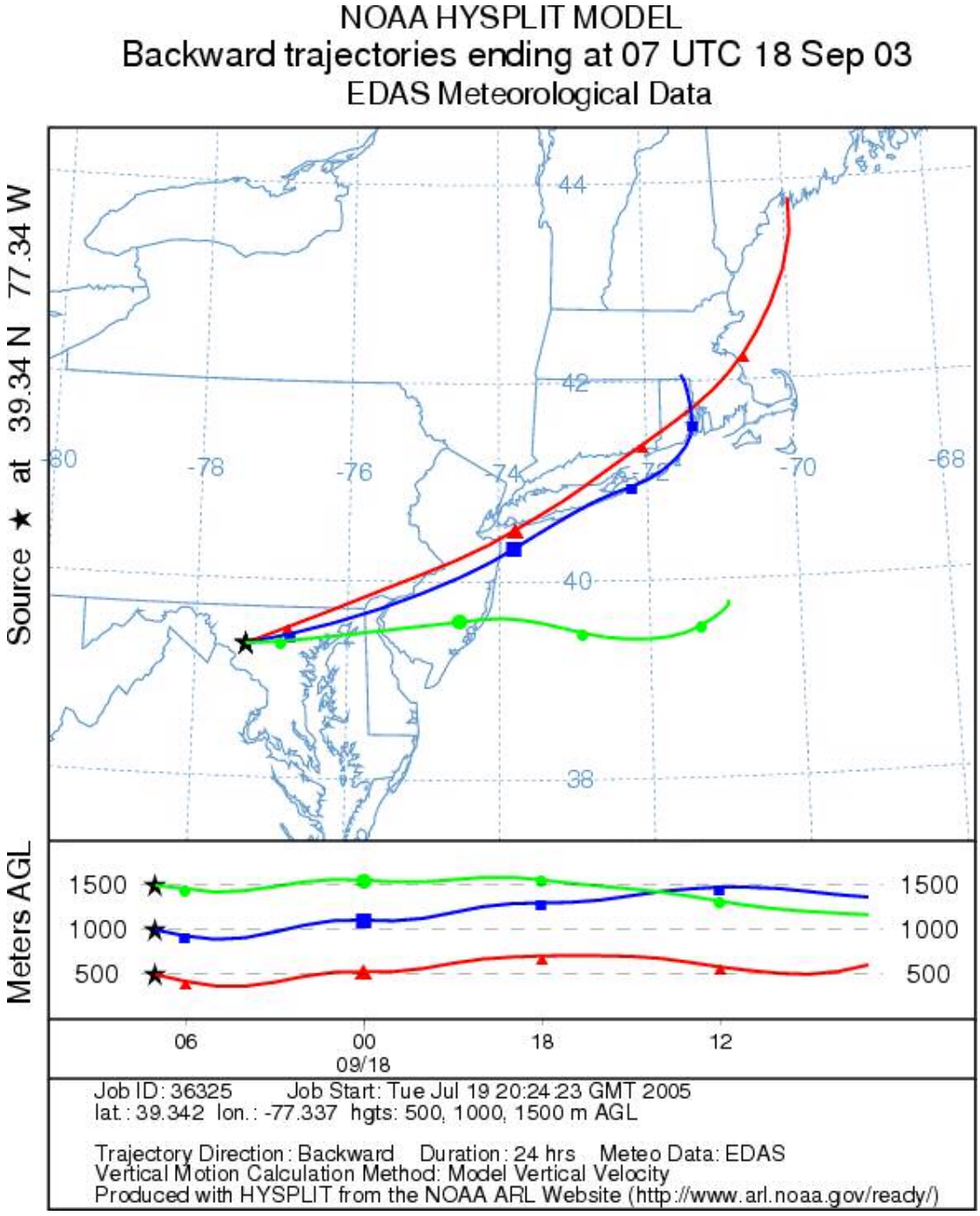

Strom track data for sample 24

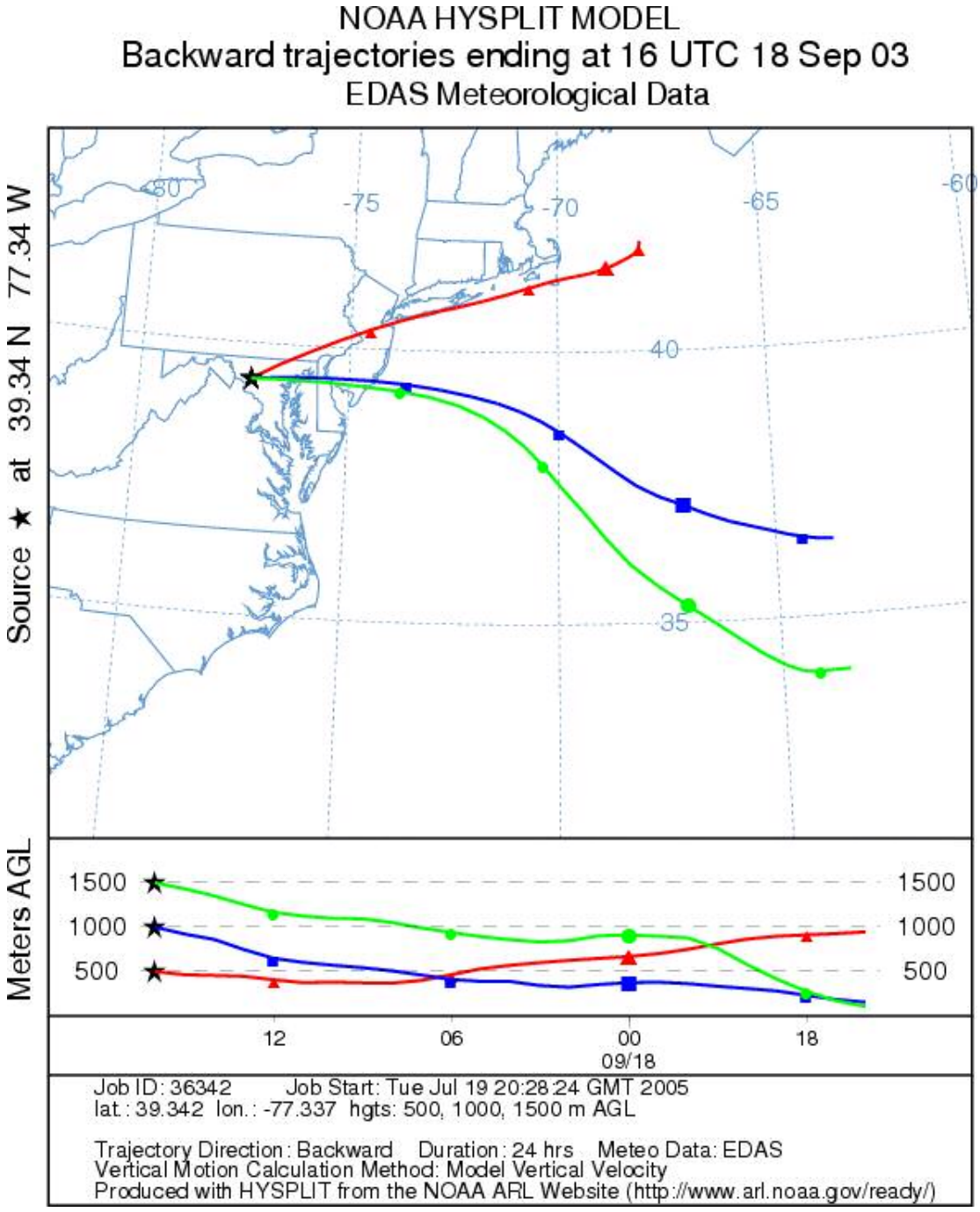

Strom track data for sample 25

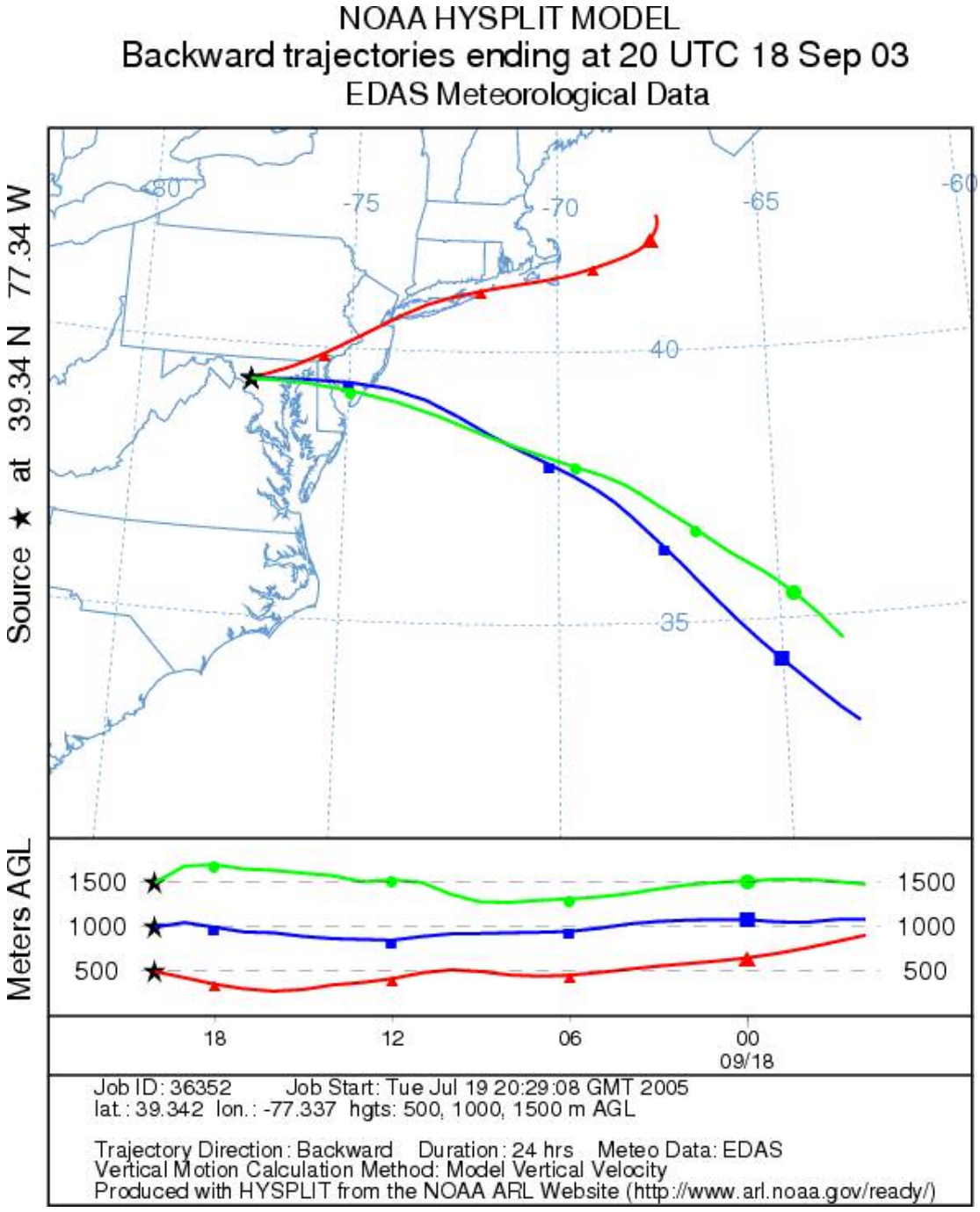

Strom track data for sample 26

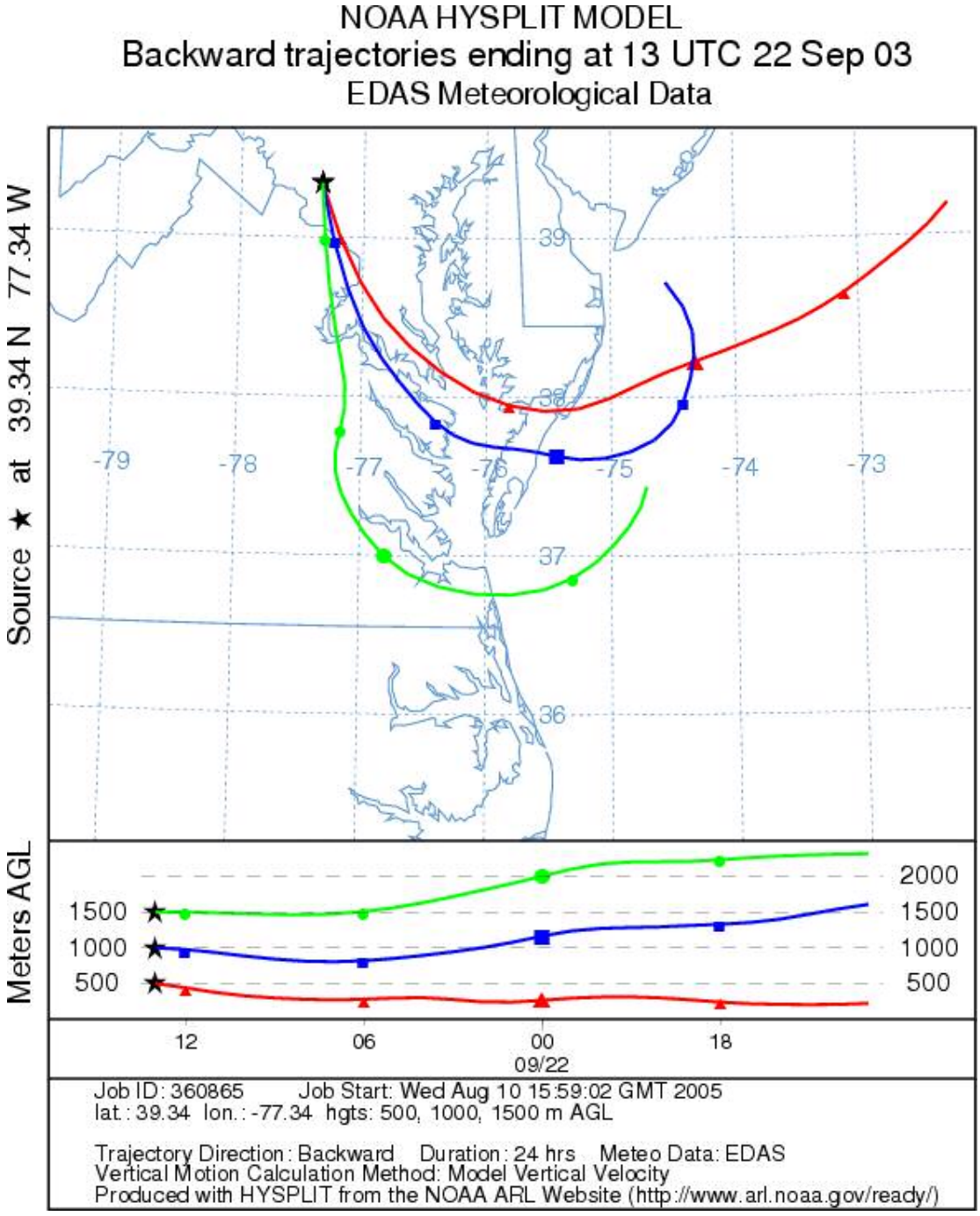

Strom track data for sample 27

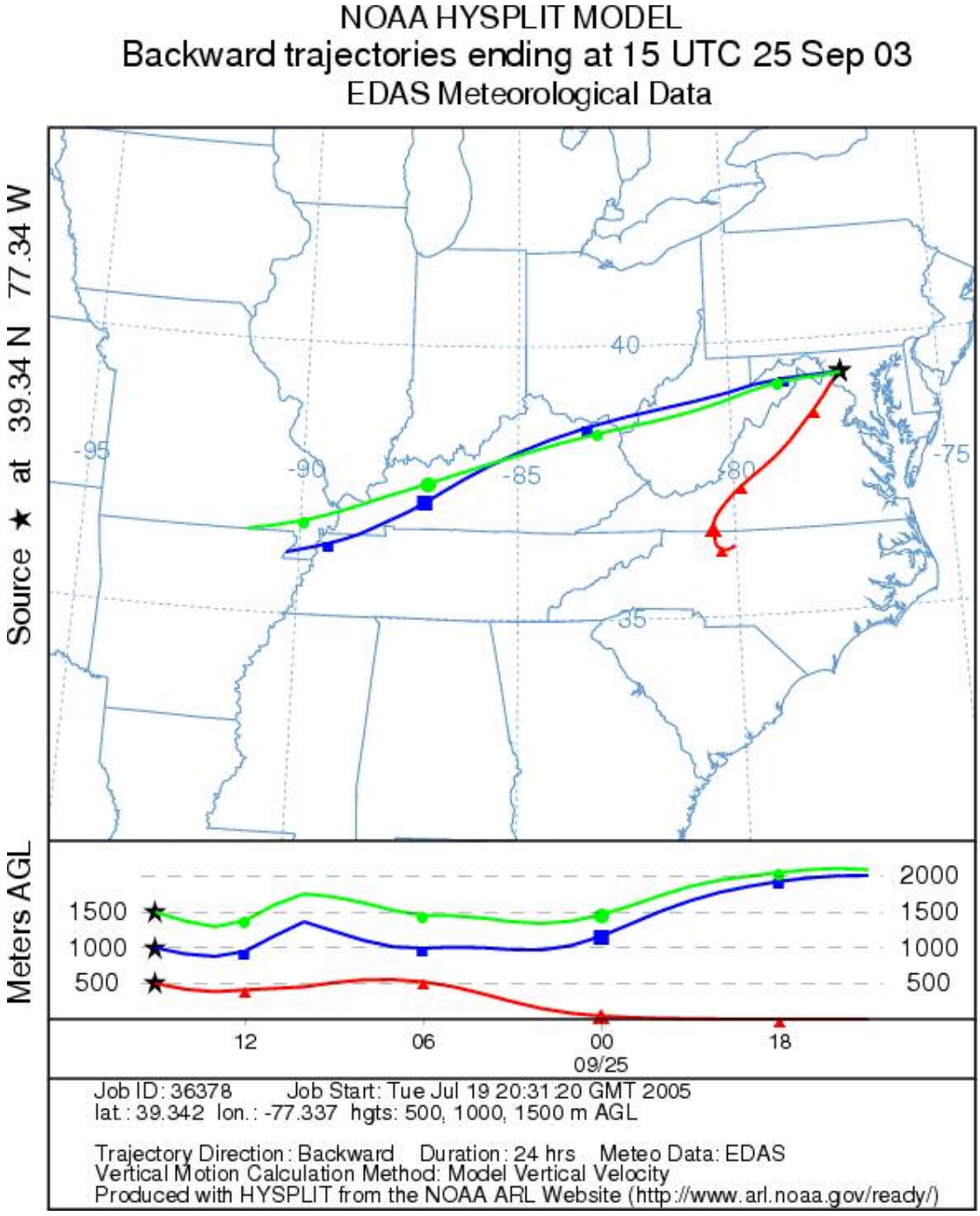

Strom track data for sample 28

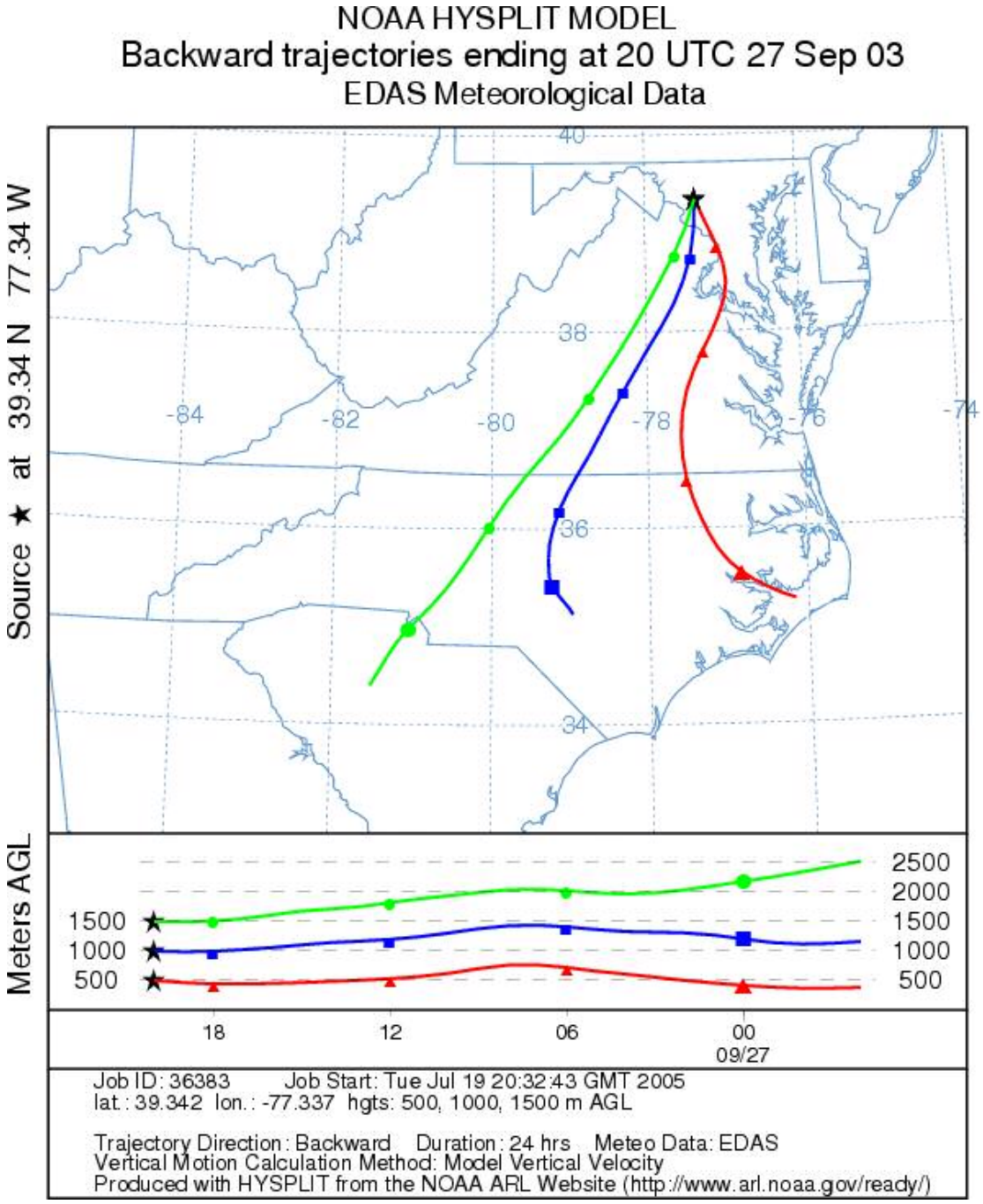

Strom track data for sample 29

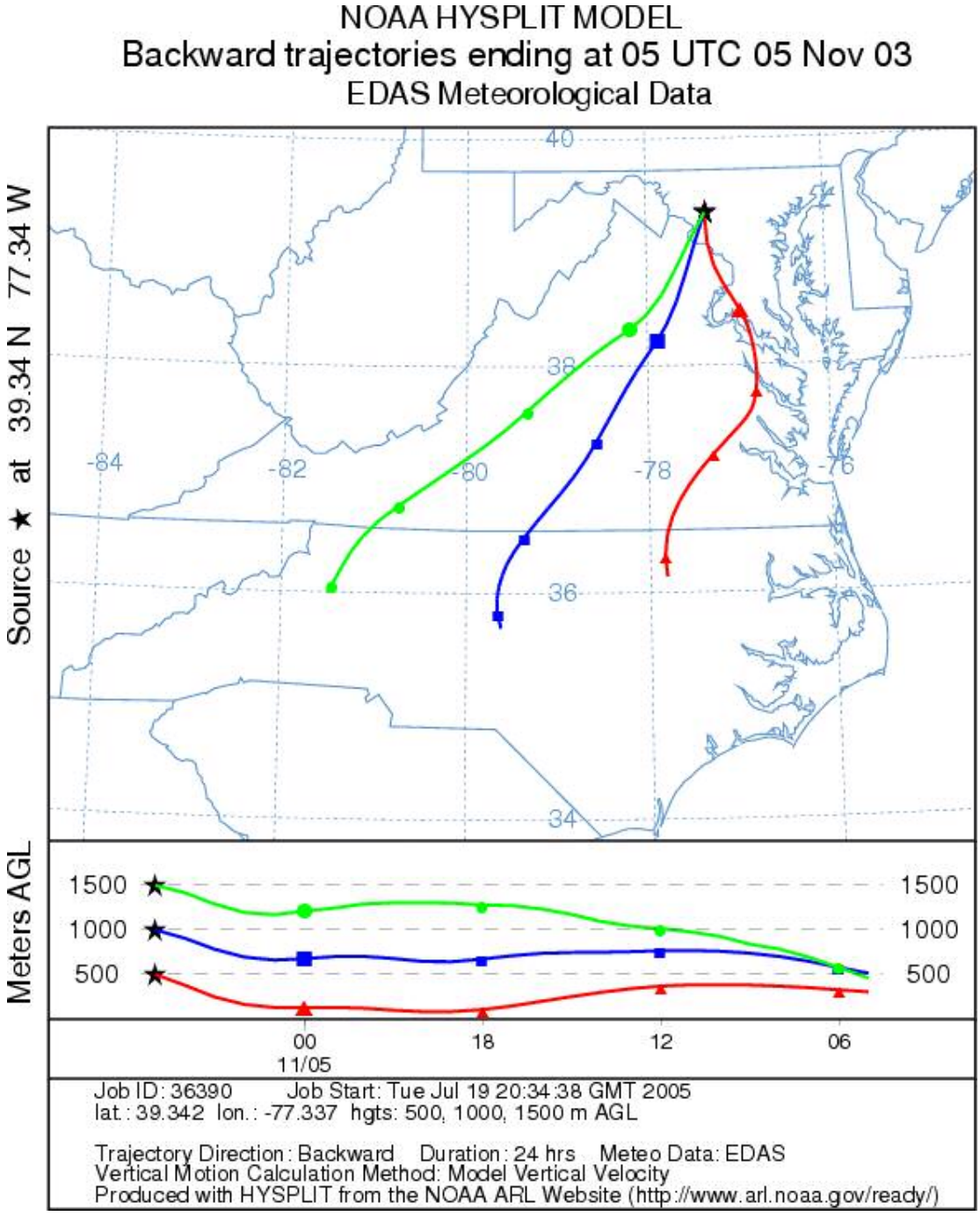

Strom track data for sample 30

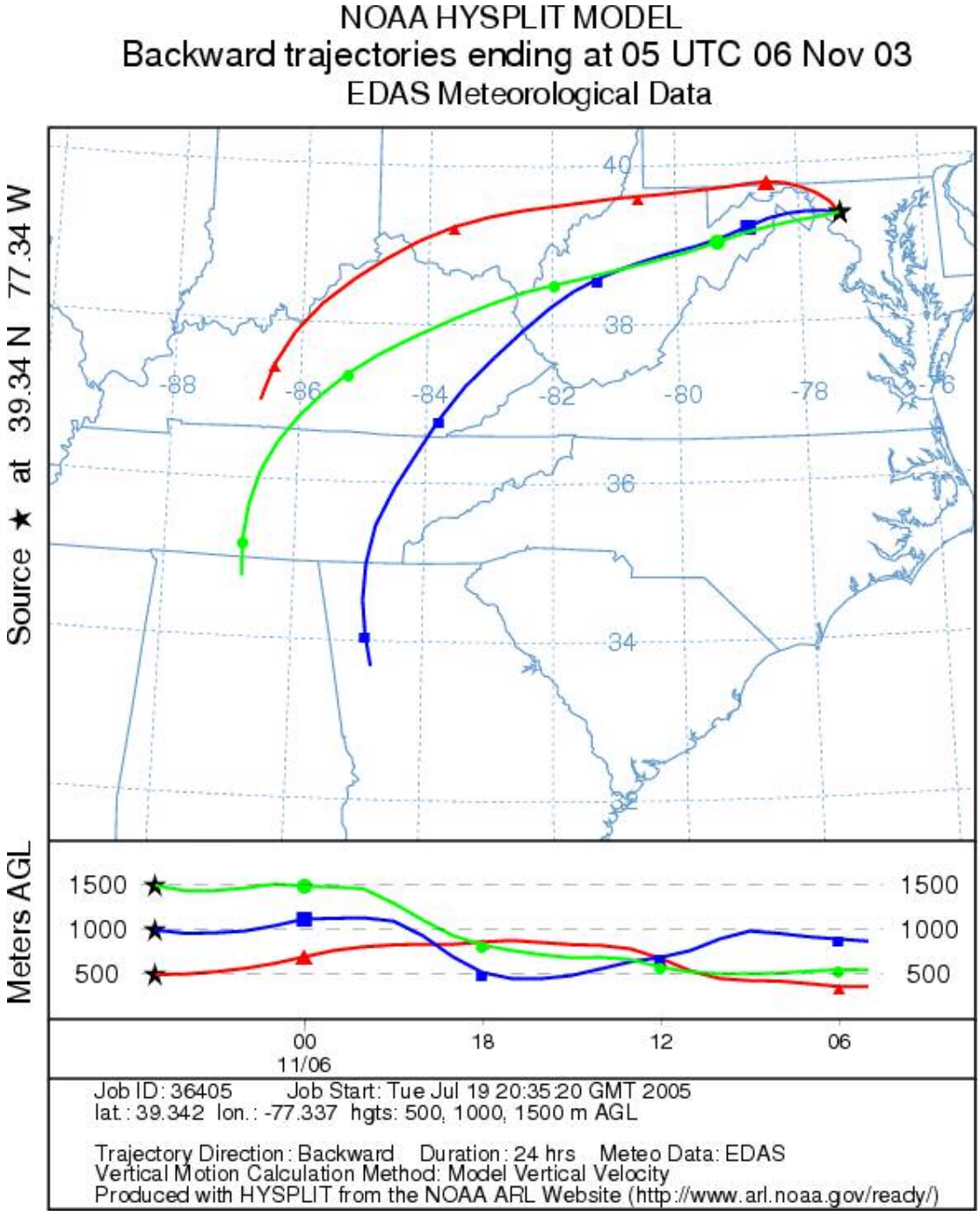

Strom track data for sample 31

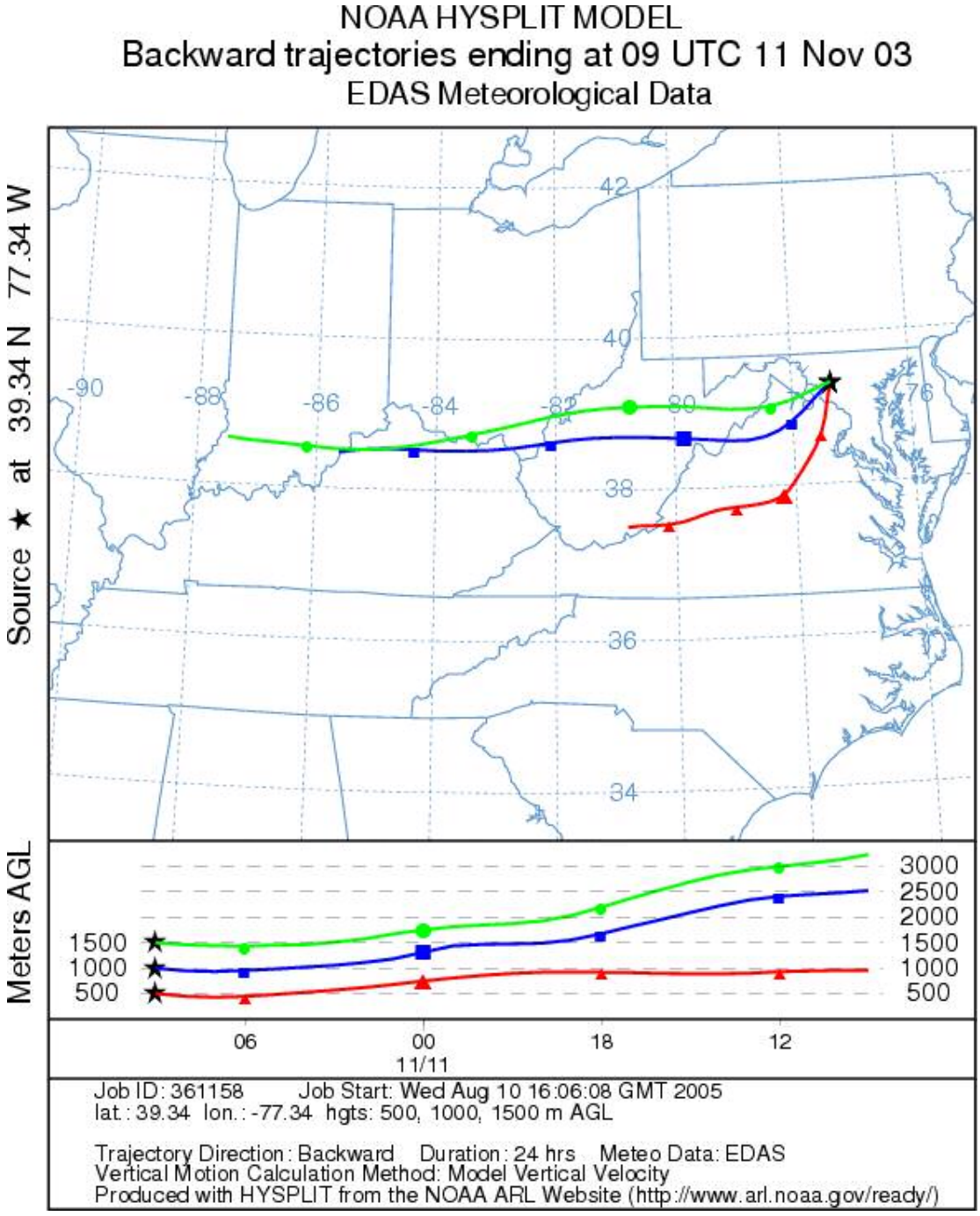

Strom track data for sample 32

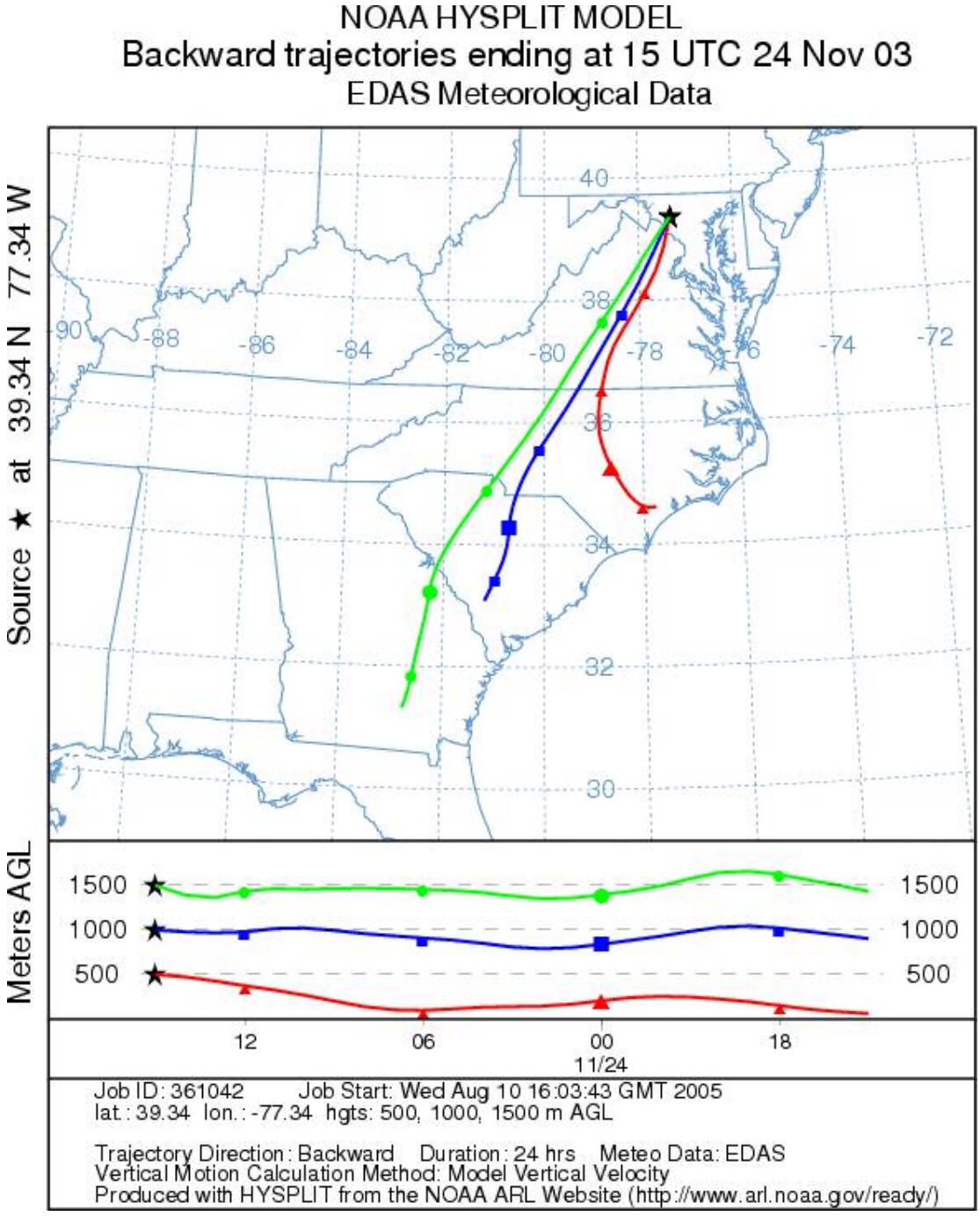

Strom track data for sample 33

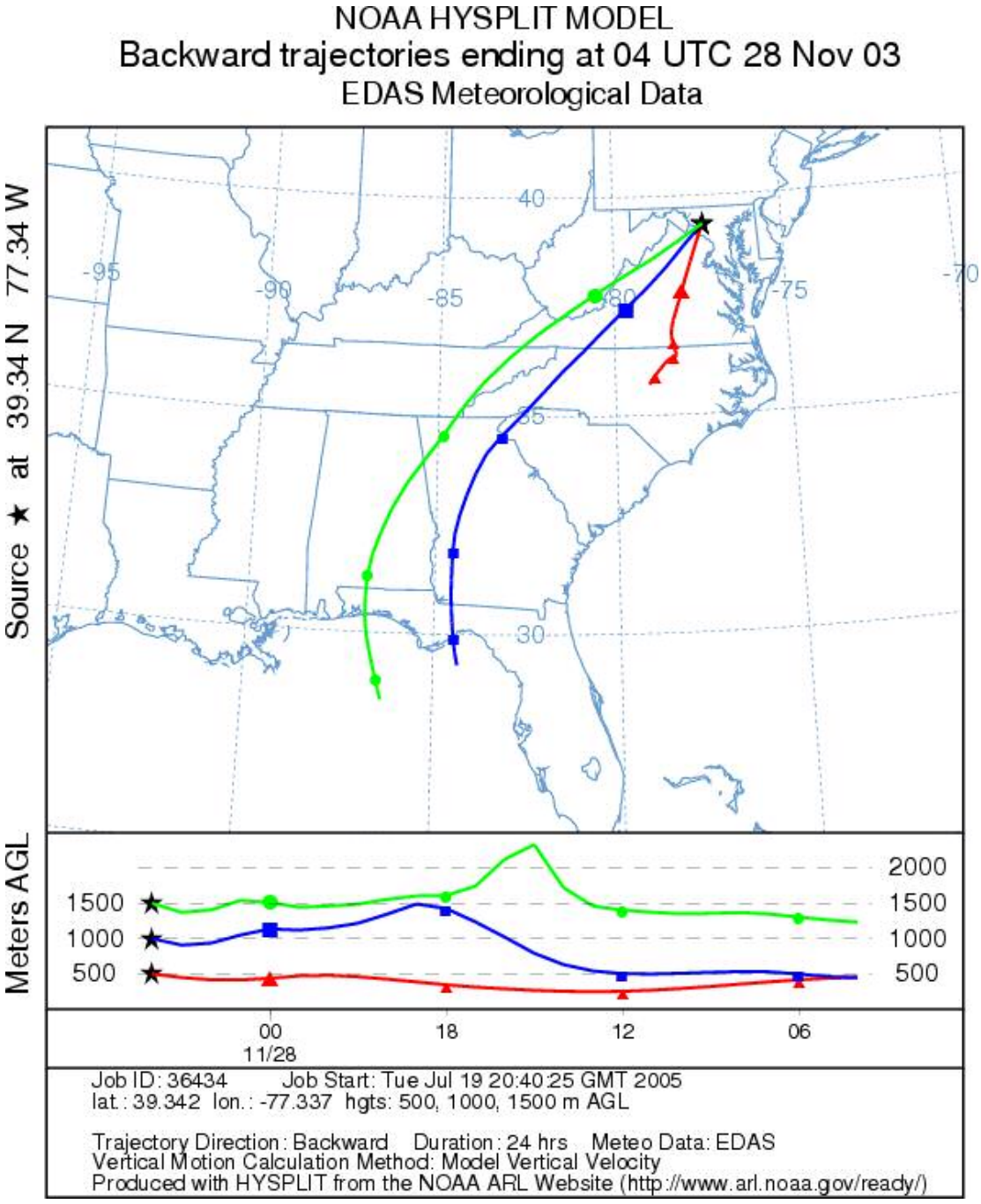

Strom track data for sample 34

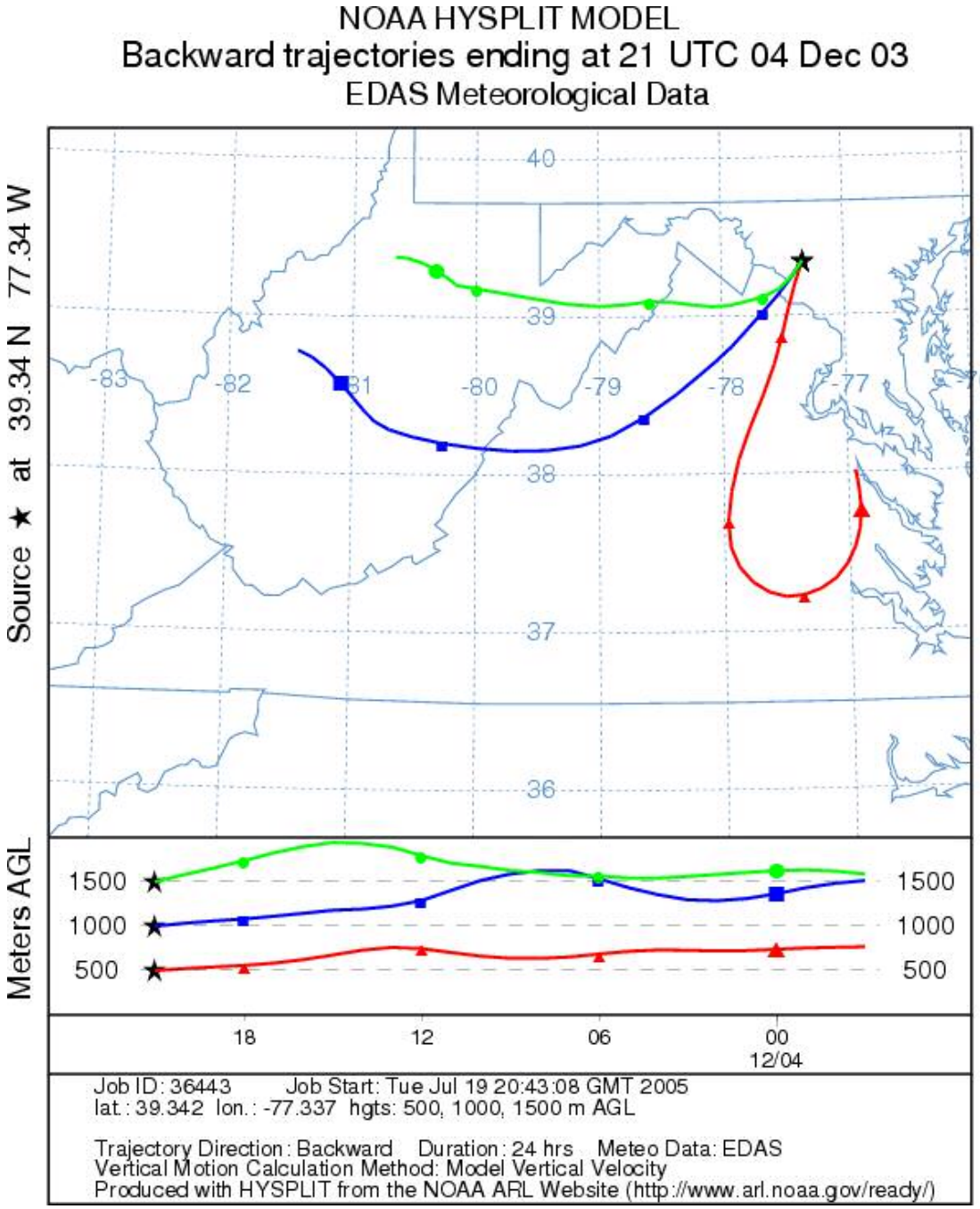

Strom track data for sample 35

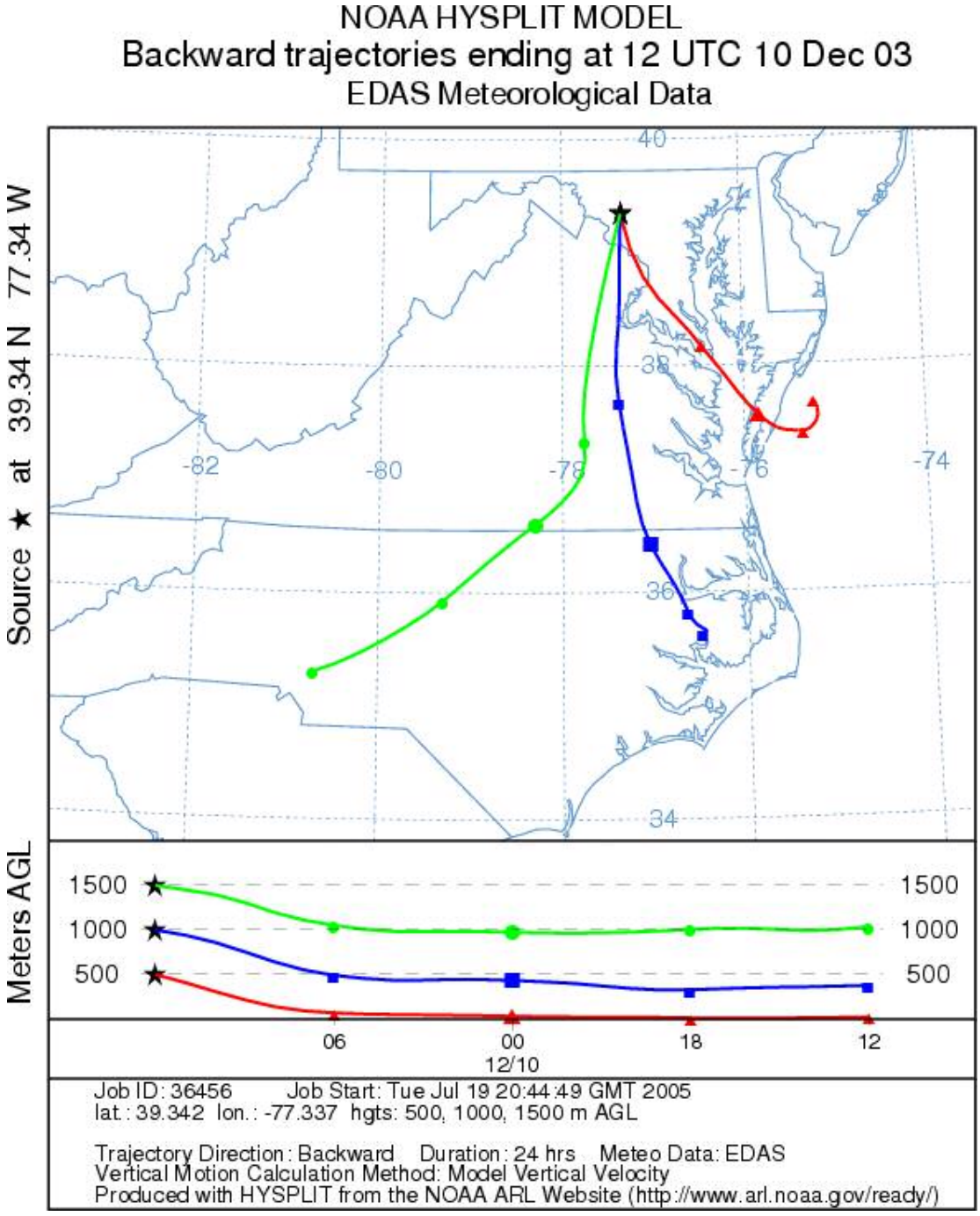

Strom track data for sample 36

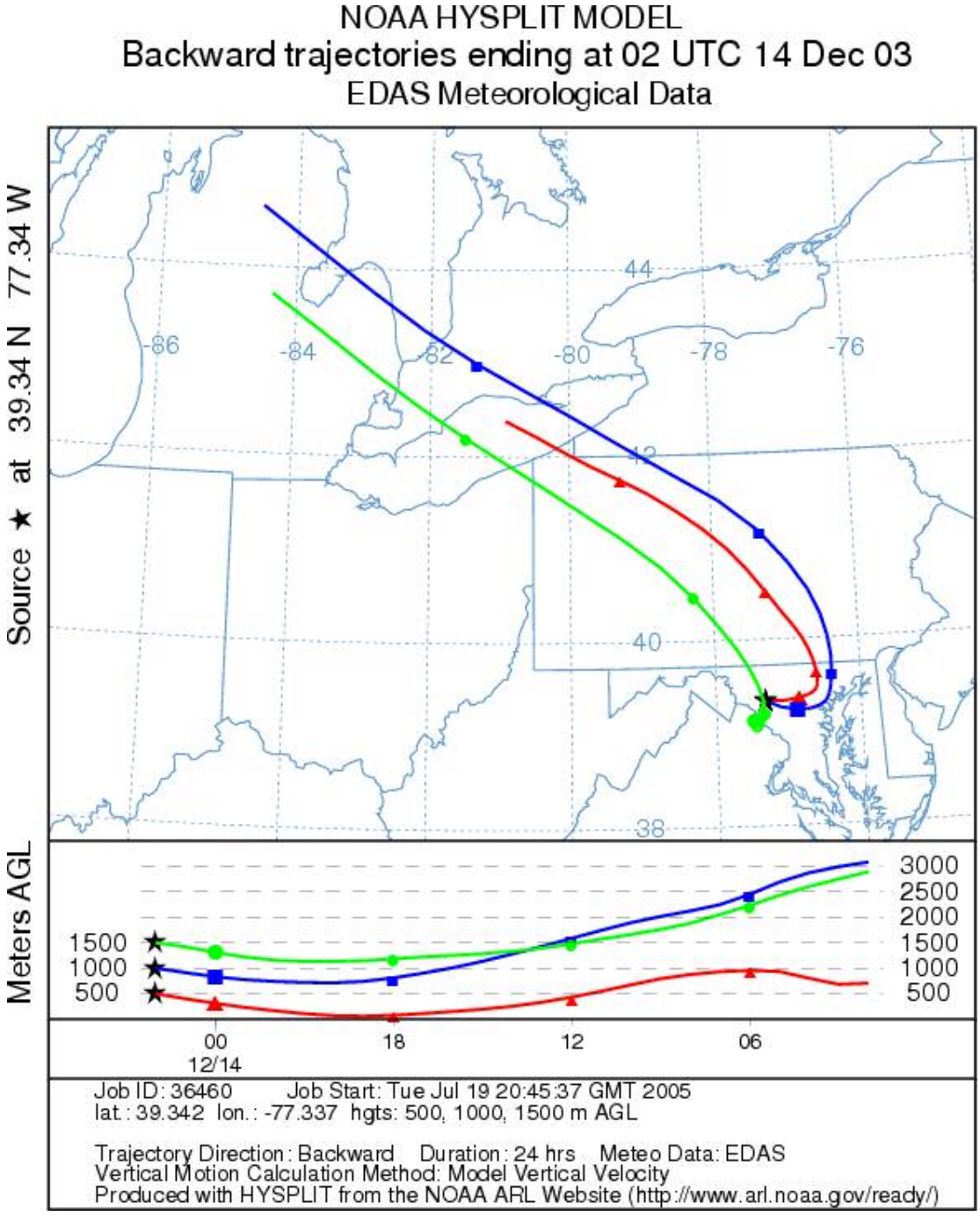

Strom track data for sample 37

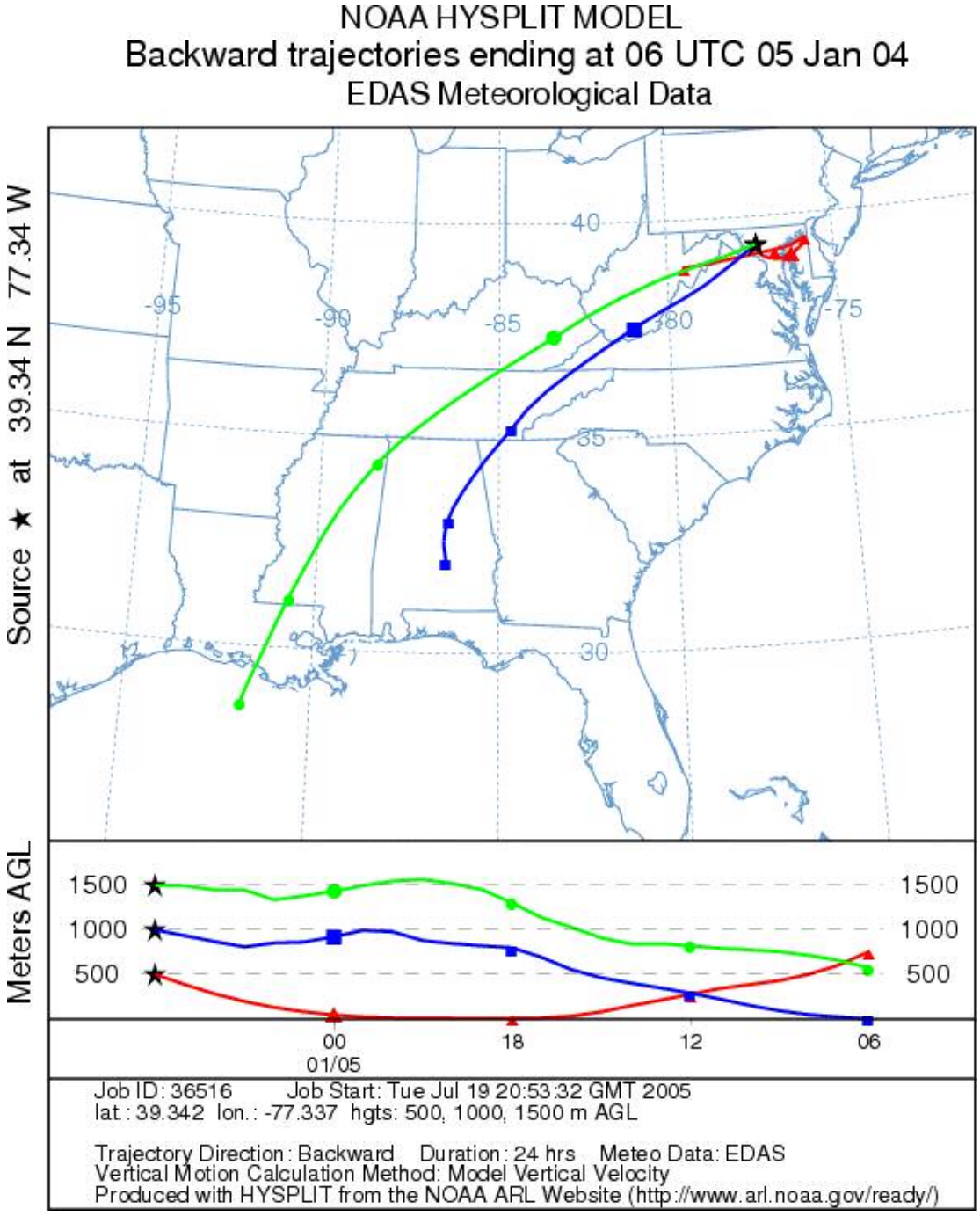

Strom track data for sample 38

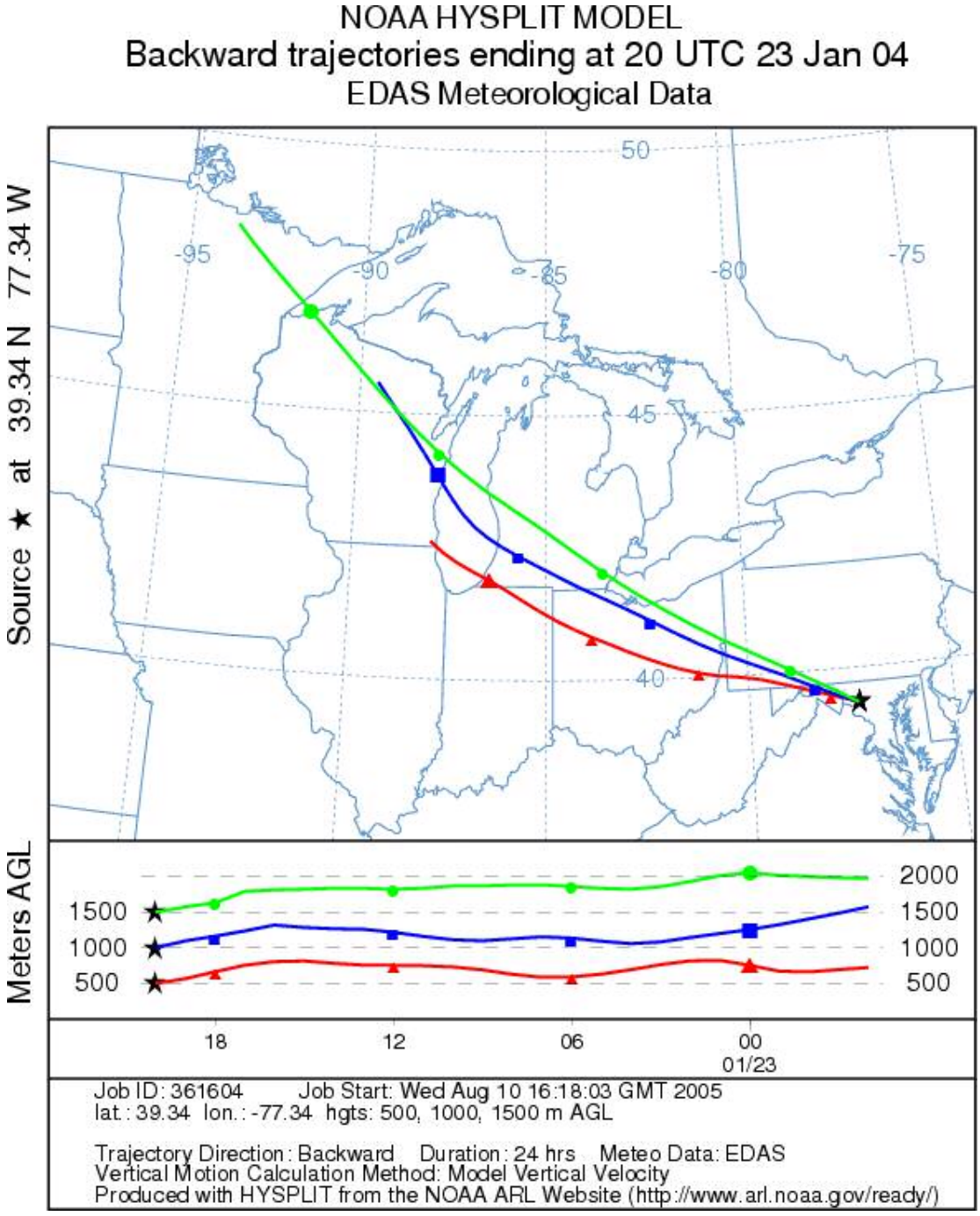

Strom track data for sample 39

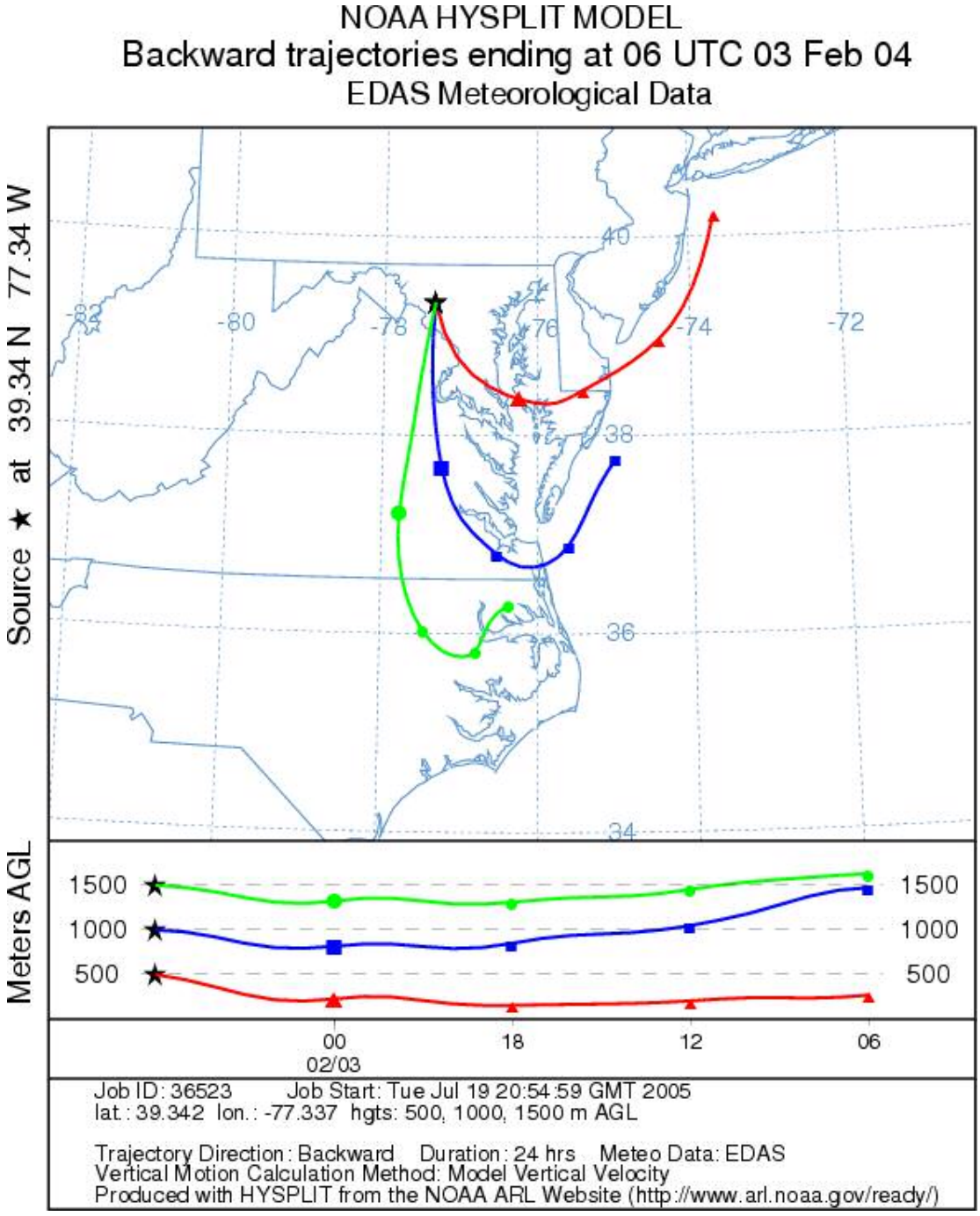

Strom track data for sample 40

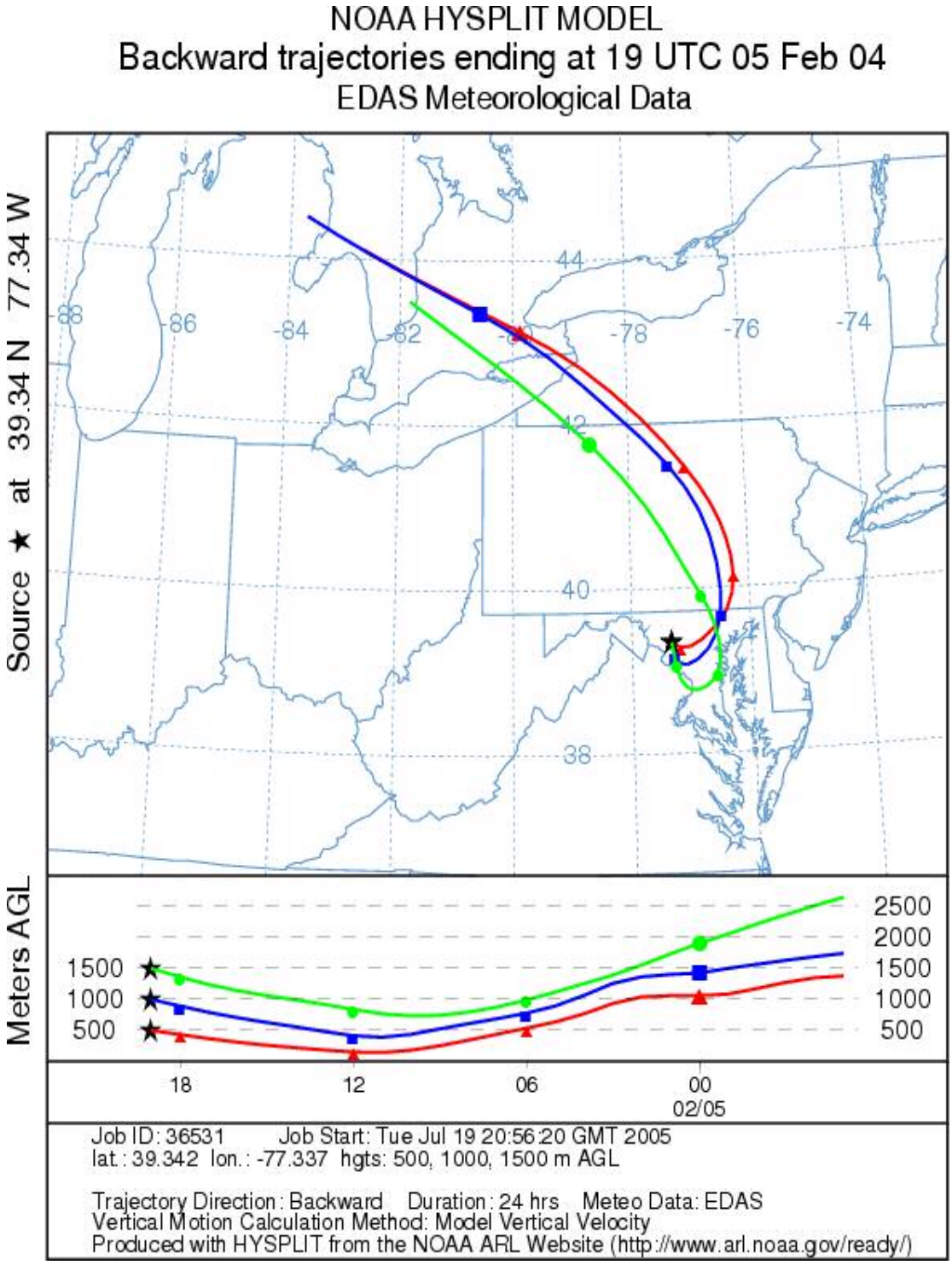

Strom track data for sample 41

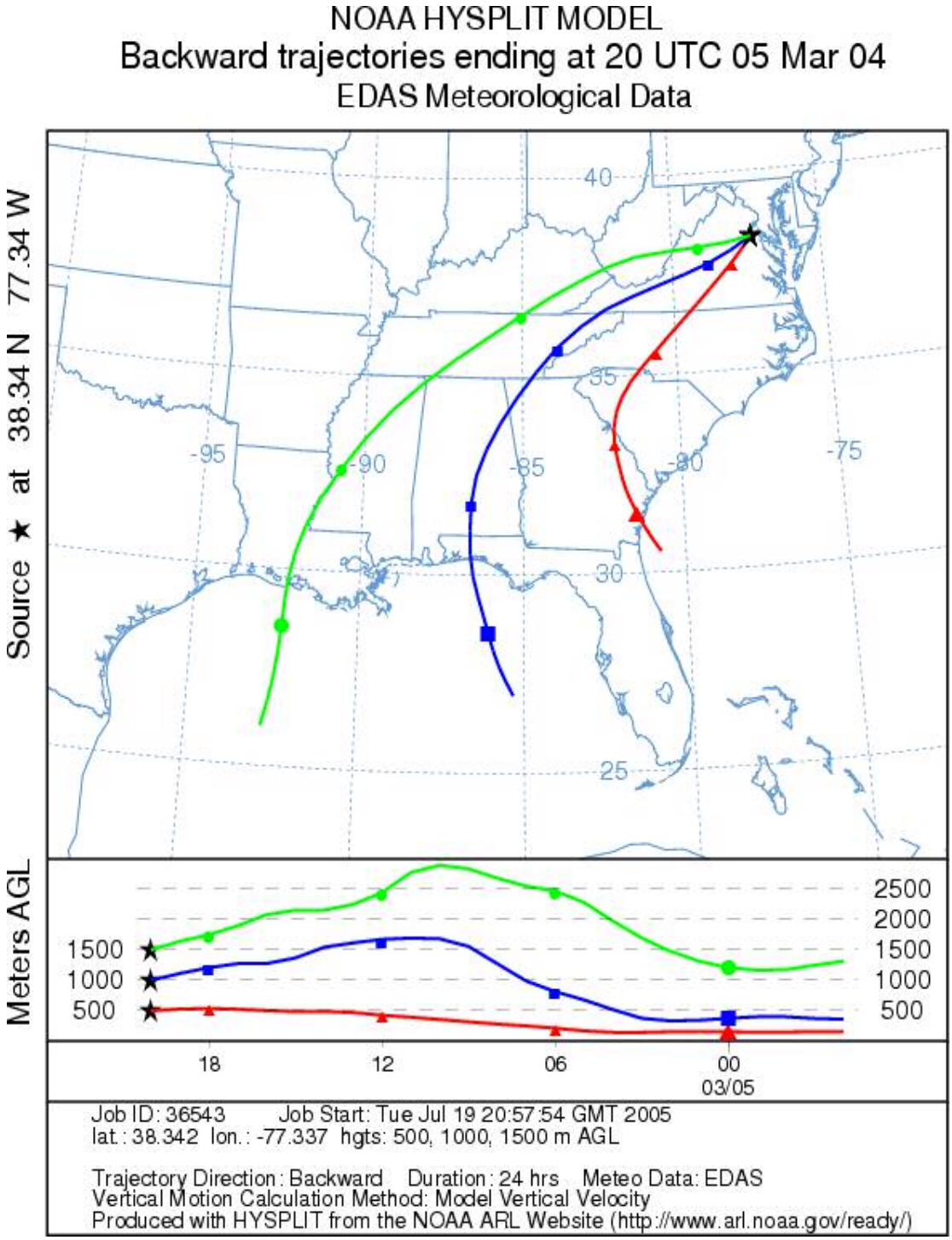

Strom track data for sample 42

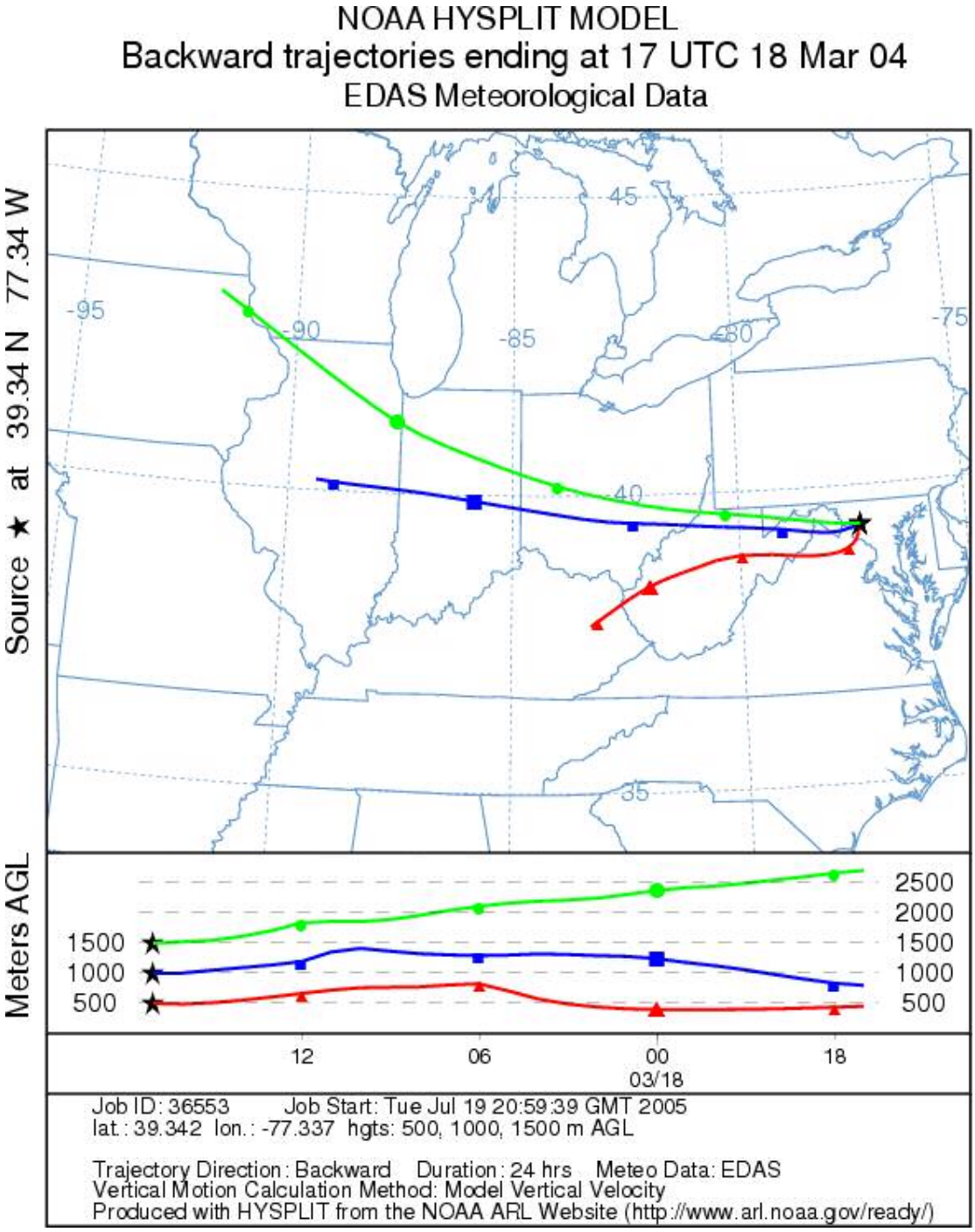

Strom track data for sample 43

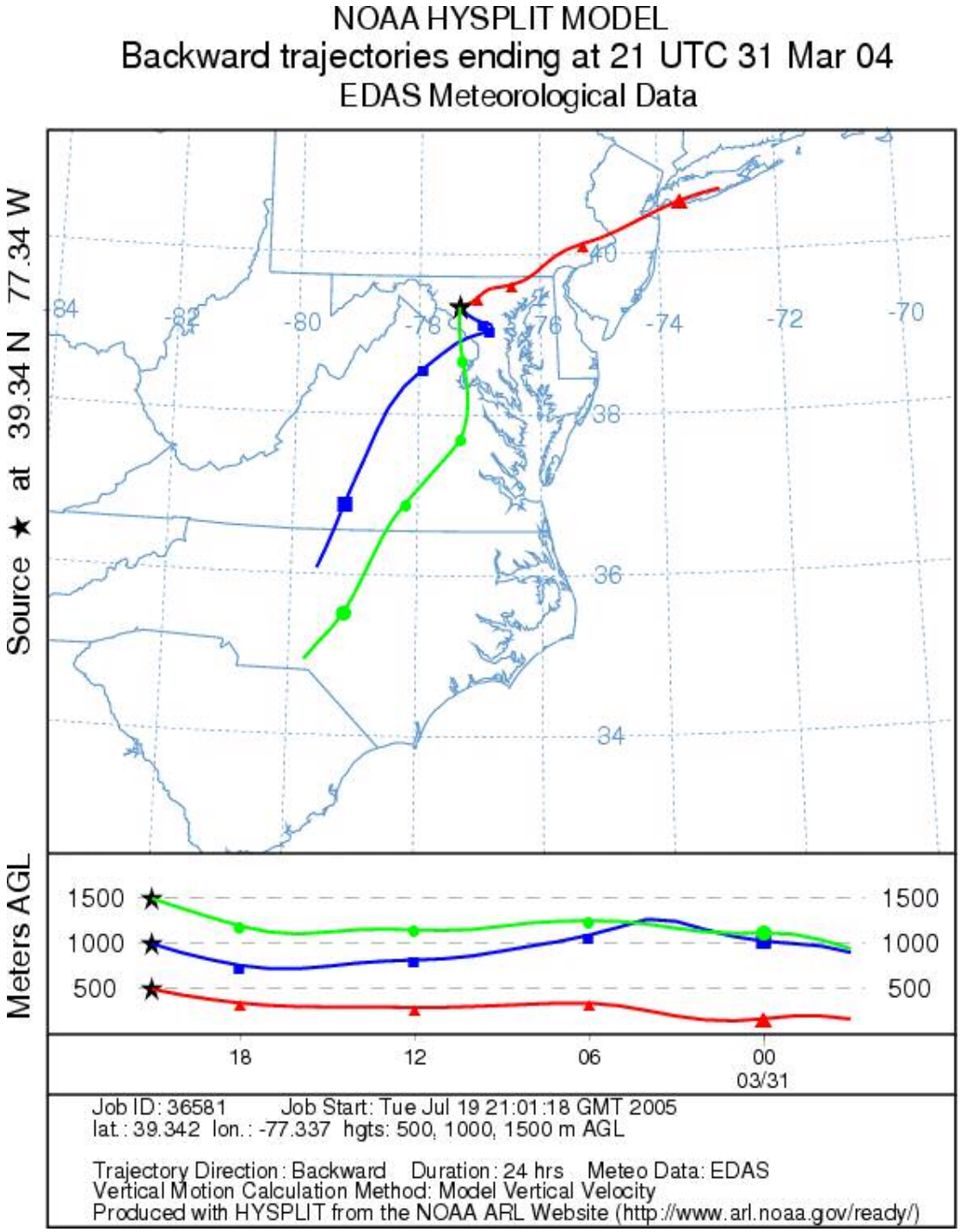

Strom track data for sample 44

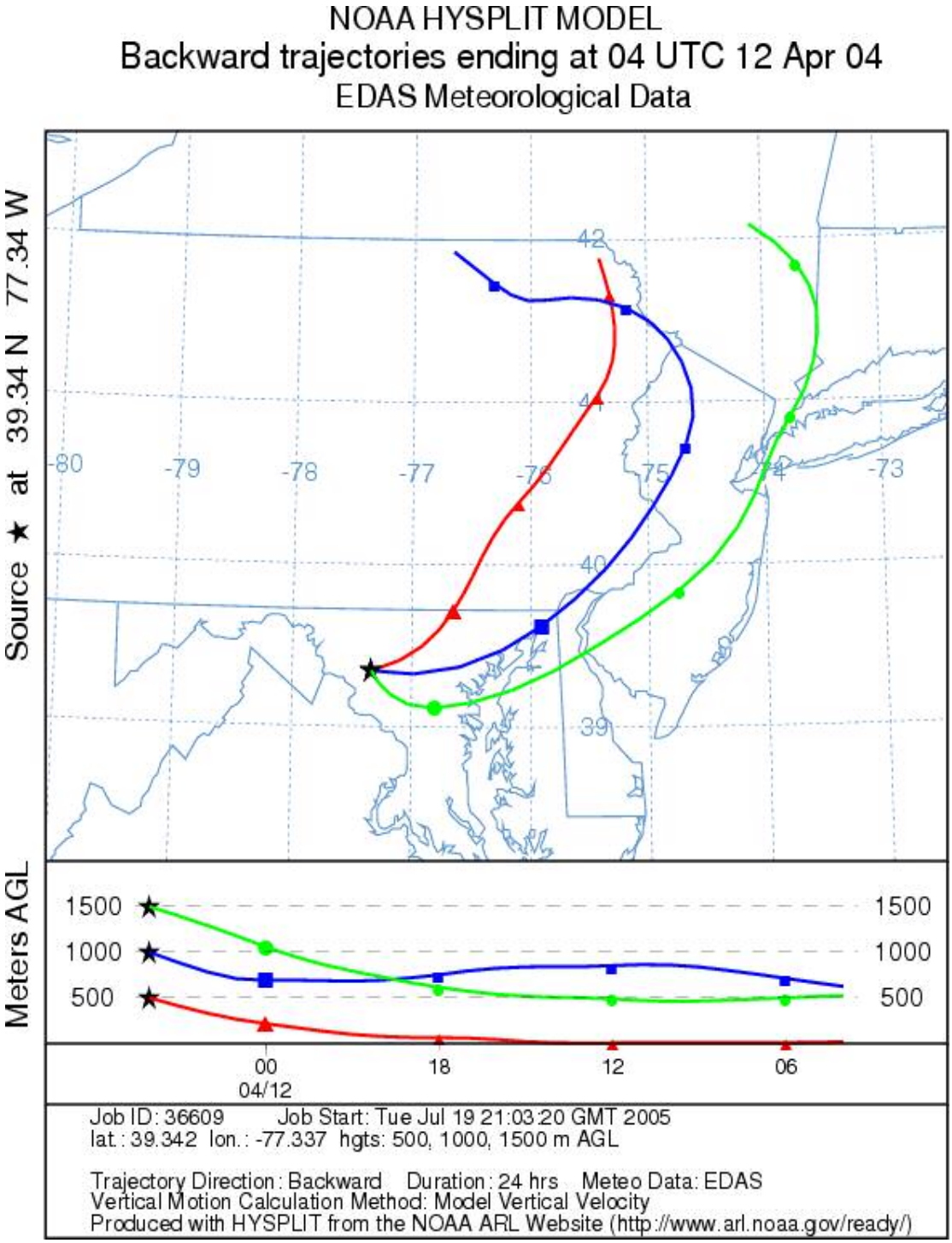

Strom track data for sample 45

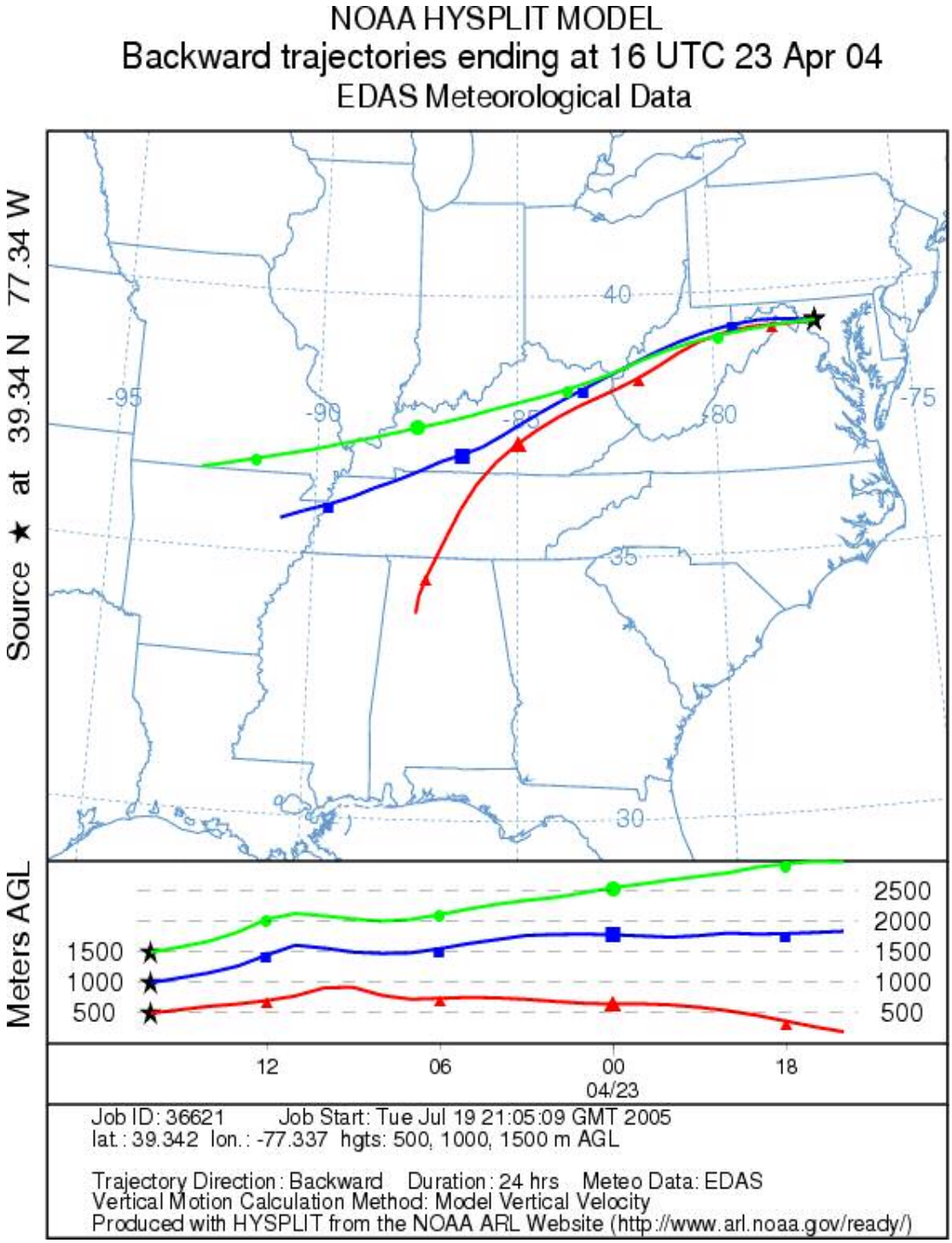

Strom track data for sample 46

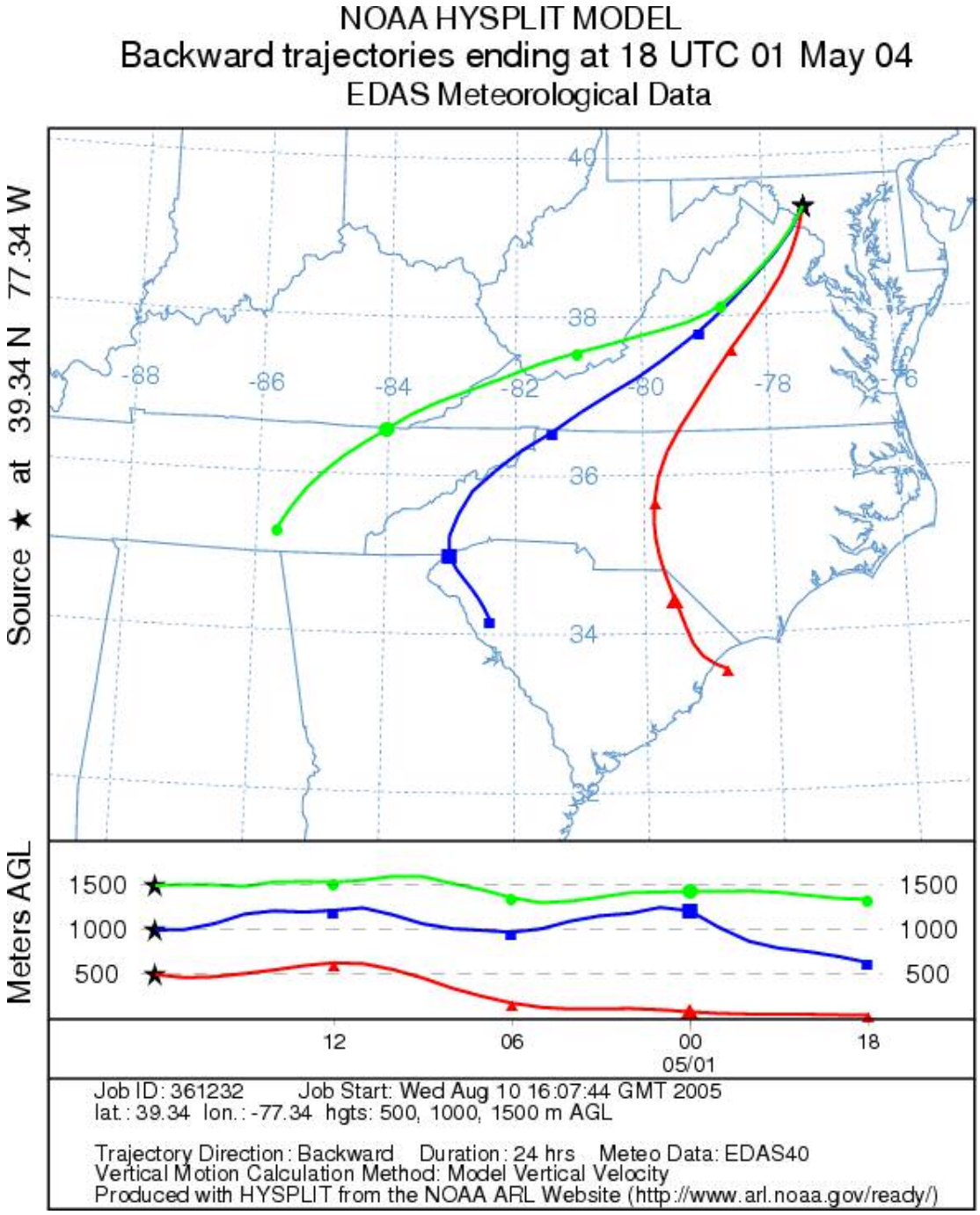

Bibliography

Alexander B., Vollmer M. K., Jackson T., Weiss R. F., and Thiemens M. H. (2001) Stratospheric CO_2 isotopic anomalies and SF6 and CFC tracer concentrations in the Arctic polar vortex. *Geophysical Research Letters* **28**(21), 4103-4106.

Alexander B., Vollmer M. K., Jackson T., Weiss R. F., and Thiemens M. H. (2002) Stratospheric CO_2 isotopic anomalies and SF6 and CFC tracer concentrations in the Arctic polar vortex (vol 28, pg 4103, 2001). *Geophysical Research Letters* **29**(5).

Amberger A. and Schmidt H. L. (1987) Naturliche isotopengehalte von nitrat als indikatoren fur dessen herkunft. *Geochimica et Cosmochimica Acta* **51**(10), 2699-2705.

Aravena R., Evans M. L., and Cherry J. A. (1993) Stable isotopes of oxygen and nitrogen in source identification of nitrate from septic systems. *Ground Water* **31**(2), 180-186.

Aravena R. and Robertson W. D. (1998) Use of multiple isotope tracers to evaluate denitrification in ground water: Study of nitrate from a large-flux septic system plume. *Ground Water* **36**(6), 975-982.

Atherton C. S. and Penner J. E. (1988) The transformation of nitrogen oxides in the polluted troposphere. *Tellus* **40B**, 380-392.

Atherton C. S. and Penner J. E. (1990) The effects of biogenic hydrocarbons on the transformation of nitrogen-oxides in the troposphere. *Journal Of Geophysical Research-Atmospheres* **95**(D9), 14027-14038.

Babikov D., Kendrick B. K., Walker R. B., Pack R. T., Fleurat-Lesard P., and Schinke R. (2003) Formation of ozone: Metastable states and anomalous isotope effect. *Journal Of Chemical Physics* **119**(5), 2577-2589.

Babikov D., Kendrick B. K., Walker R. B., Pack R. T., Fleurat-Lesard P., and Schinke R. (2003) Metastable states of ozone calculated on an accurate potential energy surface. *Journal Of Chemical Physics* **118**(14), 6298-6308.

Babikov D., Kendrick B. K., Walker R. B., Schinke R., and Pack R. T. (2003) Quantum origin of an anomalous isotope effect in ozone formation. *Chemical Physics Letters* **372**(5-6), 686-691.

Baertschi P. (1976) Absolute O-18 content of standard mean ocean water. *Earth And Planetary Science Letters* **31**(3), 341-344.

Bao H. M., Campbell D. A., Bockheim J. G., and Thiemens M. H. (2000) Origins of sulphate in Antarctic dry-valley soils as deduced from anomalous O-17 compositions. *Nature* **407**(6803), 499-502.

Bao H. M. and Gu B. H. (2004) Natural perchlorate has a unique oxygen isotope signature. *Environmental Science & Technology* **38**(19), 5073-5077.

Bao H. M., Michalski G. M., and Thiemens M. H. (2001) Sulfate oxygen-17 anomalies in desert varnishes. *Geochimica et Cosmochimica Acta* **65**(13), 2029-2036.

Bao H. M., Thiemens M. H., Farquhar J., Campbell D. A., Lee C. C. W., Heine K., and Loope D. B. (2000) Anomalous O-17 compositions in massive sulphate deposits on the Earth. *Nature* **406**(6792), 176-178.

Bao H. M., Thiemens M. H., and Heine K. (2001) Oxygen-17 excesses of the Central Namib gypcretes: spatial distribution. *Earth and Planetary Science Letters* **192**(2), 125-135.

Bao H. M., Thiemens M. H., Loope D. B., and Yuan X. L. (2003) Sulfate oxygen-17 anomaly in an Oligocene ash bed in mid-North America: Was it the dry fogs? *Geophysical Research Letters* **30**(16).

Battaglin W. A., Kendall C., Chang C. C. Y., Silva S. R., and Campbell D. H. (2001) Chemical and isotopic evidence of nitrogen transformation in the Mississippi River, 1997-98. *Hydrological Processes* **15**(7), 1285-1300.

Bhattacharya S. K., Savarino J., and Thiemens M. H. (2000) A new class of oxygen isotopic fractionation in photodissociation of carbon dioxide: Potential implications for atmospheres of Mars and Earth. *Geophysical Research Letters* **27**(10), 1459-1462.

Bhattacharya S. K. and Thiemens M. H. (1988) Isotopic fractionation in ozone decomposition. *Geophysical Research Letters* **15**(1), 9-12.

Bhattacharya S. K. and Thiemens M. H. (1989) Effect of isotopic exchange upon symmetry dependent fractionation in the O+CO-]CO_2 reaction. *Zeitschrift Fur Naturforschung Section A-A Journal Of Physical Sciences* **44**(9), 811-813.

Bigeleisen J. (1949) The relative reaction velocities of isotopic molecules. *Journal of Chemical Physics* **17**(8), 675-678.

Bigeleisen J. (1998) Second-order correction to the Bigeleisen-Mayer equation due to the nuclear field shift. *Proceedings of the National Academy of Sciences of the United States of America* **95**(9), 4808-4809.

Bigeleisen J. and Mayer M. G. (1947) Calculation of equilibrium constants for isotopic exchange reactions. *Journal of Chemical Physics* **15**(5), 261-267.

Bigeleisen J. and Wolfsberg M. (1958) Theoretical and experimental aspects of isotope effects in chemical kinetics. *Advances in Chemical Physics* **1**, 15-76.

Boering K. A., Jackson T., Hoag K. J., Cole A. S., Perri M. J., Thiemens M., and Atlas E. (2004) Observations of the anomalous oxygen isotopic composition of carbon dioxide in the lower stratosphere and the flux of the anomaly to the troposphere. *Geophysical Research Letters* **31**(3).

Bohlke J. K., Ericksen G. E., and Revesz K. (1997) Stable isotope evidence for an atmospheric origin of desert nitrate deposits in northern Chile and southern California, USA. *Chemical Geology* **136**(1-2), 135-152.

Bohlke J. K., Mroczkowski S. J., and Coplen T. B. (2003) Oxygen isotopes in nitrate: new reference materials for O-18: O-17: O-16 measurements and observations on nitrate-water equilibration. *Rapid Communications in Mass Spectrometry* **17**(16), 1835-1846.

Bottcher J., Strebel O., Voerkelius S., and Schmidt H. L. (1990) Using isotope fractionation of nitrate nitrogen and nitrate oxygen for evaluation of microbial denitrification in a sandy aquifer. *Journal of Hydrology* **114**(3-4), 413-424.

Bragazza L., Limpens J., Gerdol R., Grosvernier P., Hajek M., Hajek T., Hajkova P., Hansen I., Iacumin P., Kutnar L., Rydin H., and Tahvanainen T. (2005) Nitrogen concentration and delta N-15 signature of ombrotrophic Sphagnum mosses at different N deposition levels in Europe. *Global Change Biology* **11**(1), 106-114.

Braman R. S. and Hendrix S. A. (1989) Nanogram nitrite and nitrate determination in environmental and biological-materials by vanadium (III) reduction with chemi-luminescence detection. *Analytical Chemistry* **61**(24), 2715-2718.

Brauer K. and Strauch G. (2000) An alternative procedure for the O-18 measurement of nitrate oxygen. *Chemical Geology* **168**(3-4), 283-290.

Brenninkmeijer C. A. M., Janssen C., Kaiser J., Rockmann T., Rhee T. S., and Assonov S. S. (2003) Isotope effects in the chemistry of atmospheric trace compounds. *Chemical Reviews* **103**(12), 5125-5161.

Bruningfann C. S. and Kaneene J. B. (1993) The effects of nitrate, nitrite and N-nitroso compounds on human health - A review. *Veterinary and Human Toxicology* **35**(6), 521-538.

Bunton C. A., Halevi E. A., and Llewellyn D. R. (1952) Oxygen exchange between nitric acid and water.1. *Journal of the Chemical Society* (DEC), 4913-4916.

Burns D. A. and Kendall C. (2002) Analysis of delta N-15 and delta O-18 to differentiate NO3- sources in runoff at two watersheds in the Catskill Mountains of New York. *Water Resources Research* **38**(5).

Campbell D. H., Kendall C., Chang C. C. Y., Silva S. R., and Tonnessen K. A. (2002) Pathways for nitrate release from an alpine watershed: Determination using delta N-15 and delta O-18. *Water Resources Research* **38**(5).

Casciotti K. L., Sigman D. M., Hastings M. G., Bohlke J. K., and Hilkert A. (2002) Measurement of the oxygen isotopic composition of nitrate in seawater and freshwater using the denitrifier method. *Analytical Chemistry* **74**(19), 4905-4912.

Chacko T., Cole D. R., and Horita J. (2001) Equilibrium oxygen, hydrogen and carbon isotope fractionation factors applicable to geologic systems. In *Stable Isotope Geochemistry*, *Reviews in Mineralogy and Geochemistry*, Vol. 43 (ed. J. W. Valley and D. R. Cole), pp. 225-278. Mineralogical Society of America.

Chang C. C. Y., Kendall C., Silva S. R., Battaglin W. A., and Campbell D. H. (2002) Nitrate stable isotopes: tools for determining nitrate sources among different land uses in the Mississippi River Basin. *Canadian Journal Of Fisheries And Aquatic Sciences* **59**(12), 1874-1885.

Chang C. C. Y., Langston J., Riggs M., Campbell D. H., Silva S. R., and Kendall C. (1999) A method for nitrate collection for delta N-15 and delta O-18 analysis from waters with low nitrate concentrations. *Canadian Journal Of Fisheries And Aquatic Sciences* **56**(10), 1856-1864.

Clayton R. N. (2002) Solar System - Self-shielding in the solar nebula. *Nature* **415**(6874), 860-861.

Clayton R. N., Grossman L., and Mayeda T. K. (1973) Component of primitive nuclear composition in carbonaceous meteorites. *Science* **182**(4111), 485-488.

Coplen T. B., Bohke J. K., and Casciotti K. L. (2004) Using dual-bacterial denitrification to improve delta N-15 determinations of nitrates containing mass-independent 17O. *Rapid Communications In Mass Spectrometry* **18**(3), 245-250.

Coplen T. B., Krouse H. R., and J.K. B. (1992) Reporting of nitrogen-isotope abundances - (Technical report). *Pure and Applied Chemistry* **64**(6), 907-908.

Criss R. E. (1991) Temperature-dependence of isotopic fractionation factors. In *Stable Isotope Geochemistry: A Tribute to Samuel Epstein*, Vol. 3 (ed. H. P. Taylor, J. O'Neil, and K. I.R.), pp. 11-16. Geochem Soc Spec Pub.

Delwiche C. C. and Steyn P. L. (1970) Nitrogen isotope fractionation in soils and microbial reactions. *Environmental Science & Technology* **4**(11), 929-&.

Dentener F. J. and Crutzen P. J. (1994) A 3-Dimensional Model Of The Global Ammonia Cycle. *Journal Of Atmospheric Chemistry* **19**(4), 331-369.

Dossett S. R. and Bowersox V. C. (1999) National trends network site operation manual. National Atmospheric Deposition Program.

Durka W., Schulze E. D., Gebauer G., and Voerkelius S. (1994) Effects of forest decline on uptake and leaching of deposited nitrate determined from N-15 and O-18 measurements. *Nature* **372**(6508), 765-767.

Ehhalt D., Prather M., Dentener F., Derwent R., Dlugokencky E., Holland E., Isaksen I., Katima J., Kirchhoff V., Matson P., Midgley P., and Wang M. (2001) Atmospheric Chemistry and Greenhouse Gases. In *Climate Change 2001: Working Group I: The Scientific Basis* (ed. J. T. Houghton, Y. Ding, D. J. Griggs, M. Noguer, P. J. van der Linden, X. Dai, K. Maskell, and C. A. Johnson), pp. 881pp. Cambridge University Press.

Elliott E. M., Kendall C., Harlin K., Butler T., Carlton R., and Wankel S. (2004) Mapping the spatial and temporal distribution of N and O isotopes in precipitation across the northeastern and mid-Atlantic United States. *EOS Trans. AGU* **85**(47), Abstract H52B-02.

Elliott E. M., Kendall C., Harlin K., Butler T., Carlton R., and Wankel S. (2004) Mapping the spatial and temporal distribution of N and O isotopes in precipitaiton across the northeastern and mid-Atlantic United States. *EOS Trans. AGU* **85**(47), Abstract H52B-02.

Eriksson E. (1959) On the isotopic composition of the ammonia and the nitrate ion in rain. *Geochimica et Cosmochimica Acta* **15**(1-2), 153-153.

Fogel M. L. and Paerl H. W. (1993) Isotopic tracers of nitrogen from atmospheric deposition to coastal waters. *Chemical Geology* **107**(3-4), 233-236.

Freyer H. D. (1978) Preliminary N-15 studies on atmospheric nitrogenous trace gases. *Pure and Applied Geophysics* **116**(2-3), 393-404.

Freyer H. D. (1978) Seasonal trends of NH_4^+ and NO_3^- nitrogen isotope composition in rain collected at Jülich, Germany. *Tellus* **30**(1), 83-92.

Freyer H. D. (1978) Seasonal trends of NH_4^+ and NO_3^- nitrogen isotope composition in rain collected in Julich, West Germany. *Tellus* **30**, 83-92.

Freyer H. D. (1991) Seasonal-variation of N-15-N-14 ratios in atmospheric nitrate species. *Tellus Series B-Chemical and Physical Meteorology* **43**(1), 30-44.

Freyer H. D. (1991) Seasonal-variation of N-15/N-14 ratios in atmospheric nitrate species. *Tellus Series B-Chemical and Physical Meteorology* **43**(1), 30-44.

Freyer H. D., Kley D., Volzthomas A., and Kobel K. (1993) On the interaction of isotopic exchange processes with photochemical-reactions in atmospheric

oxides of nitrogen. *Journal Of Geophysical Research-Atmospheres* **98**(D8), 14791-14796.

Freyer H. D., Kobel K., Delmas R. J., Kley D., and Legrand M. R. (1996) First results of N-15/N-14 ratios in nitrate from alpine and polar ice cores. *Tellus Series B-Chemical and Physical Meteorology* **48**(1), 93-105.

Galloway J. N. and Likens G. E. (1981) Acid precipitation - The importance of nitric acid. *Atmospheric Environment* **15**(6), 1081-1085.

Gao Y. Q. and Marcus R. A. (2001) Strange and unconventional isotope effects in ozone formation. *Science* **293**(5528), 259-263.

Gao Y. Q. and Marcus R. A. (2002) On the theory of the strange and unconventional isotopic effects in ozone formation. *Journal of Chemical Physics* **116**(1), 137-154.

Garten C. T. (1992) Nitrogen isotope composition of ammonium and nitrate in bulk precipitation and forest throughfall. *International Journal of Environmental Analytical Chemistry* **47**(1), 33-45.

Garten C. T. (1996) Stable nitrogen isotope ratios in wet and dry nitrate deposition collected with an artificial tree. *Tellus Series B-Chemical and Physical Meteorology* **48**(1), 60-64.

Goldenbaum G. C. and Dickerson R. R. (1993) Nitric-oxide production by lightning discharges. *Journal of Geophysical Research-Atmospheres* **98**(D10), 18333-18338.

Goulding K. W. T., Bailey N. J., Bradbury N. J., Hargreaves P., Howe M., Murphy D. V., Poulton P. R., and Willison T. W. (1998) Nitrogen deposition and its contribution to nitrogen cycling and associated soil processes. *New Phytologist* **139**(1), 49-58.

Guenther J., Krankowsky D., and Mauersberger K. (2000) Third-body dependence of rate coefficients for ozone formation in O-16-O-18 mixtures. *Chemical Physics Letters* **324**(1-3), 31-36.

Haberhauer G. and Blochberger K. (1999) A simple cleanup method for the isolation of nitrate from natural water samples for O isotope analysis. *Analytical Chemistry* **71**(16), 3587-3590.

Hall N. F. and Alexander O. R. (1940) Oxygen exchange between anions and water. *Journal of American Chemical Society* **62**(12), 3455-3462.

Hastings M. G., Malcolm E., Kaiser J., and Sigman D. M. (2004) Controls on the nitrogen and oxygen isotopic composition ($\delta^{15}N$, $\delta^{18}O$, $\Delta^{17}O$) of atmospheric nitrate in Princeton, NJ. *EOS Trans. AGU* **85**(47), Abstract H52B-06.

Hastings M. G., Sigman D. M., and Lipschultz F. (2003) Isotopic evidence for source changes of nitrate in rain at Bermuda. *Journal of Geophysical Research-Atmospheres* **108**(D24).

Hastings M. G., Steig E. J., and Sigman D. M. (2004) Seasonal variations in N and O isotopes of nitrate in snow at Summit, Greenland: Implications for the study of nitrate in snow and ice cores. *Journal of Geophysical Research-Atmospheres* **109**(D20).

Hathorn B. C. and Marcus R. A. (1999) An intramolecular theory of the mass-independent isotope effect for ozone. I. *Journal of Chemical Physics* **111**(9), 4087-4100.

Hathorn B. C. and Marcus R. A. (2000) An intramolecular theory of the mass-independent isotope effect for ozone. II. Numerical implementation at low pressures using a loose transition state. *Journal of Chemical Physics* **113**(21), 9497-9509.

Hayes J. M. (2001) Fractionation of the isotopes of carbon and hydrogen in biosynthetic processes. In *Stable Isotope Geochemistry, Reviews in Mineralogy and Geochemistry*, Vol. 43 (ed. J. W. Valley and D. R. Cole), pp. 225-278. Mineralogical Society of America.

Hayes J. M. (2004) An introduction to isotopic calculations. In *National Ocean Sciences Accelerator Mass Spectrometry Facility Website,* pdf available at http://www.nosams.whoi.edu/research/staff_hayes.html.

Heaton T. H. E. (1986) Isotopic studies of nitrogen pollution in the hydrosphere and atmosphere - A review. *Chemical Geology* **59**(1), 87-102.

Heaton T. H. E. (1987) N-15/N-14 ratios of nitrate and ammonium in rain at Pretoria, South-Africa. *Atmospheric Environment* **21**(4), 843-852.

Heaton T. H. E. (1990) $^{15}N/^{14}N$ ratios of NO_x from vehicle engines and coal-fired power stations. *Tellus* **42B**, 304-307.

Heaton T. H. E., Wynn P., and Tye A. M. (2004) Low N-15/N-14 ratios for nitrate in snow in the High Arctic (79 degrees N). *Atmospheric Environment* **38**(33), 5611-5621.

Heidenreich J. E. and Thiemens M. H. (1983) A non-mass-dependent isotope effect in the production of ozone from molecular-oxygen. *Journal of Chemical Physics* **78**(2), 892-895.

Herzberg G. (1950) *Molecular spectra and molecular structure*. Van Nostrand.

Hoering T. (1955) Variations of nitrogen-15 abundance in naturally occurring substances. *Science* **122**(3182), 1233-1234.

Hoering T. (1957) The isotopic composition of the ammonia and the nitrate ion in rain. *Geochimicae et Cosmochimica Acta* **12**(1-2), 97-102.

Hulston J. R. and Thode H. G. (1965) Variations in S-33 S-34 and S-36 contents of meteorites and their relation to chemical and nuclear effects. *Journal of Geophysical Research* **70**(14), 3475-&.

Hutchinson G. E. (1944) Nitrogen in the biogeochemistry of the atmosphere. *American Scientist* **32**, 178-195.

Hutchinson G. E. (1954) *The biochemistry of the terrestrial atmosphere*. University of Chicago Press.

Janssen C., Guenther J., Krankowsky D., and Mauersberger K. (1999) Relative formation rates of O-50(3) and O-52(3) in O-16-O-18 mixtures. *Journal of Chemical Physics* **111**(16), 7179-7182.

Jaworski N. A., Howarth R. W., and Hetling L. I. (1997) Atmospheric deposition of nitrogen oxides onto the landscape contributes to coastal eutrophication in the northeast United States. *Environmental Science & Technology* **31**(7), 1995-2004.

Johnston J. C., Rockmann T., and Brenninkmeijer C. A. M. (2000) CO2+O(D-1) isotopic exchange: Laboratory and modeling studies. *Journal of Geophysical Research-Atmospheres* **105**(D12), 15213-15229.

Johnston J. C. and Thiemens M. H. (1997) The isotopic composition of tropospheric ozone in three environments. *Journal of Geophysical Research-Atmospheres* **102**(D21), 25395-25404.

Junk G. and Svec H. J. (1958) The Absolute Abundance Of The Nitrogen Isotopes In The Atmosphere And Compressed Gas From Various Sources. *Geochimica et Cosmochimica Acta* **14**(3), 234-243.

Kaiser J., Rockmann T., and Brenninkmeijer C. A. M. (2004) Contribution of mass-dependent fractionation to the oxygen isotope anomaly of atmospheric nitrous oxide. *Journal of Geophysical Research-Atmospheres* **109**(D3).

Kasibhatla P. S., Levy H., and Moxim W. J. (1993) Global NO_x, HNO_3, PAN, and NO_y distributions from fossil-fuel combustion emissions - A model study. *Journal of Geophysical Research-Atmospheres* **98**(D4), 7165-7180.

Kaye J. A. (1987) Mechanisms and observations for isotope fractionation of molecular-Species in planetary-Atmospheres. *Reviews of Geophysics* **25**(8), 1609-1658.

Kendall C. (1998) Tracing nitrogen sources and cycling in catchments. In *Isotope Tracers in Catchment Hydrology* (ed. C. Kendall and J. J. McDonnell), pp. 519-576. Elsevier Science B.V.

Kendall C. and Grim E. (1990) Combustion Tube Method For Measurement Of Nitrogen Isotope Ratios Using Calcium-Oxide For Total Removal Of Carbon-Dioxide And Water. *Analytical Chemistry* **62**(5), 526-529.

Kendall C., Silva S. R., Chang C. C. Y., Burns D. A., Campbell D. H., and Shanley J. B. (1996) *Use of the Delta 18-O and Delta15-N of nitrate to determine sources of nitrate in early spring runoff in forested catchments*.

Klein R. and Friedel R. A. (1950) Oxygen exchange between nitrates and water. *Journal of the American Chemical Society* **72**(8), 3810-3811.

Kohlmann J. P. and Poppe D. (1999) The tropospheric gas-phase degradation of NH_3 and its impact on the formation of N2O and NOx. *Journal of Atmospheric Chemistry* **32**(3), 397-415.

Kornexl B. E., Gehre M., Hofling R., and Werner R. A. (1999) On-line delta O-18 measurement of organic and inorganic substances. *Rapid Communications in Mass Spectrometry* **13**(16), 1685-1693.

Kornexl B. E., Werner R. A., and Gehre M. (1999) Standardization for oxygen isotope ratio measurement - Still an unsolved problem. *Rapid Communications In Mass Spectrometry* **13**(13), 1248-1251.

Krankowsky D., Bartecki F., Klees G. G., Mauersberger K., Schellenbach K., and Stehr J. (1995) Measurement of heavy isotope enrichment in tropospheric ozone. *Geophysical Research Letters* **22**(13), 1713-1716.

Krankowsky D., Lammerzahl P., and Mauersberger K. (2000) Isotopic measurements of stratospheric ozone. *Geophysical Research Letters* **27**(17), 2593-2595.

Krouse H. R. and Coplen T. B. (1997) Reporting of relative sulfur isotope-ratio data (technical report). *Pure and Applied Chemistry* **69**(2), 293-295.

Lammerzahl P., Rockmann T., Brenninkmeijer C. A. M., Krankowsky D., and Mauersberger K. (2002) Oxygen isotope composition of stratospheric carbon dioxide. *Geophysical Research Letters* **29**(12).

Lee C. C. W., Savarino J., and Thiemens M. H. (2001) Mass independent oxygen isotopic composition of atmospheric sulfate: Origin and implications for the present and past atmosphere of earth and mars. *Geophysical Research Letters* **28**(9), 1783-1786.

Lehmann M. F., Bernasconi M., and McKenzie J. A. (2001) A method for the extraction of ammonium from freshwaters for nitrogen isotope analysis. *Analytical Chemistry* **73**(19), 4717-4721.

Levy H., Moxim W. J., Klonecki A. A., and Kasibhatla P. S. (1999) Simulated tropospheric NOx: Its evaluation, global distribution and individual source contributions. *Journal of Geophysical Research-Atmospheres* **104**(D21), 26279-26306.

Li W. J., Ni B. L., Jin D. Q., and Zhang Q. G. (1988) Measurement of the absolute abundance of O-17 In V-SMOW. *Kexue Tongbao* **33**(19), 1610-1613.

Lyons J. R. (2001) Transfer of mass-independent fractionation in ozone to other oxygen-containing radicals in the atmosphere. *Geophysical Research Letters* **28**(17), 3231-3234.

Lyons J. R. and Young E. D. (2005) CO self-shielding as the origin of oxygen isotope anomalies in the early solar nebula. *Nature* **435**(7040), 317-320.

M.D.E. (2002-2005) Top ten sources of nitrogen oxides (NO_x) in the Baltimore area 1990, Vol. 2005.

Malan D. J. (1963) *Physics of lightning*. The English Universities Press Ltd.

Marcus R. A. (1952) Unimolecular dissociations and free radical recombination reactions. *Journal Of Chemical Physics* **20**(3), 359-364.

Marcus R. A. (1965) Dissociation and isomerization of vibrationally excited species.3. *Journal of Chemical Physics* **43**(8), 2658-&.

Mariotti A. (1983) Atmospheric nitrogen is a reliable standard for natural N-15 abundance measurements. *Nature* **303**(5919), 685-687.

Mariotti A., Germon J. C., Hubert P., Kaiser P., Letolle R., Tardieux A., and Tardieux P. (1981) Experimental-determination of nitrogen kinetic isotope fractionation- Some principles - Illustration for the denitrification and nitrification processes. *Plant and Soil* **62**(3), 413-430.

Matsuhisa Y., Goldsmith J. R., and Clayton R. N. (1978) Mechanisms of hydrothermal crystallization of quartz at 250-degrees-C and 15 kbar. *Geochimica et Cosmochimica Acta* **42**(2), 173-&.

Mauersberger K., Krankowsky D., and Janssen C. (2003) Oxygen isotope processes and transfer reactions. *Space Science Reviews* **106**(1-4), 265-279.

Mauersberger K., Lammerzahl P., and Krankowsky D. (2001) Stratospheric ozone isotope enrichments-revisited. *Geophysical Research Letters* **28**(16), 3155-3158.

Mauersberger K., Morton J., Schueler B., Stehr J., and Anderson S. M. (1993) Multi-isotope study of ozone - Implications for the heavy ozone anomaly. *Geophysical Research Letters* **20**(11), 1031-1034.

Mayer B., Bollwerk S. M., Mansfeldt T., Hutter B., and Veizer J. (2001) The oxygen isotope composition of nitrate generated by nitrification in acid forest floors. *Geochimica et Cosmochimica Acta* **65**(16), 2743-2756.

Mayer B., Boyer E. W., Goodale C., Jaworski N. A., Van Breemen N., Howarth R. W., Seitzinger S., Billen G., Lajtha L. J., Nosal M., and Paustian K. (2002) Sources of nitrate in rivers draining sixteen watersheds in the northeastern US: Isotopic constraints. *Biogeochemistry* **57**(1), 171-197.

McKinney C. R., McCrea J. M., Epstein S., Allen H. A., and Urey H. C. (1950) Improvements in mass spectrometers for the measurement of small differences in isotope abundance ratios. *Review of Scientific Instruments* **21**(8), 724-730.

Mengis M., Schiff S. L., Harris M., English M. C., Aravena R., Elgood R. J., and MacLean A. (1999) Multiple geochemical and isotopic approaches for assessing ground water NO3- elimination in a riparian zone. *Ground Water* **37**(3), 448-457.

Michalski G., Bohlke J. K., and Thiemens M. (2004) Long term atmospheric deposition as the source of nitrate and other salts in the Atacama Desert, Chile: New evidence from mass-independent oxygen isotopic compositions. *Geochimica et Cosmochimica Acta* **68**(20), 4023-4038.

Michalski G., Meixner T., Fenn M., Hernandez L., Sirulnik A., Allen E., and Thiemens M. (2004) Tracing atmospheric nitrate deposition in a complex semiarid ecosystem using Delta(17)0. *Environmental Science & Technology* **38**(7), 2175-2181.

Michalski G., Savarino J., Bohlke J. K., and Thiemens M. (2002) Determination of the total oxygen isotopic composition of nitrate and the calibration of a Delta O-17 nitrate reference material. *Analytical Chemistry* **74**(19), 4989-4993.

Michalski G., Scott Z., Kabiling M., and Thiemens M. H. (2003) First measurements and modeling of Delta O-17 in atmospheric nitrate. *Geophysical Research Letters* **30**(16).

Moore H. (1974) Isotopic measurement of atmospheric nitrogen-compounds. *Tellus* **26**(1-2), 169-174.

Moore H. (1977) Isotopic composition of ammonia, nitrogen-dioxide and nitrate in atmosphere. *Atmospheric Environment* **11**(12), 1239-1243.

Morton J., Barnes J., Schueler B., and Mauersberger K. (1990) Laboratory studies of heavy ozone. *Journal of Geophysical Research-Atmospheres* **95**(D1), 901-907.

Murdoch P. S. and Stoddard J. L. (1992) The role of nitrate in the acidification of streams in the Catskill Mountains of New-York. *Water Resources Research* **28**(10), 2707-2720.

Nadelhoffer K. J. and Fry B. (1994) *Nitrogen isotope studies in forest ecosystems*. Blackwell Scientific Publishers.

Ohte N., Sebestyen S. D., Shanley J. B., Doctor D. H., Kendall C., Wankel S. D., and Boyer E. W. (2004) Tracing sources of nitrate in snowmelt runoff using a high-resolution isotopic technique. *Geophysical Research Letters* **31**(21).

Paerl H. W. (1985) Enhancement of marine primary production by nitrogen-enriched acid-rain. *Nature* **315**(6022), 747-749.

Pardo L. H., Kendall C., Pett-Ridge J., and Chang C. C. Y. (2004) Evaluating the source of streamwater nitrate using delta N-15 and delta O-18 in nitrate in two watersheds in New Hampshire, USA. *Hydrological Processes* **18**(14), 2699-2712.

Penner J. E., Atherton C. S., Dignon J., Ghan S. J., Walton J. J., and Hameed S. (1991) Tropospheric nitrogen - A 3-dimensional study of sources, distributions, and deposition. *Journal of Geophysical Research-Atmospheres* **96**(D1), 959-990.

Prospero J. M., Barrett K., Church T., Dentener F., Duce R. A., Galloway J. N., Levy H., Moody J., and Quinn P. (1996) Atmospheric deposition of nutrients to the North Atlantic Basin. *Biogeochemistry* **35**(1), 27-73.

Revesz K. and Bohlke J. K. (2002) Comparison of O-delta 18 measurements in nitrate by different combustion techniques. *Analytical Chemistry* **74**(20), 5410-5413.

Revesz K., Bohlke J. K., and Yoshinari T. (1997) Determination of delta O-18 and delta N-15 in nitrate. *Analytical Chemistry* **69**(21), 4375-4380.

Richet P., Bottinga Y., and Javoy M. (1977) Review of hydrogen, carbon, nitrogen, oxygen, sulfur, and chlorine stable isotope fractionation among gaseous molecules. *Annual Review of Earth and Planetary Sciences* **5**, 65-110.

Rittenberg D. and Ponticorvo L. (1956) A method for the determination of the O^{18} concentration of oxygen of organic compounds. *International Journal of Applied Radiation and Isotopes* **2**, 208-214.

Robinson E. and Robbins R. C. (1970) Gaseous nitrogen compound pollutants from urban and natural sources. *Journal of the Air Pollution Control Association* **20**, 303-306.

Rockmann T., Brenninkmeijer C. A. M., Saueressig G., Bergamaschi P., Crowley J. N., Fischer H., and Crutzen P. J. (1998) Mass-independent oxygen isotope fractionation in atmospheric CO as a result of the reaction CO+OH. *Science* **281**(5376), 544-546.

Rockmann T., Kaiser J., Crowley J. N., Brenninkmeijer C. A. M., and Crutzen P. J. (2001) The origin of the anomalous or "mass-independent" oxygen isotope fractionation in tropospheric N2O. *Geophysical Research Letters* **28**(3), 503-506.

Russell A. G., McRae G. J., and Cass G. R. (1985) The dynamics of nitric-acid production and the fate of nitrogen-oxides. *Atmospheric Environment* **19**(6), 893-903.

Russell K. M., Galloway J. N., Macko S. A., Moody J. L., and Scudlark J. R. (1998) Sources of nitrogen in wet deposition to the Chesapeake Bay region. *Atmospheric Environment* **32**(14-15), 2453-2465.

Ryther J. H. and Dunstan W. M. (1971) Nitrogen, phosphorus, and eutrophication in coastal marine environment. *Science* **171**(3975), 1008-&.

Sakata M. (2001) A simple and rapid method for delta N-15 determination of ammonium and nitrate in water samples. *Geochemical Journal* **35**(4), 271-275.

Savarino J., Lee C. C. W., and Thiemens M. H. (2000) Laboratory oxygen isotopic study of sulfur (IV) oxidation: Origin of the mass-independent oxygen isotopic anomaly in atmospheric sulfates and sulfate mineral deposits on Earth. *Journal of Geophysical Research-Atmospheres* **105**(D23), 29079-29088.

Savarino J. and Thiemens M. H. (1999) Mass-independent oxygen isotope (O-16, O-17, O-18) fractionation found in H-x, O-x reactions. *Journal of Physical Chemistry A* **103**(46), 9221-9229.

Schauble E. A. (2004) Applying stable isotope fractionation theory to new systems. In *Geochemistry of Non-Traditional Stable Isotopes*, Vol. 55, pp. 65-111.

Schiff S. L., Devito K. J., Elgood R. J., McCrindle P. M., Spoelstra J., and Dillon P. (2002) Two adjacent forested catchments: Dramatically different NO3-export. *Water Resources Research* **38**(12).

Seinfeld J. H. and Pandis S. N. (1998) *Atmospheric Chemistry and Physics: From Air Pollution to Climate Change*. Wiley.

Sigman D. M., Casciotti K. L., Andreani M., Barford C., Galanter M., and Bohlke J. K. (2001) A bacterial method for the nitrogen isotopic analysis of nitrate in seawater and freshwater. *Analytical Chemistry* **73**(17), 4145-4153.

Silva S. R., Kendall C., Wilkison D. H., Ziegler A. C., Chang C. C. Y., and Avanzino R. J. (2000) A new method for collection of nitrate from fresh water and the analysis of nitrogen and oxygen isotope ratios. *Journal Of Hydrology* **228**(1-2), 22-36.

Solorzano L. (1969) Determination of ammonia in natural waters by phenolhypochlorite method. *Limnology and Oceanography* **14**(5), 799-&.

Spoelstra J., Schiff S. L., Elgood R. J., Semkin R. G., and Jeffries D. S. (2001) Tracing the sources of exported nitrate in the turkey lakes watershed using N-15/N-14 and O-18/O-16 isotopic ratios. *Ecosystems* **4**(6), 536-544.

Spoelstra J., Schiff S. L., Jeffries D. S., and Semkin R. G. (2004) Effect of storage on the isotopic composition of nitrate in bulk precipitation. *Environmental Science & Technology* **38**(18), 4723-4727.

Spokes L. J., Yeatman S. G., Cornell S. E., and Jickells T. D. (2000) Nitrogen deposition to the eastern Atlantic Ocean. The importance of south-easterly flow. *Tellus Series B-Chemical and Physical Meteorology* **52**(1), 37-49.

Stark M. S., Harrison J. T. H., and Anastasi C. (1996) Formation of nitrogen oxides by electrical discharges and implications for atmospheric lightning. *Journal of Geophysical Research-Atmospheres* **101**(D3), 6963-6969.

Stelson A. W. and Seinfeld J. H. (1982) Relative-Humidity and Temperature-Dependence of The Ammonium-Nitrate Dissociation-Constant. *Atmospheric Environment* **16**(5), 983-992.

Stickrod R. D. and Marshall J. D. (2000) On-line nitrate-delta N-15 extracted from groundwater determined by continuous-flow elemental analyzer/isotope ratio mass spectrometry. *Rapid Communications in Mass Spectrometry* **14**(14), 1266-1268.

Thiemens M. H. (1999) Atmosphere science - Mass-independent isotope effects in planetary atmospheres and the early solar system. *Science* **283**(5400), 341-345.

Thiemens M. H. and Jackson T. (1987) Production of isotopically heavy ozone by ultraviolet-light photolysis of O_2. *Geophysical Research Letters* **14**(6), 624-627.

Thiemens M. H. and Jackson T. (1988) New experimental-evidence for the mechanism for production of isotopically heavy O_3. *Geophysical Research Letters* **15**(7), 639-642.

Thiemens M. H., Jackson T., Mauersberger K., Schueler B., and Morton J. (1991) Oxygen isotope fractionation in stratospheric CO_2. *Geophysical Research Letters* **18**(4), 669-672.

Thiemens M. H., Jackson T. L., and Brenninkmeijer C. A. M. (1995) Observation of a mass-independent oxygen isotopic composition in terrestrial stratospheric CO_2, The link to ozone chemistry, and the possible occurrence in the Martian atmosphere. *Geophysical Research Letters* **22**(3), 255-257.

Thiemens M. H., Savarino J., Farquhar J., and Bao H. M. (2001) Mass-independent isotopic compositions in terrestrial and extraterrestrial solids and their applications. *Accounts of Chemical Research* **34**(8), 645-652.

Titani T. and Goto K. (1939) Austauschreaktion der sauerstoffatome zwischen einigen anorganischen anionen und wasser. *Bulletin of the Chemical Society of Japan* **14**, 77-85.

Turro N. J. (1983) Influence of nuclear-spin on chemical-reactions - Magnetic isotope and magnetic-field effects (A review). *Proceedings of the National Academy of Sciences of the United States of America-Physical Sciences* **80**(2), 609-621.

Urey H. C. (1947) The thermodynamic properties of isotopic substances. *Journal of the Chemical Society* (MAY), 562-581.

Valentini J. J. (1987) Mass-independent isotopic fractionation in nonadiabatic molecular-collisions. *Journal of Chemical Physics* **86**(12), 6757-6765.

Vitousek P. M., Aber J. D., Howarth R. W., Likens G. E., Matson P. A., Schindler D. W., Schlesinger W. H., and Tilman D. G. (1997) Human alteration of the global nitrogen cycle: Sources and consequences. *Ecological Applications* **7**(3), 737-750.

Voerkelius S. (1990) Isotopendiskriminierung bei der nitrifikation und denitrifikation: Grundlagen und andwendungen der herkunfts-zuordnung von nitrat and distickstoffmonoxyd., Technical University of Munich.

Wada E., Kadonaya, T. and Matsuo, S. (1975) ^{15}N abundance in nitrogen of naturally occurring substances and global assessment of denitrification from isotopic viewpoint. *Geochemistry Journal* **9**(3), 139-148.

Wang Y., DeSilva A. W., Goldenbaum G. C., and Dickerson R. R. (1998) Nitric oxide production by simulated lightning: Dependence on current, energy, and pressure. *Journal of Geophysical Research-Atmospheres* **103**(D15), 19149-19159.

Wassenaar L. I. (1995) Evaluation of the origin and fate of nitrate in the abbotsford aquifer using the Isotopes of N-15 and O-18 in NO_3. *Applied Geochemistry* **10**(4), 391-405.

Wen J. and Thiemens M. H. (1991) Experimental and theoretical-Study of isotope effects on ozone decomposition. *Journal of Geophysical Research-Atmospheres* **96**(D6), 10911-10921.

Wen J. and Thiemens M. H. (1993) Multi-isotope study of the $O(^1D)+CO_2$ exchange and stratospheric consequences. *Journal of Geophysical Research-Atmospheres* **98**(D7), 12801-12808.

Weston R. E. (1999) Anomalous or mass-independent isotope effects. *Chemical Reviews* **99**(8), 2115-2136.

Williard K. W. J., DeWalle D. R., Edwards P. J., and Sharpe W. E. (2001) O-18 isotopic separation of stream nitrate sources in mid-Appalachian forested watersheds. *Journal Of Hydrology* **252**(1-4), 174-188.

Xiao H. Y. and Liu C. Q. (2002) Sources of nitrogen and sulfur in wet deposition at Guiyang, southwest China. *Atmospheric Environment* **36**(33), 5121-5130.

Yeatman S. G., Spokes L. J., Dennis P. F., and Jickells T. D. (2001) Can the study of nitrogen isotopic composition in size-segregated aerosol nitrate and ammonium be used to investigate atmospheric processing mechanisms? *Atmospheric Environment* **35**(7), 1337-1345.

Yeatman S. G., Spokes L. J., Dennis P. F., and Jickells T. D. (2001) Comparisons of aerosol nitrogen isotopic composition at two polluted coastal sites. *Atmospheric Environment* **35**(7), 1307-1320.

Yeatman S. G., Spokes L. J., and Jickells T. D. (2001) Comparisons of coarse-mode aerosol nitrate and ammonium at two polluted coastal sites. *Atmospheric Environment* **35**(7), 1321-1335.

Young E. D., Galy A., and Nagahara H. (2002) Kinetic and equilibrium mass-dependent isotope fractionation laws in nature and their geochemical and cosmochemical significance. *Geochimica et Cosmochimica Acta* **66**(6), 1095-1104.

Zel'dovich Y. B., Sadvnikov P. Y., and Frank-Kamenetskii D. A. (1947) *Oxidation of nitrogen in combustion (translated by M. Shelef)*. Academy of Sciences, USSR.